Performance Analysis of Multicell Coordination in Cellular Wireless Networks

By: Murtadha Al-Saedy

A Thesis Submitted in Fulfilment of the Requirements
for the Degree of Doctor of Philosophy (PhD)
in
Communications

Department of Electronic and Computer Engineering,
College of Engineering, Design and Physical Sciences
Brunel University London
London, United Kingdom

Supervised By: Professor Hamed Al-Raweshidy

January 2016

In memory of my beloved parents.

Abstract

In this thesis, multicell coordination for wireless cellular networks is studied, whereby various approaches have been conducted to tackle this issue.

Firstly, the coverage probability and effective capacity in downlink multiple-input multiple-output (MIMO) cellular system are considered. Two scenarios are investigated; in the first scenario, it is assumed that the system employs distance-based fractional power control with no multicell coordination. For the second scenario, it is assumed that the system implements multicell coordinated beamforming so as to cancel inter-cell interference. The base stations (BS) are modelled as randomly uniformly distributed in the area according to Poisson point process (PPP). Using tools from stochastic geometry, tractable, analytical expressions for coverage probability and effective capacity are derived for both scenarios.

Secondly, an adaptive strategy for inter-cell interference cancellation and coordination is proposed for downlink multicarrier cellular random networks. The adaptive strategy coordinates and cancels the interference on the both frequency and spatial domains. Based on this adaptive strategy, two interference management schemes have been proposed. The adaptation process is implemented based on measured instantaneous signal-to-interference and noise ratio (SINR) of the considered user. Furthermore, the locations of base stations BSs are modelled as an independent spatial PPP. Using tools from stochastic geometry, the proposed schemes have been analytically evaluated. Analytical expressions for coverage probability are derived for both schemes. In addition, an expression for average rate has been derived using the coverage probability analysis.

Thirdly, low complexity algorithms for user scheduling have been proposed for coordinated MIMO multicell network. The algorithms consist of two stages: multicell scheduling stage and precoding stage. The algorithm works on sequential distributive manner. Two variants of multicell scheduling are proposed. The first algorithm has less complexity but leads to more difference in sum rate among cells. While the second algorithm results in better fairness in terms of system performance but causes

frequent signalling among the cells. Moreover, the algorithm is extended to multi-mode selection in addition to the user selection.

Finally, an adaptive coordination scheme for energy-efficient resource allocation has been developed for orthogonal frequency division multiple access (OFDMA) cellular networks. The proposed scheme consists of centralised and distributed stages for allocating resources to cell-edge and cell-centre users, respectively. The optimisation problems are formulated as integer linear fractional and integer linear problems for the first stage and second stages, respectively. The spectral-energy trade-off is analysed under the constraint of fairness among users. In summary, the research work presented in this thesis reveals statistical approach to analyse the multicell coordination in random cellular networks. It also offers insight into the resource allocation and scheduling problems within multicell coordination framework, and how to solve them with a certain objective.

Acknowledgements

First of all, I would like to express my appreciation and gratefulness to the higher committee for education development (HCED) in Iraq for funding my PhD study.

I would also like to offer my sincere gratitude to my supervisor Professor Hamed Al-Raweshidy for his guidance, useful advice, and encouragement. His unfailing belief in me, enthusiastic support, and useful discussion with him have been so precious and helpful. This work would have not been possible without his help and support. The thing that I appreciate most about him is his patience and understanding whilst allowing me the room to work in my own way.

My special thanks goes to Dr. Maysam Abbod for his encouragement and support.

I am also indebted to my family for their precious moral support and encouragement throughout the years of my study, whose love and inspiration travelled alongside me on my PhD journey. This work would not have materialised without their encouragement and support.

Finally, I am deeply grateful for my colleagues and friend who always urge me to pursue my study and inspire me to complete this thesis.

Table of Contents

List of Figures

List of Abbreviations

Abbreviation	Definition
AWGN	Additive White Gaussian Noise
BD	Block Diagonalisation
BER	Bit Error Rate
BS	Base Station
CBF	Coordinated Beamforming
CLT	Central Limit Theorem
CSI	Channel State Information
CCDF	Complementary Cumulative Distribution Function
CDMA	Code Division Multiple Access
CoMP	Coordinated Multiple Point
DFP	Dynamic Frequency Planning
DoF	Degrees of Freedom
DPC	Dirty Paper Coding
EE	Energy Efficiency
FDD	Frequency-Division Duplex
FDMA	Frequency-Division Multiple Access
FFR	Fractional Frequency Reuse
FRF	Frequency Reuse Factor
GSO	Gram Schmidt Orthogonalisation
HSDPA	High Speed Downlink Packet Access
ICI	Inter-cell Interference
ICIC	Inter-cell Interference Coordination
i.i.d	Independent and Identically Distributed
ISI	Inter-symbol Interference
LTE	Long Term Evolution
LoS	Line-of-Sight
MIMO	Multiple-Input Multiple-Output

MISO	Multiple-Input Single-Output
MRT	Maximal Ratio Transmission
MU-MIMO	Multi-User MIMO
NLoS	Non-Line-of-Sight
OFDMA	Orthogonal Frequency Division Multiple Access
PDF	Probability Density Function
PF	Proportional Fairness
PPP	Point Poisson Process
QoS	Quality of Service
RBF	Random Beamforming
r.v.	Random Variable
SDMA	Space Division Multiple Access
SIC	Successive Interference Cancellation
SIR	Signal-to-Interference Ratio
SINR	Signal-to-Interference-plus-Noise Ratio
SISO	Single-Input Single-Output
SFR	Soft Frequency Reuse
SNR	Signal-to-Noise Ratio
SU-MIMO	Single-User MIMO
SVD	Singular Value Decomposition
TDD	Time-Division Duplex
TDMA	Time-Division Multiple Access
UE	User Equipment
ZF	Zero Forcing
1G	First Generation
2G	Second Generation
3G	Third Generation
3GPP	Third Generation Partnership Project
4G	Fourth Generation
5G	Fifth Generation

List of Symbols

Notation	Definition
$\Gamma(.)$	Gamma function
$\Gamma(.,.)$	upper incomplete function
$\gamma(.,.)$	lower incomplete function
$\ln(.)$	natural logarithm
$\log_2(.)$	logarithm to base 2
${}_2F_1(.,.;.;.)$	Gaussian hypergeometric function
$I_0(.)$	modified Bessel function of the zero-th order
erfc(.)	complementary error function
$\mathrm{D}_{-n}(.)$	parabolic cylinder function
$Q(.)$	Gaussian-Q function
$Q^{-1}(.)$	inverse-Q function
$(\varepsilon)_j$	Pochhammer symbol
$\mathbb{E}\{.\}$	expectation
$\mathbb{V}\mathrm{ar}\{.\}$	variance
$f_\gamma(.)$	probability density function of γ
$F_\gamma(.)$	cumulative distribution function of γ
$\mathscr{L}_\gamma(.)$	Laplace transform of γ
$\mathbb{P}(X)$	probability of X
$\mathbb{P}_{\|y}(X)$	probability of X given that y has occurred
$\sum$	sum
$\prod$	product
$\binom{a}{b}$	binomial coefficient
$(x)^+$	equivalent to max(x, 0)
$\arg\min f(x)$	the point for which the function $f(x)$ has minimum value
$\arg\max f(x)$	the point for which the function $f(x)$ has maximum value
$\mathcal{A}$	set of elements
$\mid \mathcal{A} \mid$	cardinality of set $\mathcal{A}$

$\cup$	union of sets
$\cap$	intersection of sets
$\mathbb{R}$	set of real numbers
$\mathbf{a}$	a vector
$\mathbf{A}$	a matrix
$\mathbf{I}_n$	identity matrix with $n \times n$ dimension
$\mathbb{C}^{n \times m}$	the space of $n \times m$ complex matrix
$\mathcal{N}(.)$	null space of matrix
$\mathcal{R}(.)$	row space of matrix
$(.)^{\mathsf{H}}$	Hermitian operation on matrix
$(.)^{\dagger}$	pseudoinverse of a matrix
$\| \, . \, \|$	norm on a vector
$\mathsf{tr}(.)$	trace of matrix
$\mathsf{Rank}(.)$	rank of matrix
$\det(.)$	determinate of matrix
$\mathcal{P}_{\mathbf{A}}$	Projection on matrix $\mathbf{A}$
$\mathcal{O}$	big $\mathcal{O}$ notation for the asymptotic upper bound of a function.

Chapter 1

Introduction

1.1 Problem Statement

Wireless communication technology has become indispensable part of our life. It allows people to communicate with each other anywhere at any time, and affords us the possibility of accessing email, browsing, and digital resources, not to mention many others. Thus, it penetrates almost all our life aspects. During the last decades, wireless communication witnessed a rapid growth owing to its dramatic success of cellular technology. From its conventional functionality of voice service, text messaging, to the recent services such as multimedia and Internet applications, wireless communication has occupied a central place in computing and communication technology. The evolution process in wireless technology creates an expectation of universal seamless connectivity with high speed transmission anywhere at any time. With such increasing interest in fast Internet download and seamless high speed connectivity, traffic demands grow unprecedentedly as reported by the annual visual network index (VNI) reports released by Cisco [1]. Furthermore, the number of mobile devices is expected to grow exponentially as predicted by [2].

This motivates both industry and academia to meet the increasing demands for high

data rate services via new innovative wireless technologies that are smart and highly efficient. Currently, an extensive research has already been ignited to investigate and develop the potential candidate technologies for future mobile cellular system, i.e. fifth generation (5G) [3]. 5G is envisioned to be a paradigm shift that breaks backward compatibility, and expected to include very high carrier frequencies with very large bandwidths, extreme base station density, and massive number of antennas, with the objective of providing high system capacity with better quality of service (QoS) [3] [4].

1.2 Motivation

Meeting the ever-increasing demands for large volume of traffic and better QoS implies fast data rate transmission, which is fundamentally limited by wireless radio resources, mainly spectrum, which is scarce and very expensive. To deal with the dilemma of resource scarcity, the spectrum should be efficiently reused in conjunction with utilisation of highly sophisticated transmission techniques [4]. Spectrum reuse almost contributes for the most part of system spectral efficiency, i.e. a metric of how much traffic can be transmitted over a limited spectrum band [4].

The adoption of OFDMA and MIMO has also played a significant role in achieving high spectral efficiency. However, aggressive spectrum reuse results in strong interference in multicell networks, caused by the simultaneous transmission of neighbouring BSs over the same frequency band [4]. Intercell interference severely degrades users performance, especially those users at the cell boundaries. Thus, while spectrum re-utilisation yields high wide-system spectral efficiency, the performance of individual users, especially cell-edge users, will be degraded as a result. This gives rise to a trade-off between system spectral efficiency and individual user spectral efficiency, where attaining both is a challenging problem.

One of the effective approaches to deal with inter-cell interference is to enable co-ordination among neighbouring BSs. Multicell coordination can be implemented on

time, frequency, and space domain. This technique has attracted great attention recently, and investigated in LTE-A under the name of coordinated multipoint processing (CoMP) [5]. It is also regarded as a candidate technique for future wireless networks. In multicell coordination, neighbouring BSs exchange channel state information of users upon which they can coordinate their transmission so as to avoid or exploit inter-cell interference. Multicell coordination is most useful for cell-edge users who suffer from both weak signal quality and strong interference from neighbouring cells [6]. Multicell coordination on space domain has attracted great attention last years. One of such main techniques is the interference alignment (IA), which is shown to be capacity optimal for high signal-to-noise (SNR) regime [7]. In IA, the desired signals can be retrieved by using signal processing techniques working on space domain.

Implementation of multicell coordination is challenging in practice due to complexity, overhead signalling cost, and other limitations. Moreover, multicell coordination may not always bring an advantage, as determining whether it is advantageous or not depends on the distribution of BSs and users that are usually randomly located. For example, users at the cell-centre typically enjoy good channel condition and the interference is weak, hence, coordination may be unnecessary. In contrast, users at the cell-edge typically suffer from bad channel condition and strong interference, hence, cancelling interference can be helpful for them. Thus, more adaptive strategies are required to make use of multicell coordination.

In general, previous wireless networks have been evaluated in terms of spectral efficiency. Since future wireless networks are expected to provide services with high QoS requirements, it is of paramount importance to create a new paradigm shift to QoS-oriented design and evaluation of wireless networks [3]. Moreover, energy consumption has also nowadays been considered as a major issue to be considered both economically and environmentally [4]. Since increasing spectral efficiency results in more energy consumption, there is always a fundamental trade-off between spectral efficiency and energy consumption. This motivates the research to consider this trade-off as the set point for future wireless networks.

In this thesis, coordination in multicell setting is analysed, and different approaches of implementing coordination over space and frequency domains are investigated. The aim is to propose adaptive strategies for implementing coordination using MIMO. Moreover, algorithms for multicell resource allocation and scheduling schemes are developed and analysed. Throughout this thesis, different performance metrics are considered such as spectral efficiency, energy efficiency, and QoS. The main work in this thesis can be classified into two main different approaches; statistical analysis and optimisation approaches. In the first, statistical methodology is conducted to analyse and evaluate the proposed schemes assuming random system layout. In the later, resource allocation and scheduling schemes are developed aiming at maximising system performance in OFDMA-based multicell coordination and MIMO-based multicell coordination, respectively.

1.3 Contributions

The key contributions of the thesis are summarised as follows:

- **Analysing the coverage probability and effective capacity for downlink MIMO cellular networks with power control and coordination**

  The coverage probability is analysed for downlink random MIMO cellular networks. The BSs are modelled as randomly located in the network area. Two scenarios are investigated and analysed. In the first scenario, the system is assumed to employ distance-based fractional power control to compensate for path-loss, and no coordination is implemented among cells. Two cases are investigated for the this scenario; single user MIMO and multiuser MIMO. In the second scenario, the system is assumed to employ coordinated beamforming to cancel the inter-cell interference. For both scenarios, analytical tractable expressions are derived for coverage probability. Based on coverage probability analysis, the analysis is also extended to the effective capacity to investigate the impact of power control on delay QoS requirement.

- **Proposing adaptive coordination inter-cell interference cancellation for downlink cellular networks**

  Adaptive coordination with inter-cell interference cancellation schemes are proposed for multi-carrier downlink cellular network. The coverage probability and average rate are analysed for both cell-edge and cell-centre users in both schemes. The proposed schemes adaptively employ coordination over both space and frequency domains to serve cell-edge and cell-centre users with different beamforming strategies, where the beamforming strategies are selected based on channel condition. The BSs are assumed to be randomly distributed in the network area. Using tools from stochastic geometry, analytical expressions are derived for coverage probability for the proposed schemes in terms of the main system parameters such as BSs density and antenna number. In addition, analytical expression for average rate is derived based on coverage probability.

- **Designing multicell coordination algorithm for joint user selection and user scheduling in cellular networks**

  The problem of user scheduling is studied in coordinated MIMO multicell network. The objective is to schedule the best set of users such that the system sum rate is maximised. In addition to user scheduling, adaptive spatial modes algorithm is introduced so as to allocate varying number of spatial modes to users as well as to leverage full potential of spatial diversity. Then, two low complexity algorithms are proposed for multicell scheduling. The algorithms consist of two stages; scheduling and precoding stages. In scheduling stage, users are selected by each cell in sequential distributed manner using limited information exchange. In precoding stage, the precoding matrices are designed by each cell separately from all other cells. Then, the algorithm is extended to proportional fairness scheduling to account for heterogeneity of users. The performance and complexity of algorithms are studied and analysed.

- **Designing energy efficient multicell resource allocation schemes for downlink OFDMA cellular networks**

The problem of resource allocation and bit loading is studied in multicell OFDMA network. The objective is to minimise energy consumption per transmitted bit for a given spectral efficiency. We propose two stage adaptive resource allocation scheme based on coordination among the cells. In the first stage (centralised stage), the cell-edge users in the neighbouring cells are allocated orthogonal subchannel resources with the objective of minimising energy consumption. While, in the second stage (distributed stage), cell-centre users are allocated the remaining resources with the objective of minimising power to reduce interference on the the other cells. The first stage is implemented via a central unit, while the second stage is implemented by each cell independently. The energy efficient optimisation problem is formulated as an integer linear fractional programming for which the fractional problem can be iteratively solved by a parametric approach. The second stage problem is formulated as an integer linear programming. Using the proposed adaptive scheme of coordination and resource allocation, the trade-off between spectral efficiency is analysed under the constraint of guaranteeing minimum throughput per each user and total transmit power.

1.4 Thesis Organisation

The remainder of this thesis is organised as follows:

Chapter 2 provides an essential introductory background for the research work of this thesis. It begins by giving an overview of the importance of wireless communication and how the cellular networks have evolved over the last years in response to urgent demands for high data rate technology. Next, it discusses the fundamental issues and concepts of wireless channel, performance metrics of wireless systems, and cellular networks. It then addresses MIMO techniques and issues, single-user MIMO, multiuser MIMO, precoding techniques, and challenges of multiuser MIMO. This section is followed by providing an overview of multicell MIMO and its two

variants; cooperative MIMO and coordinated MIMO, and discussing some of their issues and challenges. Finally, an overview of OFDMA system, resource allocation and scheduling, and inter-cell interference coordination techniques is presented.

Chapter 3 analyses coverage probability and effective capacity for downlink random cellular network. It begins by introducing the concept of effective capacity and its relation to Shannon capacity, followed by presenting the system model and the mathematical framework of effective capacity. Next, the analysis of coverage probability of single user MIMO and multiuser MIMO with fractional power control is presented. This is followed by an analysis of coverage probability of the system employing coordinated beamforming. Finally, An analysis of effective capacity is presented.

Chapter 4 analyses the performance of adaptive coordination and interference cancellation in downlink random MIMO cellular networks. It begins with an essential background and literature review on interference management and multicell MIMO techniques. Then, the system model of random cellular system is presented, followed by explaining the two proposed adaptive schemes for coordination and interference cancellation on both space and frequency domain. It then provides the mathematical analysis of the two proposed schemes, whereby analytical expressions for coverage probability are derived for both schemes. Following this, analytical expression for average rate is derived.

Chapter 5 studies the user scheduling in coordinated MIMO multicell networks. It begins with reviewing the literature related to user selection algorithms, coordinated MIMO, and multimode selection. Next, the system model is presented and the problem of multicell scheduling is defined. Following that, an algorithm for user selection in single cell scenario is introduced and explained, and then extended to multimode selection. Then, the proposed algorithms for multicell scheduling are introduced and analysed. It then presents an extension of the algorithm to proportional fairness scheduling scheme. Following that, complexity analysis of the algorithms are provided.

Chapter 6 studies the energy efficiency in multicell downlink OFDMA cellular net-

works. It begins with reviewing the literature related to this issue. Next, the system model is presented whereby the network setting and system parameters are introduced. Following that, the proposed coordination schemes is explained, and the algorithm of the two stages of resource allocation is presented. Then, the resource allocation problem of both stages are formulated as optimisation problems, whereby the objective of the first stage is to minimise energy consumption for a given spectral efficiency and minimum user rate, and the objective of second stage is to minimise power under the same constraints of the first stage.

Lastly, Chapter 7 concludes the thesis and suggests future research directions.

Chapter 2

Background

2.1 Future Wireless Networks

2.1.1 Importance of Telecommunication Technology

The world of telecommunications has witnessed dramatic changes during the last years due to technological and cultural revolution. The advancement of electronic technology has also led to great developments in many areas, particularly in digital communication. Thus, digital communication is fast becoming indispensable to governmental bodies, business and education institutions, industries, daily people's life. This creates a cultural climate dramatically changing daily people's life in various aspects. Nowadays applications such as web services, E-mails, video streaming are becoming highly important for daily people's life, hence creating new demands in terms of internet and communications services, which are more facilitated by the growth of global network of computers and internet servers. In addition, the advancement of smart phones and other handheld devices results in a significant growth in the data traffic recently. As a response to these demands, the technology of telecommunication has been pushed forward to fulfil these needs; also it introduces a new great opportunity of profits from an economic point of view. The significance of

telecommunication revolution both culturally and economically is so important that governments have established organisational bodies aiming solely for promotion of telecommunication technology, to ensure that even disadvantaged countries will be able to have an opportunity to access cutting-edge communication technologies, and to entirely engage with the information technology pace.

2.1.2 Wireless Communication Systems

Internet services such as web browsing, email, video streaming, have become urgent needs for the people's daily life, not only on the traditional wired networks, but also on the wireless networks, particularly cellular systems [1]. Wireless communication uses electromagnetic spectrum to carry the modulated information data to the receiver. First generations of cellular systems are mainly designed for only voice and text services. With the advancement of smart phone technology, the devices are nowadays equipped with sophisticated capabilities, thus, new demands for multimedia and high data rate applications are generated [2]. While high data rates services can be reliably provided on wired networks, providing such services on the wireless networks, however, is not a trivial matter to accomplish due to the limited resources and the unpredictable nature of wireless channel. Besides, the number of subscribers all around the world is still increasing, making provisioning of high data rate services over cellular systems very challenging problem for both manufacturers and operators. Consequently, the main issue becomes the problem of how to provide high data rate services over limited wireless resources such that the quality of service (QoS) is satisfied. Thus, wireless communication requires very different approaches than that of wired networks.

2.1.3 Evolution of Cellular Networks

The first generations of wireless mobile networks were voice-oriented systems, providing low data rate services such as voice. With the dramatic evolution of wireless

mobile systems over the last decades, wireless systems have become more multimedia-oriented mobile networks, and hence raising the expectations for higher data rates. The first generation (1G) was based on analogue technology, deployed in USA and Europe in in the early of 1980's, followed by the digital technology-based second generation system (2G) deployed in 1991 in Europe. In 2001, third generation (3G) system based on code-division multiple access (CDMA) technology was first operated. The dramatic enhancement for the mobile systems occurred in high-speed downlink packet access (HSDPA) supporting a speed of up to 21 Mbps. Then, it is evolved to HSPA+ with speed reaching up to 42 Mbps. Later on, long-term evolution (LTE) is introduced by third generation partnership (3GPP) to provide high data rate up to 160 Mbps within 20 MHz channel bandwidth. LTE is based on orthogonal frequency division multiple access (OFDMA) technique for resources sharing among users, and incorporates advanced technologies such as MIMO, adaptive modulation, and link adaptation [8]. In 2008, the technical requirements of fourth generation (4G) has been identified in international mobile telecommunications-Advanced (IMT-A) [9]. In this direction, 3GPP targeted the candidate cellular technologies that are meeting IMT-A requirements, and proposed LTE-advanced (LTE-A) [10]. The key technologies that make LTE-A superior over LTE and 3G systems are carrier aggregation, OFDMA, CoMP technique for interference management, and deploying heterogeneous networks to improve spectral efficiency and provide uniform coverage [10]. Nowadays, researchers all over the world have been targeting 5G cellular , which is expected to be a groundbreaking technology, overcoming the limitations faced by previous cellular generation. 5G is envisioned to include massive bandwidth with high frequencies, dense BSs deployment, massive number of antennas, heterogeneous network deployment, cognitive radio, highly adaptive multicell coordination strategies, and energy efficient technology, not to mention others [3].

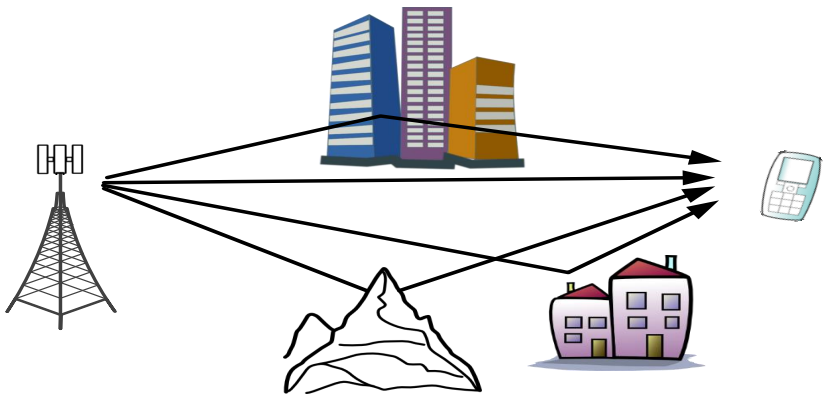

Figure 2.1: An illustartion of multipath phenomenon where different signal replicas arrive at the reciver side.

2.2 Wireless Communication Channel

Wireless channel is the air medium over which wireless transmission is performed via electromagnetic waves. Since the wave is not restricted to take single path, it suffers reflection, diffraction, scattering by buildings, hills, bodies, and other objects when travelling from transmitter to receiver, hence multiple copies of the signal arrive at the receiver as shown in Fig. 2.1. Each copy of the signal has different delay, phase, and gain, and thus they interfere constructively or destructively. This is referred to as multipath phenomenon. To fully characterise the random time varying properties of multipath channel, statistical models have been developed [11]. In general, wireless channel is affected by three factors: path-loss, shadowing, and small-scale fading [11] as illustrated in Fig. 2.2.

Path-loss refers to the signal power dissipation in proportion to the distance between transmitter and receiver. In free space, path-loss is given by

$$L = \frac{\varepsilon G_t G_r}{(4\pi d)^2} \tag{2.1}$$

where ε is the wavelength, G_t is the transmitter antenna gain, G_r is the receive

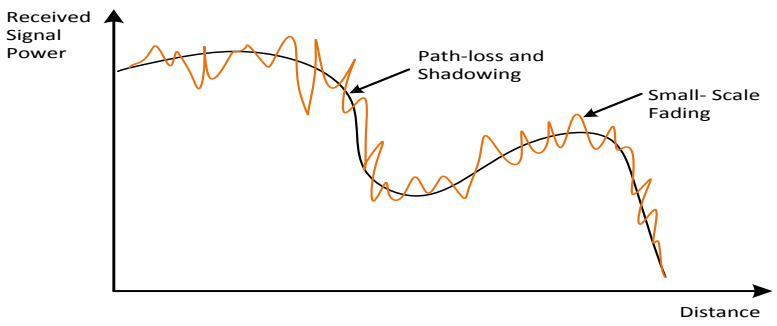

Figure 2.2: The composite effect of path-loss, shadowing, and small-scale fading in wirelss channel.

antenna gain, d is the distance between the transmitter and receiver. This model is only valid provided that there is only one single path between two points, i.e. line-of-sight (LoS), or few multipath components. In cellular communication, the signal propagates through different paths between transmitter and receiver, for which the path-loss is commonly modelled as [11]

$$L = \varsigma d^{-\alpha} \tag{2.2}$$

where ς represents a constant that captures the antenna characteristics and channel attenuation, and α is the path-loss exponent that varies from 2 to 6 depending on the communication environment [11].

Shadowing is a random variation experienced by signal power due to obstacles between transmitter and receiver that attenuate the signal through scattering, reflection, and diffraction [11], [12]. Statistical methods are usually used to model shadowing where log-normal shadowing model is the most accurately validated model [11]. The

probability density function (PDF) of a log-normal random variable y is given as

$$f(y) = \frac{1}{y\sigma\sqrt{2\pi}} e^{-\frac{(\ln y - \mu)^2}{2\sigma^2}}, y > 0. \tag{2.3}$$

where μ and σ represent the mean and the standard deviation of y given in dB.

Small-scale fading refers to the microscopic channel variations due to constructive and destructive addition of multipath signal replicas. Since each signal replica experiences different attenuation, delay, and phase, the superposition of all components results in a destructive and constructive addition, thus attenuating and amplifying the received signal, respectively [11], [12]. When the drop of the signal is severe, it is referred to as deep fade, and usually results in temporary outage in communication.

Fading variations and its impact on frequency domain can be characterised by the notion of coherence bandwidth W_c. This parameter measures the range of frequencies over which the channel is highly correlated, in other word the channel does not change over the entire signal bandwidth (or flat). Coherence bandwidth is connected to the delay spread arising from multipath phenomenon as $W_c \approx \frac{1}{T_d}$, where T_d is defined as the difference between delays spread associated with the most significant multipath component and the latest component. If the signal bandwidth w is smaller than the coherence bandwidth, the channel exhibits a constant gain transfer function over the entire signal bandwidth. However, when the coherence bandwidth is larger than the signal bandwidth, the channel response exhibits frequency-selective behaviour, in other words, different parts of signal bandwidth experience uncorrelated fading, giving rise to signal distortion or what is so-called inter-symbol interference (ISI). To overcome this problem, sophisticated equalisation needs to be utilised at the detection side, which is costly in implementation. The other widely adopted solution in recent advanced wireless technologies is to use low rate multicarrier transmission such as orthogonal frequency division multiplexing (OFDM), whereby each subcarrier has smaller bandwidth to ensure that the channel is flat over each subcarrier bandwidth [11], [12].

On the other hand, fading variations in time domain are characterised through the notion of coherence time T_c, which refers to the time duration at which the channel remains correlated. Coherence time is related to the Doppler spread parameter f_d as $T_c \approx \frac{1}{f_d}$, which is the broadening in the signal bandwidth caused by relative mobility of the transmitter and receiver. Channel with larger Doppler spread changes faster, thereby having shorter coherence time [11]. The rate at which the variation in the signal takes place determines how fast the fading is; fast fading occurs with multipath phenomenon as it takes place over very small time scale (on the order of milliseconds), while slow fading occurs with path-loss and shadowing as it happens over relatively larger time scale on the order of tens of seconds.

To model small-scale fading, several statistical models have been proposed and utilised. The two most common models are Rayleigh and Rician models. Here, we will briefly describe the two models.

2.2.1 Rayleigh Channel Fading

This is based on the assumption that there is no line-of-site component between transmitter and receiver, and there is a large number of independent signal paths. According to Central Limit Theorem (CLT), when there is a large number of random variables, the limiting distribution will approximate Gaussian distribution [11]. Thus, the fading channel can be modelled as a zero-mean complex-valued Gaussian random variable $x \sim \mathcal{CN}(0, \sigma^2)$ with channel envelope $y = \mid x \mid$ and PDF given by

$$p(y) = \frac{y}{\sigma^2} e^{-\frac{y^2}{2\sigma^2}}, y > 0 \tag{2.4}$$

where σ^2 is the average received power.

2.2.2 Rician Channel Fading

When there is a line-of-site component between transmitter and receiver, the signal will be composed of large number of independent paths plus line-of-site components. The signal envelope is modelled by Rician distribution given by

$$p(y) = \frac{2y(K+1)}{\sigma^2} e^{-K-\frac{(K+1)y^2}{\sigma^2}} I_0(2y\sqrt{\frac{K(K+1)}{\sigma^2}}) \tag{2.5}$$

where K denotes the ratio of the power of the line-of-site component to the power of other multipath components, and I_0 is the modified Bessel function of the zero-th order given by

$$I_0(y) = \sum_{k=0}^{\infty} \frac{(\frac{1}{4}y^2)^k}{(k!)^2} \tag{2.6}$$

2.3 Performance of Wireless Networks

The performance of wireless networks is typically measured by several major parameters such as capacity (equivalently spectral efficiency), quality of service (QoS) guarantee, fairness. In the early cellular systems, since the main services were voice and text messaging, which require low data rate, much emphasis has been put on coverage and capacity. However, with the advancement of smart phone technology, the demand for high data rate multimedia applications shifts the interest towards both capacity (spectral efficiency) and QoS guarantee. Recently, energy efficiency has also attracted an important interest in both industry and academia due to the impact of energy consumption on environment and other economic reasons. In the subsequent discussion, we will briefly describe three key performance metrics, namely capacity, effective capacity, and energy efficiency.

2.3.1 Shannon Capacity

In his pioneering work on the information theory [13], Shannon introduced the notion of channel capacity, which means the achievable data rate that can be transmitted over the channel with arbitrarily small error probability. Capacity has become an important metric for analysing performance of wireless networks, it possessed even high importance for future mobile networks that are expected to provide high data rate applications. In an additive white Gaussian noise (AWGN) channel, Shannon capacity is defined as

$$C = W\log_2(1 + \frac{P}{N_0 W}), [\text{bits/sec}] \tag{2.7}$$

where W is signal bandwidth in Hz, N_0 is the noise spectral density in Watt/Hz, and P is the transmit power. The term $\frac{P}{N_0 W}$ is commonly referred to as signal-to-noise ratio (SNR). Shannon capacity gives an upper bound limit on the achievable rate, it could be achieved by advanced signal processing and coding techniques. It can be observed from the above formula that the two factors fundamentally limiting the capacity are power and bandwidth, which represent the main wireless resources. Two extreme regimes can be deduced from Shannon formula; when SNR gets very large, the capacity becomes logarithmic in power and linear in bandwidth, i.e. $C = W\log_2(\frac{P}{N_0 W})$, this is referred to as bandwidth-limited regime. On the other hand, when SNR gets very small, capacity becomes insensitive to bandwidth, i.e. $C = \frac{P}{N_0}\log_2 e$, where e is the base of the natural logarithm. In the first regime, it is more advantageous to increase bandwidth for capacity increase, whereas in the second regime, increasing power is the best strategy.

2.3.2 Effective Capacity

Effective capacity is an important concept for evaluating wireless systems with QoS provisioning. QoS provisioning includes all mechanisms that are responsible for guaranteeing QoS when providing multimedia and internet services. QoS is defined as

the capability of the network to provide satisfactory service to the users. The satisfaction of service depends on factors such as throughput, delay, jitter, packet error rate, and reliability. QoS provisioning has been extensively studied in wired networks under the concept of effective bandwidth [14], [15]. Now QoS provisioning is rapidly becoming an essential feature in advanced cellular systems. Inspired by the concept of effective bandwidth, which statistically models a source traffic in wired networks with constant service rate, Wu and Negi have proposed a new concept termed as effective capacity using large deviation theory [15], [16]. Effective capacity is the dual of effective bandwidth, and it models service rate in wireless channel with constant arrival rate [16]. They define the effective capacity as the achievable constant arrival rate that a given service rate process can support in order to guarantee a statistical QoS requirement specified by QoS exponent θ. Let $S(t) \triangleq \sum_{\tau=1}^{t} R(\tau)$ represent the aggregate service rate over the time period $[0, t)$, where $R(\tau)$ is the service rate at time τ, the effective capacity E_c is defined as

$$E_c(\theta) = -\lim_{t\to\infty} \frac{1}{\theta t} \log\mathbb{E}\{e^{-\theta S(t)}\} \tag{2.8}$$

when $\{R(t)\}$ stationary and ergodic process, E_c can be reduced to:

$$E_c(\theta) = -\frac{1}{\theta} \log\mathbb{E}\{e^{-\theta R(t)}\} \tag{2.9}$$

where θ represents QoS constraint, and can be incorporated into scheduling process. More specifically, when $\theta \to 0$, this indicates loose QoS constraints, and the effective capacity approaches Shannon capacity, whereas when $\theta \to \infty$, it implies stringent QoS requirement (delay is not tolerated). Hence, instead of the conventional cross-layer design approaches in which Shannon capacity is maximised subject to delay constraints, here the effective capacity is maximised for a given θ [14].

2.3.3 Energy Efficiency

Energy efficiency has attracted great attention nowadays, since increasing spectral efficiency results in more energy consumption. The energy consumption increase in wireless communication systems results in an increase of CO_2 emission, which represents big threat to the environment [17], and there is a consensus on the necessity of protecting the environment from the dangers of modern technology. Moreover, the radio access part of cellular systems consumes about 70% of the electricity power bills as reported by mobile systems operators, which means high operational cost from economical point of view [18]. Additionally for uplink radio access it is very reasonable to reduce energy consumption for mobile devices in order to save the battery power [18], [19]. For theses reasons, reducing energy consumption motivates research circles to investigate new energy efficient techniques in wireless networks technology.

There is an inherent conflict in enhancing spectral efficiency and decreasing energy consumption at the same time; reducing energy consumption leads to decrease in spectral efficiency and vice versa [18], [19]. Consequently, there always exists a trade off between spectral and energy efficiencies. Thus, the spectral-energy efficiency trade-off can be set off as a mile stone for the research to investigate the problem of how much energy consumption for a given spectral efficiency, or how much spectral efficiency can be obtained for a given energy consumption [18].

Two different definitions are used to define the energy efficiency [20]. The first definition is to take the ratio of transmission bits rate (or spectral efficiency) to the transmitted power, measured in bit/Joule [21], [22]. This definition has been widely used in literature. The other definition of energy efficiency (Joule/bit) is to take the ratio of consumed power over bit rate or spectral efficiency [20]. In this thesis, the second definition of energy efficiency will be used as it implies the energy consumption.

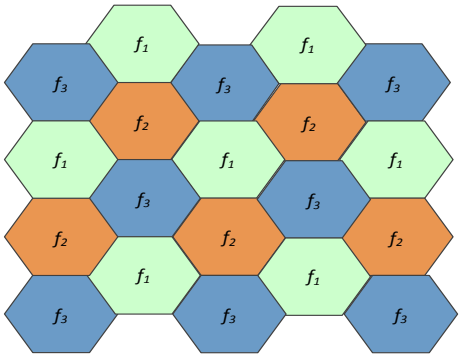

Figure 2.3: An example of hexagonal cellular system with frequency reuse factor 3.

2.4 Cellular Network Models

The main concept of cellular systems is to divide the coverage area into non-overlapping smaller areas referred to as cells while reusing the available spectrum bands at different cells. The frequency reuse factor (FRF) determines the frequency pattern scheme, for example, FRF = N corresponds to the case of utilising a subband at every N cell, as shown in Fig. 2.3. When FRF = 1, we have the conventional full spectrum reuse, where the spectrum is reutilised at each cell.

In cellular systems, the major problem arising from frequency reuse is the inter-cell interference (ICI) caused by neighbouring cells [23], [24]. It degrades the system performance, especially for the cell-edge users. Let the instantaneous signal-to-interference and noise (SINR) given by:

$$\text{SINR} = \frac{P_s}{P_n + P_I} \tag{2.10}$$

where P_s, P_n, and P_I denote the desired signal power, noise power, and inter-cell interference (ICI) power, respectively. Instantaneous rate is given by

$$R(t) = \log_2(1 + \text{SINR}), [\text{bits/sec/Hz}] \tag{2.11}$$

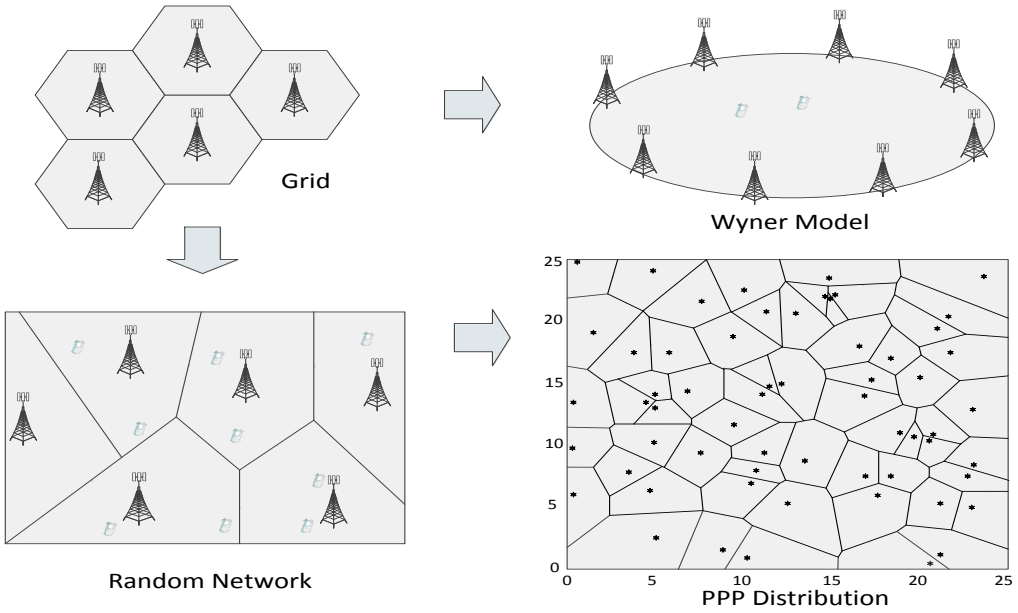

Figure 2.4: An illustration of hexagonal cellular system, circular Wyner model, random cellular system, and PPP model

Note that in (2.10), the interference is treated as a Gaussian noise, i.e. no successive interference cancellation (SIC) technique is used. It can be clearly observed that increasing the power of desired signal does not improve the performance, as it results in an additional interference on the other cell. However, with suitable interference management strategy implemented across cells, P_I can be either cancelled or reduced to small value. Inter-cell interference management strategies require coordination and an exchange of necessary information among neighbouring cells.

Hexagonal and other grid models shown in Fig. 2.4 have been widely used to evaluate and analyse cellular networks. In these models, BSs locations follow deterministic grid, and all cells have the same size and shape. Grid models are quite easy to simulate, and have been thought to closely approximate realistic cellular system layout [25]. Due to analytical complexity inherent in such models, researchers have resorted to more simplified architecture to analyse cellular systems such as widely known Wyner model [25], [26]. In this model, it is assumed that users have deterministic average SINR regardless of where they are located. It has been extensively used in

literature due to its simplicity and analytical tractability. However, it is proven to be inaccurate in most cases [27]. An alternative approach adopted recently is to model BSs as randomly positioned, which may resemble the realistic BSs layout that exhibits random pattern, especially heterogeneous networks [28]. Counter-intuitively, such random model yields analytical tractability, and accurate expressions can be obtained for SINR distributions. Stochastic geometry mathematical tools can be efficiently applied to analyse these models [29]. It is shown that while grid models provide an upper bound optimistic upper bound on system performance, random models gives the lower bound [28].

2.5 Multi-Antenna Cellular Systems

The use of multiple antenna systems creates a new dimension (i.e. space dimension) that can be potentially exploited in addition to frequency and time. The pioneering works of winters [30], Foschini [31]-[32], and Telatar [33] have predicted enormous spectral efficiency for wireless systems using multiple antennas in a rich scattering channel with the channel state being perfectly known at the transmitter. The role of scattering environment is to provide independent channel directions from each transmit antenna to each receive antenna. Thus, by spatially multiplexing different symbol streams and simultaneously transmitting them over N_t transmit antennas, the spectral efficiency linearly scales by a factor of $\min(N_t, N_r)$ where N_r is the number of receive antennas [34]. In the following discussion, capacity analysis is introduced for MIMO channels with different scenarios, namely single user MIMO (SU-MIMO) and multiuser MIMO (MU-MIMO). We start with SU-MIMO as it represents the simple point-to-point MIMO channel.

2.5.1 SU-MIMO Capacity

In SU-MIMO, a transmitter equipped with multiple antennas spatially multiplexes different streams for transmission to multiple antenna receiver. Consider a BS equipped with N_t antennas and receiver with N_r antennas as shown in Fig. 2.5. The received signal is given by

$$\mathbf{y} = \mathbf{H}\mathbf{x} + \mathbf{n} \tag{2.12}$$

where $\mathbf{H} \in \mathbb{C}^{N_r \times N_t}$ is the channel gain matrix between the transmitter and the receiver, $\mathbf{x} \in \mathbb{C}^{N_t \times 1}$ is the transmitted symbol vector, $\mathbf{n} \in \mathbb{C}^{N_r \times 1}$ is the AWGN vector, where $\mathbf{n} \sim \mathcal{GN}(0, \sigma^2 \mathbf{I}_{N_r})$, and $\mathbf{y} \in \mathbb{C}^{N_r \times 1}$ is the received signal vector. The capacity can be obtained by decomposing the channel matrix into a set of parallel, independent scaler sub-channel. Assuming CSI is perfectly known at the transmitter and applying singular value decomposition (SVD) to the channel matrix, $\mathbf{H} = \mathbf{U}\mathbf{\Lambda}\mathbf{V}^{\mathsf{H}}$, where $\mathbf{V} \in \mathbb{C}^{N_t \times N_t}$ and $\mathbf{U} \in \mathbb{C}^{N_r \times N_r}$ are orthogonal matrices, and $\mathbf{\Lambda}$ is a diagonal matrix whose jth entries λ_j represents the jth singular value of $\mathbf{H}$, then $\mathbf{H}\mathbf{H}^{\mathsf{H}} = \mathbf{U}\mathbf{\Lambda}^2\mathbf{U}^{\mathsf{H}}$, and the following are defined [12]

$$\tilde{\mathbf{x}} := \mathbf{V}^{\mathsf{H}}\mathbf{x}, \tag{2.13}$$

$$\tilde{\mathbf{y}} := \mathbf{U}^{\mathsf{H}}\mathbf{y}, \tag{2.14}$$

$$\tilde{\mathbf{n}} := \mathbf{U}^{\mathsf{H}}\mathbf{n}, \tag{2.15}$$

the received signal can be written as

$$\tilde{\mathbf{y}} = \mathbf{\Lambda}\tilde{\mathbf{x}} + \tilde{\mathbf{n}}, \tag{2.16}$$

now the capacity is given by [12]

$$C = \sum_{j=1}^{M_{min}} \log_2 \left(1 + \frac{p_j \lambda_j^2}{\sigma^2}\right) \text{ bits/s/Hz}, \tag{2.17}$$

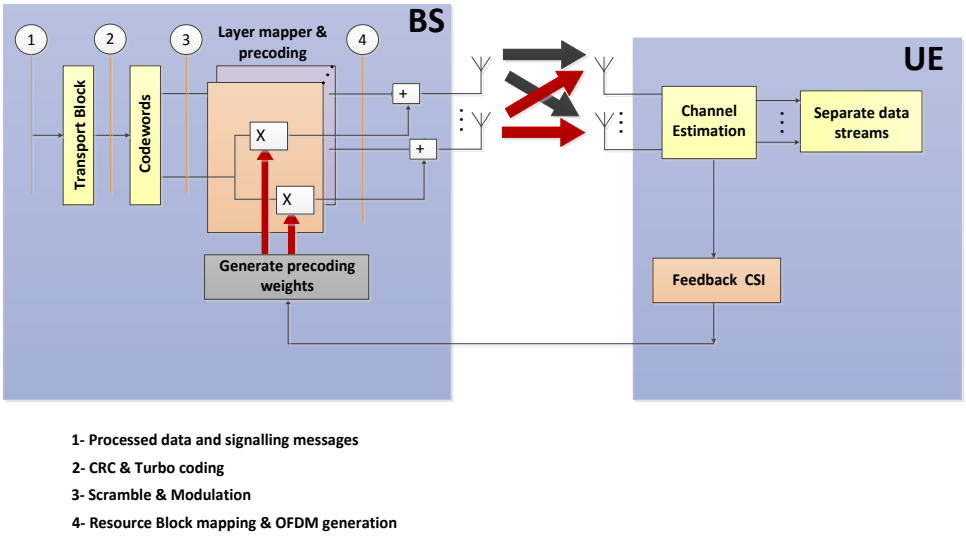

Figure 2.5: SU-MIMO transmitter and reciver structure where the BS with N_t antennas spatially multiplexes M_{min} spatial streams to a reciever with N_r antennas, where $M_{min} = \min(N_t, N_r)$.

where $M_{min} = \min\{N_t, N_r\}$, and the optimal power allocation is given by waterfilling over the eigenvalues of the diagonal matrix $\mathbf{\Lambda}^2$ as [12]

$$p_j = \left(\mu - \frac{\sigma^2}{\lambda_j^2}\right)^+, 1 \leq j \leq M_{min} \tag{2.18}$$

where $(x)^+$ denotes $\max(x, 0)$, and μ is the so-called waterfilling-level chosen such that $\sum_{j=1}^{M_{min}} p_i = P$. Waterfilling is always optimal, however, for high SNR regime constant power allocation performs as good as waterfilling [34], [35].

2.5.2 MU-MIMO Capacity

If the BS can be equipped with a large number of antenna, the multiplexing gain associated with single user MIMO will be limited by the number of receive antenna at the user side. Hence, to overcome this limitation, MIMO can be extended to

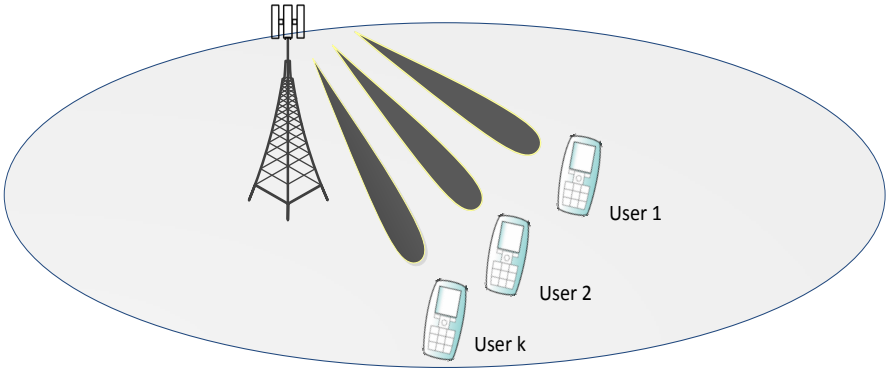

Figure 2.6: Illustration of MU-MIMO transmission where a BS serves multiple users simulteneously.

multiuser level, where, instead of transmitting multiple streams to a single user, the BS simultaneously serves multiple users over the same frequency band as shown in Fig. 2.6. In this technique, inter-user interference (also known as intra-cell interference) results as a consequence of simultaneous transmission. Since, in MU-MIMO, there is assumed no coordination among users due to power and complexity limitations, inter-user interference cancellation responsibility is transferred to the BS [36]. This requires perfect CSI acquisition at the BS, which is, however, a challenging issue. Note that CSI acquisition is necessary for MU-MIMO in the downlink scenario. In SU-MIMO, it may not necessary to have perfect knowledge of CSI, though [35].

Consider a BS equipped with N_t antennas serves K users, each equipped with N_r receive antennas, such that $N_t \geq KN_r$. The received signal at user k is given by

$$\mathbf{y}_k = \mathbf{H}_k\mathbf{x} + \mathbf{n}_k \tag{2.19}$$

where $\mathbf{H}_k \in \mathbb{C}^{N_r \times N_t}$ is the channel gain matrix between the BS and kth user, $\mathbf{x} = \sum_{k=1}^{K} \mathbf{x} \in \mathbb{C}^{N_t \times 1}$ is the superposition of all users transmitted symbol vectors, $\mathbf{n}_k \in \mathbb{C}^{N_r \times 1}$ is the AWGN vector, and $\mathbf{y}_k \in \mathbb{C}^{N_r \times 1}$ is the received signal vector at user k. We impose the power constraint as $\mathbb{E}\{\mathrm{tr}\{\mathbf{x}\mathbf{x}^{\mathsf{H}}\}\} \leq P$, and both channel and noise are

normalised to 1. For MU-MIMO, or so-called MIMO broadcast (MIMO BC) [34]-[35], the capacity is characterised by the notion of capacity region [34], which is the set of all achievable rates with arbitrarily small error probability, and is given by

$$R(\mathbf{Q}_1, ..., \mathbf{Q}_K) = [R_1, ..., R_K] \tag{2.20}$$

where R_k is the rate of kth user. The channel capacity of SU-MIMO is a single real number, while, for MU-MIMO the capacity is characterised by a convex region of K-dimensional space, where K is the number of users, and each vector in the K-dimensional convex hall represents the achievable rates by all users [34]-[35]. The optimal strategy transmission for MU-MIMO that achieves Shannon capacity limit is dirty paper coding (DPC) proposed by Costa [37]. Based on this technique, the inter user interference is pre-subtracted at the BS before transmission [34]-[37]. Thus it mimics SIC at the receiver side. It is proven in [37] that for single antenna systems if the transmitter knows non-causally the interference, it can subtract it in advance and thereby the capacity will be the same as if there were no additive interference [38]-[40].

2.5.3 Linear Precoding Techniques

For MIMO to accomplish its task, precoding technique must be used. Precoding techniques are used to cancel interference among sub streams, i.e. inter-user interference. Despite the optimality of DCP, it is very hard to be implemented practically due to high complexity incurred by successive encodings and decodings [34]. Therefore, sub-optimal, low complexity techniques have been proposed instead.

Let $\mathbf{x}_k \in \mathbb{C}^{N_t \times 1}$ denote the transmitted symbol vector for user k. By encoding this symbol vector by precoding matrix $\mathbf{T}_k \in \mathbb{C}^{N_t \times N_r}$ and combining the resultant vector with all other users encoded symbol vectors for transmission, the transmitted signal

is written as

$$\mathbf{x} = \sum_{k=1}^{K} \mathbf{T}_k \mathbf{x}_k \tag{2.21}$$

After transmission, the received signal at user k is given by

$$\mathbf{y}_k = \underbrace{\mathbf{H}_k \mathbf{T}_k \mathbf{x}_k}_{\text{desired signal}} + \underbrace{\sum_{i=1, i\neq k}^{K} \mathbf{H}_k \mathbf{T}_i \mathbf{x}_i}_{\text{inter-user interference}} + \mathbf{n}_k \tag{2.22}$$

The second term in (2.22) represents the inter-user interference caused by simultaneous transmission of users symbol vectors. To fully eliminate inter-user interference, the precoding matrix $\mathbf{T}_k$ of a user k is designed such that it lies in the null space of other users channels, $i = 1, ...K, i \neq k$, in other words, the precoding matrix of user k should be orthogonal to other users channels such that:

$$\mathbf{H}_i \mathbf{T}_k = 0, \qquad \forall k \neq i \tag{2.23}$$

Thereby, the interference is eliminated at each user. The null space dimension space should be non-empty, which is only possible if the number of non intended users is less than N_t. In this thesis, the following linear precoding techniques are briefly discussed, namely zero-forcing (ZF), signal-to-leakage-and-noise ratio maximising (SLNR-MAX) beamforming, and block diagonalization (BD). Maximum ratio transmission (MRT) precoding technique will be also presented, despite the fact that it is not to be used for cancelling interference from non intended users.

1- ***ZF beamforming***: ZF beamforming is a signal processing technique implemented by a BS to cancel out inter-user interference. Assuming single antenna users, the BS multiplies the data symbol of each user by its so-called beamforming precoding vector [41], then combines the resultant vectors of the other users for transmission through multiple antennas.

   Let $\mathbf{h}_k \in \mathbb{C}^{N_t \times 1}$ is the channel vector between a BS and single antenna user k,

and $\mathbf{H} = [\mathbf{h}_1^{\mathsf{H}}, ..., \mathbf{h}_K^{\mathsf{H}}]^{\mathsf{H}}$ is the concatenated channel matrix of K users, the ZF precoding vectors are the column vectors of the Moore-Penrose pseudo inverse of $\mathbf{H}$ given as [41]

$$\mathbf{W} = \mathbf{H}^{\dagger} = \mathbf{H}^{\mathsf{H}}(\mathbf{H}\mathbf{H}^{\mathsf{H}})^{-1} \tag{2.24}$$

ZF technique, while being suboptimal and practical, is proven to be optimal and asymptotically approach the performance of dirty paper coding in the high SNR regime when the number of users gets very large [41]. This is due to multiuser diversity, which can be increased with the increase of users number, thereby providing plentiful channel directions with better quality. As a result, a BS will have an opportunity to schedule a set of users with best channel conditions and perfect spatial separation [41].

2- ***MRT beamforming***: MRT beamforming is a precoding vector that maximise the desired channel gain. It is designed by choosing the vector that spans the channel direction [42], [43]. For a single antenna user $\mathbf{h}_k$, MRT precoder $\mathbf{w}_k$ is given as

$$\mathbf{w}_k = \frac{\mathbf{h}_k}{\| \mathbf{h}_k \|} \tag{2.25}$$

Hence, the inner product between two vectors is maximised. MRT beamforming is used to benefit from the spatial diversity offered by multiple antennas. MRT is optimal in low SNR regime, while ZF performs better in high SNR regime. This is because when SNR is low, it is more beneficial to improve the quality of desired signal power than to cancel the interference, while, in high SNR case, a user can afford losing some of its signal quality for the sake of cancelling interference via by ZF.

3- ***SLNR-MAX beamforming***: SLNR-MAX is defined as the signal to leakage interference caused by user k on the signal received by other users in the system,

thus SLNR for user k is written as [44]

$$\text{SLNR}_k = \frac{\parallel \mathbf{h}_k \mathbf{w}_k \parallel}{\sigma_k^2 + \sum_{i=1, i\neq k}^{K} \parallel \mathbf{h}_i \mathbf{w}_k \parallel} \tag{2.26}$$

where $\sum_{i=1,i\neq k}^{K} \parallel \mathbf{h}_i \mathbf{w}_k \parallel$ represents the leakage interference caused by user k on other users. Hence, the beamforming of user k $\mathbf{w}_k$ can be obtained by maximising the SLNR value. SLNR-MAX beamforming balances between the desired signal and the interference [44]. As such, its operation region lies between the two extremes of ZF and MRT.

4- ***BD precoding***: when each user is equipped with multiple antennas, and is able to receive and decode multiple streams, then using ZF is suboptimal because it treats each antenna as one user, and thereby reducing the quality of desired signal. Let us re-write the concatenated users channels matrices as $\mathbf{H} = [\mathbf{H}_1^{\mathsf{H}}, ..., \mathbf{H}_K^{\mathsf{H}}]^{\mathsf{H}}$, where $\mathbf{H}_1 \in \mathbb{C}^{N_r \times N_t}$ is the channel matrix of kth user. Let the concatenated precoding matrices defined as $\mathbf{T} = [\mathbf{T}_1^{\mathsf{H}}, ..., \mathbf{T}_K^{\mathsf{H}}]^{\mathsf{H}}$. The optimal precoding matrices should be chosen such that $\mathbf{H}_k \mathbf{T}_i = \mathbf{0}, \forall k \neq i$, i.e. $\mathbf{HT}$ is block diagonal. To satisfy this condition, $\mathbf{T}_k$ should be chosen such that it lies in the null space of other users channel matrices $\mathbf{H}_i, \forall i = 1, ..., K, i \neq k$. Define $\widehat{\mathbf{H}}_k \in \mathbb{C}^{(K-1)N_r \times N_t}$ as [45]

$$\widehat{\mathbf{H}}_k = [\mathbf{H}_1^{\mathsf{H}} ... \mathbf{H}_{k-1}^{\mathsf{H}} \mathbf{H}_{k+1}^{\mathsf{H}} ... \mathbf{H}_K^{\mathsf{H}}] \tag{2.27}$$

By applying SVD to $\widehat{\mathbf{H}}_k$ as

$$\widehat{\mathbf{H}}_k = \widehat{\mathbf{U}}_k \widehat{\mathbf{\Lambda}}_k [\widehat{\mathbf{V}}_k^{(1)} \widehat{\mathbf{V}}_k^{(0)}]^{\mathsf{H}}, \tag{2.28}$$

Here, $\widehat{\mathbf{V}}_k^{(1)}$ holds the $\hat{R} = \mathsf{Rank}(\widehat{\mathbf{H}}_k)$ right singular vectors corresponding to the non-zero singular values, while $\widehat{\mathbf{V}}_k^{(0)}$ consists of the remaining $N_t - \hat{R}$ right singular vectors corresponding to the zero singular values, which forms the orthonormal basis for the null space of $\widehat{\mathbf{H}}_k$. By projecting user k channel to the orthonormal basis of $\widehat{\mathbf{H}}_k$ null space [45], $\mathbf{H}_k \widehat{\mathbf{V}}_k^{(0)}$, the inter-user interfer-

ence is perfectly eliminated. Denote the effective channel as $\widetilde{\mathbf{H}}_k = \mathbf{H}_k \widehat{\mathbf{V}}_k^{(0)}$ with $\mathsf{Rank}(\widetilde{\mathbf{H}}_k) = \tilde{R}$. The necessary condition for transmission in the null space of $\widehat{\mathbf{H}}_k$ is that $\tilde{R} \geq 1$ [45], [46]. Similar to SU-MIMO, to maximise the achievable capacity the transmission directions should be aligned with the eigenvectors directions of effective channel $\mathbf{H}_k \widehat{\mathbf{V}}_k^{(0)}$ and waterfilling the power across the eigenvalues [45]. Thus, applying SVD to $\mathbf{H}_k \widehat{\mathbf{V}}_k^{(0)}$

$$\widetilde{\mathbf{H}}_k = \widetilde{\mathbf{U}}_k \begin{bmatrix} \widetilde{\mathbf{\Lambda}}_k & \mathbf{0} \\ \mathbf{0} & \mathbf{0} \end{bmatrix} [\widetilde{\mathbf{V}}_k^{(1)} \widetilde{\mathbf{V}}_k^{(0)}]^{\mathsf{H}} \tag{2.29}$$

Finally, the precoding matrix is constructed as $\mathbf{T}_k = \widetilde{\mathbf{V}}_k^{(1)} \widehat{\mathbf{V}}_k^{(0)}$ [45].

2.5.4 Issues and Challenges of MU-MIMO

Although MU-MIMO is promising technique for enhancing spectral efficiency, however it is quite challenging in practical implementation. To achieve full multiplexing gain of MU-MIMO, the system requires an acquisition of instantaneous perfect CSI. The system can acquire the CSI through two different ways depending on the duplexing scheme adopted. In time division duplex (TDD), both transmitter and receiver utilise the same frequency band for transmission and reception, spacing them apart by multiplexing the downlink and uplink signals on different time slots. A user transmits specific pilot symbol training signal and the BS can learn the CSI through channel reciprocity. This necessitate that the time coherence should be long enough to span the interval of both uplink signalling and downlink transmission [47]. On the other hand, in frequency division duplex (FDD), where the downlink and uplink use different frequency bands, the user can feed back the necessary information to the BS through dedicated low rate uplink channel [47]. To overcome this limitation, earlier works proposed random beamforming [48]-[51]. In random beamforming, the BS constructs several orthogonal beams and let the user feedback only the beam index for which it experiences highest SNR value. Hence only one real number is needed for

CSI learning. Although it is advantageous in terms of feedback signalling, however, random beamforming is shown to have worse performance as compared with ZF [36].

The other approach that has recently attracted great attention in both academia and industry is the limited feedback based on vector quantisation technique [52]-[55]. In limited feedback, the transmitter and receiver shares a codebook consisting of set of essential degrees of freedom of the channel, which is tailored to the channel model and receiver design [52]. When estimating the channel, a user finds the best vector in the codebook that has maximum product with estimated channel vector, and feeds back its index to the BS. With this technique, the residual interference caused by inaccuracy in CSI limits the performance of MU-MIMO system, and the problem gets even worse in high SNR regime. Thus, full multiplexing gain may not be achievable unless the feedback bit rate (hence, codebook size) is linearly increased with the SNR [53]. Although the codebook-based limited feedback has been incorporated in the latest standards bodies such as in 3GPP LTE, the problem of designing an optimal codebook is still a rich area of research [52].

2.6 Multicell MIMO Networks

As mentioned earlier, the performance of wireless networks is limited by scarcity of resources and degraded by inter-cell interference, especially for cell-edge users. In such interference-limited systems, the multiplexing gain vanishes to zero when the power gets very large [56]. In other words, increasing the transmit power to a large value does not help increase system capacity. Hence, interference management is necessary to combat the deteriorating effect of inter-cell interference, and thereby leveraging full potential of spectrum reuse. Multicell MIMO is viewed as one of such techniques that is recently attracted large attention [56]. The basic idea of multicell MIMO is to allow a set of BSs to form a cluster and coordinate their transmission to the users in neighbouring cells. This requires the CSI and user data to be exchanged among the BSs over bakhaul links. In fact, multicell coordination can be traced back to

macroscopic diversity technique (or soft handoff) used in code division multiple access (CDMA) 3G systems [57], whereby a user can simultaneously communicate with multiple BSs to provide diversity large-scale channel fading. Then, selection diversity is used to select the best link at any given time. By this means, selection diversity, combined with power control, allows full frequency reuse, and thereby enhance both coverage and capacity. However, the system capacity is still limited by inter-cell interference, which is not handled in the previous systems. In multicell MIMO, the coordination among BSs is implemented over space dimension using MIMO signal processing techniques. Two levels of operation are envisioned for multicell MIMO; coordinated MIMO and cooperative MIMO (a.k.a network MIMO) [56]. In this section, an overview of multicell MIMO operation and strategies is introduced, and some its challenges are discussed.

2.6.1 Cooperative MIMO

Cooperative MIMO is based on the idea of viewing the inter-cell interference as a signal to be exploited rather than a waste signal to be avoided. This vision has evolved as a consequence of incorporating spatial domain into the classical realm of frequency-time domain, and in the same way that MIMO technique has emerged by taking the advantage of multipath copies of the signal, which was previously considered as a harmful phenomenon, so has cooperative MIMO emerged by looking at the interference signal as a useful signal to be used [56].

Under cooperative MIMO operation, a user is connected with a set of nearest BSs, denoted as $\mathcal{B}$, where each BS is equipped with N_t transmit antennas as shown in the Fig. 2.7. The BSs in the cluster are connected via high speed, error-free links so that they cooperatively convey the data and CSIs of their users to a central unit. Having collected the CSIs of users, the central unit then computes the precoding vectors (or precoding matrices in case of BD) and sends them back to each BS, that are to jointly transmit to their users [56], [58]-[65]. This cluster of BSs can be viewed as a one giant BS transmitting to several users simultaneously using spatial multiplexing,

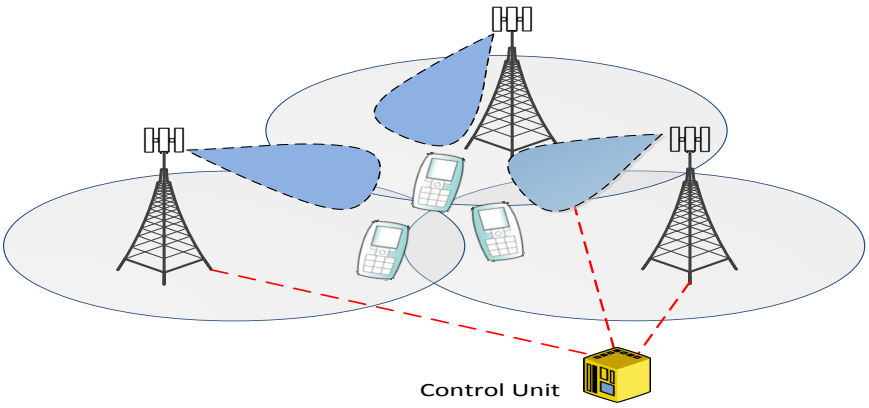

Figure 2.7: Schematic illustration of cooperative MIMO system, where the data of all their users are jointly processed and simulateneously transmitted from the BSs

where the interference channels are turned into useful channels in the same way as that of MU-MIMO scenario. Denote the set of users in the cluster as $\mathcal{U}$, where each user is equipped with only one antenna. Focusing on the intra-cell interference and neglecting the other cluster interference at the moment, the received signal of a user u in cell $b \in \{1, .., \mid \mathcal{B} \mid\}$ in the cluster, can be written as

$$y_u = \underbrace{\sum_{b=1}^{|\mathcal{B}|} \mathbf{h}_{u,b}^{\mathsf{H}} \mathbf{v}_{u,b} x_u r_{u,b}^{-\alpha/2}}_{\text{desired signal}} + \underbrace{\sum_{b=1}^{|\mathcal{B}|} \mathbf{h}_{u,b}^{\mathsf{H}} r_{u,b}^{-\alpha/2} \sum_{m \neq u}^{|\mathcal{U}|} \mathbf{v}_{m,b} x_m}_{\text{intra-cluster inteference}} + z \tag{2.30}$$

where $\mathbf{v}_{u,b} \in \mathbb{C}^{N_t \times 1}$ is the precoding vector used by bth BS for transmission to the uth user; x_u is the data symbol transmitted for the uth user such that $\mathbb{E}\{\mid x_u \mid^2\} \leq P$, where P is the power used by BS, which is assumed to be constant; $\mathbf{h}_{u,b} \in \mathbb{C}^{N_t \times 1}$ is the small-scale channel fading between the user u and bth BS, and each component of which is an independent and identically distributed (i.i.d) complex Gaussian random variable with zero mean and unit variance. $r_{u,b}$ is the distance from bth BS to the uth user, and α is the path-loss exponent. z is the noise received at the user which is

assumed to be a Gaussian random variable with zero mean and unit variance.

The precoders vectors are concatenated as

$$\mathbf{V} = [\mathbf{v}_1^{\mathsf{H}}, \mathbf{v}_2^{\mathsf{H}}, ..., \mathbf{v}_{|\mathcal{B}|}^{\mathsf{H}}]^{\mathsf{H}} \tag{2.31}$$

$$\mathbf{v}_m = [\mathbf{v}_{m,1}^{\mathsf{H}}, \mathbf{v}_{m,2}^{\mathsf{H}}, ..., \mathbf{v}_{m,|\mathcal{B}|}^{\mathsf{H}}]^{\mathsf{H}} \tag{2.32}$$

where $\mathbf{V} = \mathbf{H}(\mathbf{H}^{\mathsf{H}}\mathbf{H})^{-1}$, and

$$\mathbf{H} = [\mathbf{h}_1^{\mathsf{H}}, \mathbf{h}_2^{\mathsf{H}}, ..., \mathbf{h}_{|\mathcal{B}|}^{\mathsf{H}}]^{\mathsf{H}} \tag{2.33}$$

$$\mathbf{h}_m = [\mathbf{h}_{m,1}^{\mathsf{H}}, \mathbf{h}_{m,2}^{\mathsf{H}}, ..., \mathbf{h}_{m,|\mathcal{B}|}^{\mathsf{H}}]^{\mathsf{H}} \tag{2.34}$$

Using ZF precoding, the intra-cluster interference in (2.30) is perfectly eliminated.

2.6.2 Coordinated MIMO

In coordinated MIMO, on the other hand, the inter-cell interference is considered as a deteriorating factor that should be avoided; therefore its approach to deal with interference is the same as conventional interference management techniques [66]-[68]. In this scenario, BSs share only CSIs of their users so that they can design beamforming precoders (or BD matrices) to eliminate the interference experienced by the users in the neighbouring cells as illustrated in Fig. 2.8. More specifically, each BS transmits to only its own users, while attempting to cancel interference on the other cells users [66]-[68]. Coordinated MIMO has lower complexity compared to cooperative MIMO as it requires only CSIs and does not require synchronisation among BSs, i.e. the BSs can work in a distributive manner. Using the same notations, the received signal at user u_b in cell b in this scenario is given by:

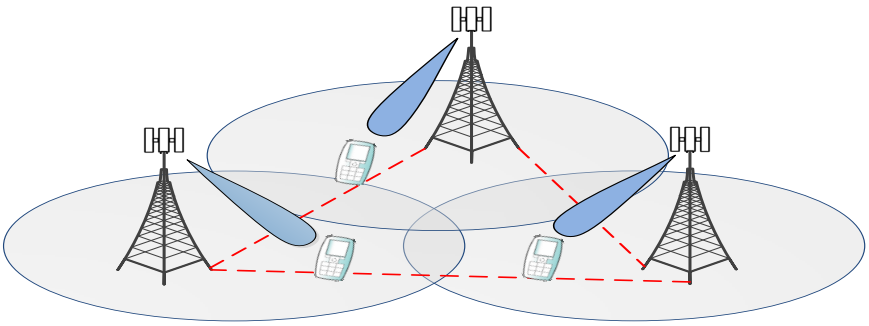

Figure 2.8: Schematic illustration of coordinated MIMO system, where each BS coordinates transmission beamforming towards users sevrd by neighbouring BSs.

$$y_{u_b} = \underbrace{\mathbf{h}_{u_b,b}^{\mathsf{H}} \mathbf{v}_{u_b,b} x_{u_b} r_{u_b,b}^{-\alpha/2}}_{\text{desired signal}} + \underbrace{\sum_{k \neq b}^{|\mathcal{B}|} \mathbf{h}_{u_b,k}^{\mathsf{H}} \mathbf{v}_{u_k,k} x_{u_k} r_{u_b,k}^{-\alpha/2}}_{\text{intra-cluster inteference}} + z \tag{2.35}$$

Similarly, the precoder of a user u_b should be designed such that it lies in the null space of other users channel spaces so that inter-cell interference is eliminated at the users.

2.6.3 Challenges and Issues

Despite its promising benefits, there are key challenges in implementing multicell MIMO in practice. In the following, some of the important challenges are discussed, and some of research directions to deal with them are highlighted.

1- ***CSI Feedback***: coordinated MIMO requires acquisition of CSIs of all users in a cluster (data are required for cooperative MIMO as well). Data and CSIs can be shared with other BSs through backhaul links. As discussed previously,

for FDD systems, a user utilises a dedicated feedback channel to feedback CSIs from all BSs (both serving and other BSs) to its serving BS. The cost of feedback increases proportionally to the number of BSs involved in coordination, thereby consuming an amount of the uplink resources. For saving system resources, it is desirable to set the best trade-off between feedback overhead and system performance [56], [69]-[70]. In TDD, on the other hand, the channel can be estimated through pilot training symbols transmitted by users. By reciprocity, BS can estimate the downlink channel. The number of required pilot symbols is now proportional to the number of users, hence putting limitation on training symbols resources when the number of users gets large [56]. Moreover, CSI has to be learned by BS in an interval within the time coherence, otherwise CSI is outdated. In high speed mobility scenario, feeding back instantaneous CSI may become problematic, therefore channel statistics could be the preferred choice in these scenarios [69]. Limited-feedback technique is also investigated for multicell MIMO, whereby the resources dedicated for limited-feedback is partitioned or adaptively allocated between desired and interference links [70]. These issue are still under investigation by the research communities.

2- ***Synchronisation and Backhaul Latency***: in cooperation scenario, BSs require perfect synchronisation among BSs, otherwise the imperfect synchronisation causes inter-symbol interference (ISI). Particularly, when the BSs involved in operation have incomparable distances from the user, resulting in different propagation delays [71]. In addition, the optimal system performance requires an exchange of data and CSIs among BSs over error-free high capacity links, especially for centralised schemes. However, in practice the capacity of backhaul links are limited, and subject to delay [56]. Future wireless networks are expected to have high capacity optical fibre links, its latency is expected to be within the allowable values required for multicell MIMO operation.

3- ***Complexity and Clustering***: in multicell MIMO, the problems of resource allocation, scheduling, and beamforming design are usually cast as optimisation problems, for which the optimal solution can be obtained through cen-

tralised processing. However, this incurs very high computational complexity, especially when the problem has non-convexity property, which is a common case in multicell scenarios. Additionally, the complexity increases with number of BSs involved in operation, hence limiting the implementation of multicell MIMO in practice. This motivates the research towards designing suboptimal low-complexity algorithms to lift the burden of complicated processing [56], [72]-[74]. Moreover, distributed-based algorithms strategies performing close to the optimal centralised strategy have been investigated so as to minimise the cost of overhead signalling. In addition, when traffic varies over time and space, or the spatial distributions of BSs are random, multicell MIMO may need to be implemented in adaptive manner in accordance with the traffic dynamics. Hence, dynamic clustering strategies, by which a cluster of BSs can be adaptively formed, are recently attracted much attention [56], [61].

2.7 Frequency Domain Multicell Coordination

OFDMA is a highly efficient transmission technique, it has been utilised in recently developed wireless networks such as LTE and LTE-A, and considered as a best candidate transmission technique for future mobile systems. Here, OFDMA systems is briefly discussed as well as resource management schemes related to OFDMA and types of multicell coordination implemented within OFDMA system framework.

2.7.1 OFDMA System

OFDMA is based on dividing the system spectrum into orthogonal equal-bandwidth subchannels; each subchannel carries certain stream of data. In recent OFDMA systems such as LTE, each subchannel consists of a consecutive orthogonal non-overlapping subcarriers. Time is also divided into smaller time slots consisting of multiple OFDMA symbols [75], as illustrated in Fig. 2.9. Then, a single smallest

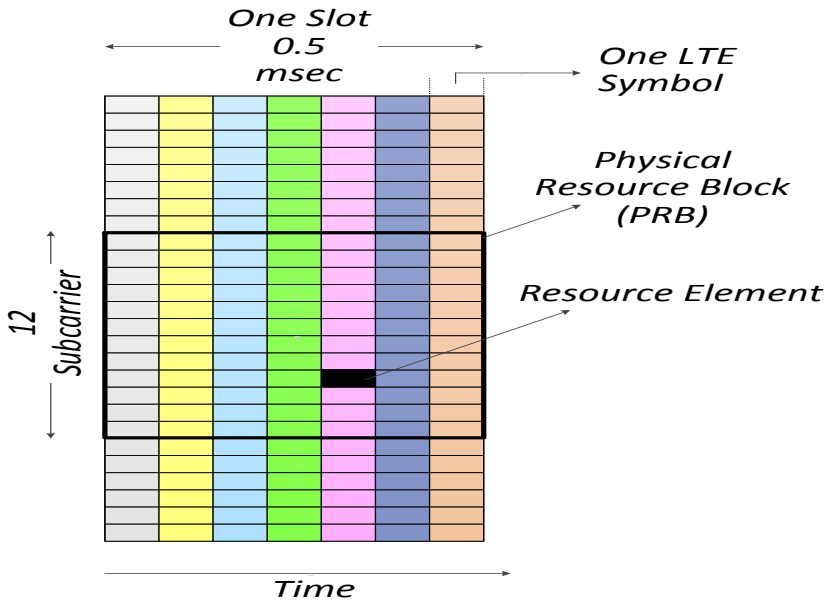

Figure 2.9: Schematic illustration of resource RB in LTE. It consists of a consequetive sets of subcarriers in frequency domain and multiple symbols in time domain.

resource unit is the resource block (RB), which is a single subchannel for the period of one time slot. OFDMA is very effective transmission technique that could cope with unpredicted nature of wireless channel and combats the intersymbol interference caused by multipath effect [76].

Since, each subchannel is chosen to be less than coherence bandwidth, the channel can be considered flat over each subchannel, and fading parameter can be considered as a random variable. This can greatly simplify the management of radio resource, allows flexibility in resource allocation, and results in better QoS provisioning [75]. More specifically, since the subchannels fades independently for different users, the probability that a subcarrier is in deep fade for all users is very low for large number of users, this is called multiuser diversity. Based on this fact, the system can treat each subchannel separately, and by knowing each user's CSI over each subchannel the BS can allocate each subchannel to the user with best channel condition, thus multiuser diversity plays an important role in maximising throughput [76]. However,

multiuser diversity results in unfairness among users, particularly for the users far away from the BS and suffer from bad channel condition for long period of time, thereby giving rise to fundamental trade-off between spectral efficiency and fairness. Moreover, when QoS constraints are considered, the adaptive resource allocation is shown to perform far better in terms of QoS guarantees thanks to fine-tuning nature of resource allocation [76].

2.7.2 Radio Resource Management (Resource allocation and scheduling)

Radio resource management (RRM) is an important functionality in multiuser wireless networks. It has triggered a great deal of research in the last decades. The main objective of resource allocation is to define how to efficiently assign users with the needed resources assuming certain objectives in time-space varying environment.

RRM problem can be formulated as an optimisation problem with certain objective function and constraints. For OFDMA, different classes for dynamic resource allocation strategies have been proposed in literature [76], namely rate adaptive, margin adaptive, and utility-based algorithms [76]. In rate adaptive resource allocation, the objective is to maximise the total data rate for the whole system while keeping the total power consumption under certain target value. In this class of resource allocation schemes, the sum capacity provides a good indication of the whole system performance, however it does not give insight on each users satisfaction, for example in time-varying channel environment the system sum rate of the whole system can be maximised by choosing the best channel condition for every user and assigning the subchannel to this user, however, users suffering from bad channel conditions will be deprived of resources they require, giving rise to long term unfairness. To overcome this limitation, it may be possible to impose additional constraint dictating minimum rate per each user. Another way to deal with this is to modify the objective function by incorporating weights ensuring fairness among users, as implemented in

proportional fairness scheduling [76]-[78].

On the other hand, for margin adaptive, the objective function is to minimise the total transmission power while satisfying the required rate per each user (or sum rate in the system) in order to guarantee minimum QoS. In the third class, which is utility-based resource allocation, the objective function is mathematically formulated to reflect the system preference, such certain QoS measure [77]-[79]. It is worth mentioning that energy efficiency has also been adopted as an objective in the resource allocation strategy, whereby the energy efficiency (or energy consumption) is maximised (or minimised) subject to given constraints.

Scheduling is another functionality to deal with multiuser systems. In time division multiplexed networks, where the time is divided into time slots, scheduling process decides which user to be served at each time slot [76]. Scheduling decision is made based on channel condition and their QoS requirements. When only CSI is considered, the scheduler always selects a user with best channel condition, and is called as maximum rate scheduler (Max.Rate), which is well known to provide maximum system throughput and result unfairness among users. Round robin (RR) is another classical class of scheduling algorithm which is proposed mainly to guarantee fairness among users, wherein the time is divided equally evenly among users to be served. However, RR results in loss in system throughput. Between these two extremes, proportional fairness (PF) scheduler has been proposed to balance between throughput maximisation and fairness guarantee. In PF, at each time slot the system schedules a user $k \in \mathcal{K}$, where $\mathcal{K}$ denotes the set of users, such that

$$R_k(t) = \arg\max_{k \in \mathcal{K}} \sum_{k=1}^{\mathcal{K}} \frac{R_k(t)}{\bar{R}_k(t)}, \tag{2.36}$$

where $R_k(t)$ is the instantaneous rate of user k, and $\bar{R}_k(t)$ is the average rate until time slot t. $\bar{R}_k(t)$ is adaptively updated according to the rule

$$\bar{R}_k(t) = (1 - \frac{1}{T})\bar{R}_k(t-1) + (\frac{1}{T})R_k(t), \tag{2.37}$$

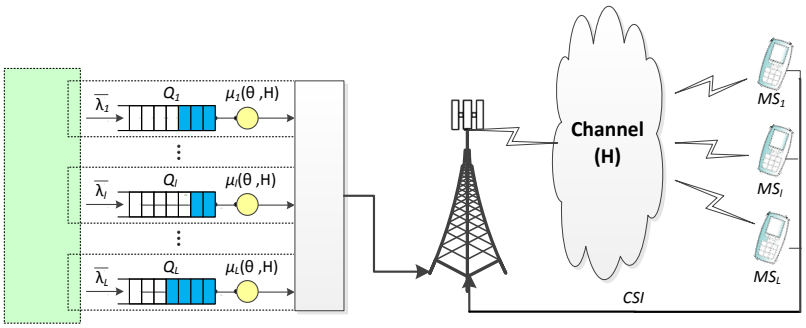

Figure 2.10: An example of scheduler in a BS, where $\bar{\lambda}_l$ is the arrival packet rate of lth user, Q_l is its queue, and μ_l is its assigned rate based on QoS exponenet θ and its channel state H.

where $\frac{1}{T}$ is constant that controls the average window size [76].

It is worth mentioning that various scheduling algorithms tailored for certain objectives have been proposed in literature, especially in cross-layer based schedulers. In cross-layer approach, the parameters of higher networks layers are incorporated in the physical layer transmission strategies as illustrated in Fig. 2.10. For example, when an arrival packet is to be served within time interval such as voice packet, queue information state (QSI) should be considered by the scheduler such that high priority is given for such an urgent packet [79], [80]. One way to incorporate QSI in the scheduling process is through QoS exponent parameter θ, as discussed previously, which can be obtained through an estimation process, for more detail refer to [16].

2.7.3 Inter-Cell Interference Coordination (ICIC)

In OFDMA cellular systems, inter-cell interference coordination (ICIC) technique has been considered as a promising strategy to avoid inter-cell interference in the downlink multicell scenario [81]-[83]. In this technique, a cluster of neighbouring cells coordinate their resource management strategies, whereby orthogonal resource block resources

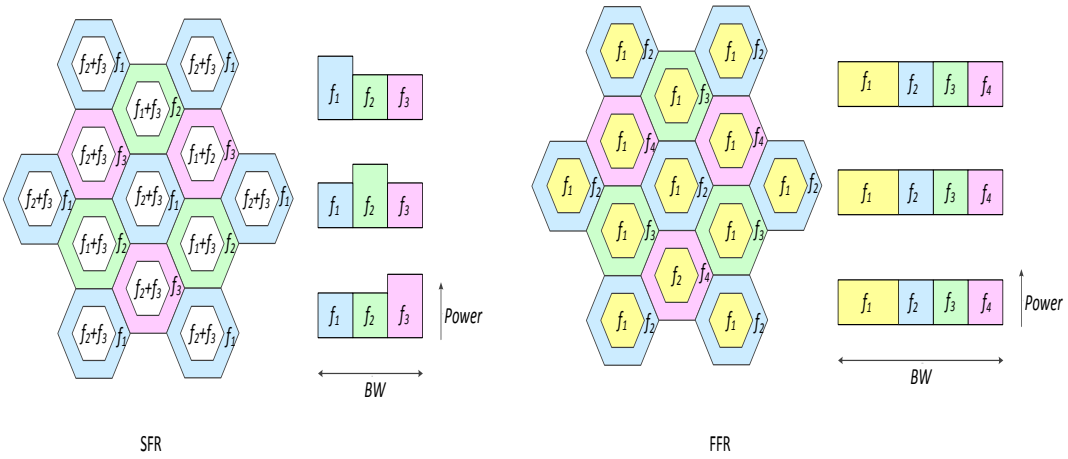

Figure 2.11: SFR and FFR frequency pattern.

are allocated to their overlapping highly interfered regions. Two main variants of ICIC strategies are proposed; Fractional Frequency Reuse (FFR) and Soft Frequency Reuse (SFR) [81]-[83]. In FFR, the whole spectrum is divided into two groups, w_e and w_c for cell-edge region and cell-centre region, respectively, where $w = w_e + w_c$. w_c is reused at each cell centre region, while w_e is further partitioned among the neighbouring cells [81] as can be seen in Fig. 2.11. On the other hand, in SFR, the spectrum is divided into N subbands. SFR allows utilisation of full spectrum reuse in the cell centre region with low power levels, while the cell-edge users can use only $1/N$ with high transmit power [83]. FFR and SFR are first introduced as static ICIC strategies. However, the static strategies often penalise the system performance in ever-changing operating environment due to failure in adaptation to traffic load variation. On the other hand, dynamic FFR and SFR are flexible to traffic variations and can better balance the spectrum resources between cell edge and cell centre users, thus providing near optimal performance at the cost of additional high complexity [83].

Chapter 3

Analysis of Multicell MIMO Networks with Power Control and Coordination

This chapter investigates the coverage probability and effective capacity for downlink MIMO random cellular networks. The system performance is analysed for different scenarios; power control, SU-MIMO, MU-MIMO, and coordinated MIMO. Analytical expressions for coverage and effective capacity are derived for these scenarios.

3.1 Introduction

With the rapidly growing number of smart phones and the ever-increasing demands for services such as web browsing, multimedia services, and video streaming, future wireless networks are expected to support high data rate services with diverse QoS requirements [1], [84]-[86]. The delay-sensitive applications impose the challenge of the service reliability, where different delay QoS requirements are to be guaranteed to

the end users [85]. As a response to these challenges, a great part of research has been devoted to develop highly spectrally efficient wireless network technologies [86], [87]. Consequently, wireless networks nowadays tend to be more densified with aggressive frequency reuse [86]. However, this comes at the price of higher inter-cell interference experienced by users at the cell-edge, resulting in degradation in system performance of the currently deployed mobile systems.

The framework adopted for evaluating cellular systems is mainly based on the concept of Shannon capacity. Shannon capacity dictates the maximum achievable data rate achievable in the system with arbitrarily small error probability [88]-[89], and is related to coverage, which is the distribution of SINR in the cellular system. While this information-theoretic framework is suitable for an analysis of system spectral efficiency, it does not impose any delay QoS constraints. Thus, for future wireless network with diverse delay QoS requirements, it is necessary to account for delay QoS constraints when analysing the whole system performance [90]-[92] so as to evaluate the the system capability of QoS provisioning. To this end, a powerful concept termed as effective capacity is proposed in [16], it gives maximum arrival rate that a given service process can support so that a QoS requirement specified by a certain QoS measure can be guaranteed [16]. Hence, it gives the statistical QoS guarantees [14], where delay is required to be lower than a threshold value only for a certain percentage of time. The effective capacity is known to be the dual of effective bandwidth previously studied in wired networks[15]-[91].

Using this effective capacity concept, the delay-QoS constraint is characterized by the QoS exponent θ such that a small value of θ corresponds to a looser QoS constraint (no delay constraint), i.e. (system can tolerate an arbitrarily long delay), and the effective capacity is reduced to Shannon capacity. While a larger value of θ corresponds to the case of stringent delay QoS constraint [92].

Based on the effective capacity concept, various scheduling and power allocation schemes are proposed for single cell scenario. In [92], [93], the optimal rate and power adaptation policies are analysed for effective capacity maximization in cognitive ra-

dio systems. In [89], the trade-off between power and delay is characterised assuming only noise with no interference. In [16],[94], TDMA-based scheduling scheme for cellular networks is developed. In [94], [96], it is shown that when the QoS constraint gets looser, the optimal power allocation converges to the classical water-filling that achieves Shannon capacity, while it converges to the scheme operating at a constant rate, i.e., channel inversion. For efficient QoS provisioning, the two main wireless resources, i.e. power and bandwidth, should be very efficiently utilised, and algorithms for this purpose are introduced in [95], [96]. In this regard, power control has also been utilised to guarantee that SINR is above a target value required to maintain wireless communication, hence resulting in better QoS. All the aforementioned works are only limited to single cell scenario, hence, they do not consider a cellular systems with inter-cell interference, where the inter-cell interference has non-negligible impact. Besides, there is a noticeable lack in research considering the effective capacity in multicell scenario. To bridge the gap in this area and characterise delay QoS using effective capacity in interference-limited cellular networks, analytical framework is necessary from this perspective.

The traditional deterministic multicell models, namely hexagonal, lattice, and Wyner models, have been extensively utilised for evaluating cellular networks performance [97]. However, in reality, BSs are generally non-regularly-deployed; therefore the deterministic hexagonal models are not sufficient for predicting the real system performance. Moreover, hexagonal and lattice deterministic models do not allow tractability in the analysis [97]. The inadequacy of the aforementioned models has motivated the research towards using random spatial models for analysing cellular systems [97], [98]. The advantage of random spatial models is that they allow analytical tractability and lead to closed-form or semi closed-form expressions for the main system performance metrics, such as capacity, coverage probability. Furthermore, they are more accurate for analysing densely-deployed networks that are rapidly gaining interest nowadays [97].

Power control is an important technique, which has been widely studied in multicell networks. Power control to compensate the effect of small-scale fading is studied in

[99], however, such power allocation strategy requires the knowledge of instantaneous CSI at each scheduling instant, hence imposing heavy feedback signalling. Moreover, the signal attenuation due to path-loss may outweigh the signal deterioration caused by small-scale fading. Thus, small-scale fading based power control may not always be the suitable strategy for QoS provisioning, and therefore it is worth considering distance-based power control that keeps the average SINR at a certain level necessary to signal decoding. Distance-dependent power control is proposed for downlink systems in [100], [101], and uplink systems in [102]. In [101], discrete power allocation scheme is proposed for ad hoc systems.

Unlike the aforementioned works, in this chapter MIMO downlink random cellular system employing fine-grained (continuous) distance-based fractional power control is studied, whereby coverage probability and effective capacity for this system are analysed. The locations of BSs are modelled as homogeneous spatial PPP [97],[98], whereby stochastic geometry provides mathematical tools for dealing with such random processes. Two scenarios are considered for cellular networks. In the first scenario, it is assumed that distance-based power control is employed by each BS when transmitting to its respective users, and it is assumed that no coordination among BSs to cancel the interference takes place. Under this scenario, two cases are investigated; SU-MIMO and MU-MIMO. In SU-MIMO, a BS serves only one user over single frequency-time slot via MRT technique, thereby, providing spatial diversity. For MU-MIMO, on the other hand, the system utilises ZF technique to spatially multiplexes several multiple users data for simultaneous transmission, this technique is known under the name of space division multiple access (SDMA). Minimum mean square error (MMSE) precoding can also be used for SDMA, but it is analytically difficult, while MRT and ZF are amenable to analytical tractability, and represent the main two extremes of beamforming strategies as described in the previous chapter.

In the second scenario, its is further assumed that several BSs can form a cluster and coordinate their transmission so as to cancel the inter-cell interference at the unintended users by using coordinated beamforming (CBF) technique. Although, cancelling out interference is beneficial in general, however, it comes at the price

of loosing degrees of freedom. Therefore, the analysis is conducted based on coordination range (the relative distance between the serving and last BS involved in coordination). The coordination range can generally determine whether it is more useful to coordinate or it might be better to transmit using the maximum eigen mode of transmission channel. For both scenarios, analytical expressions are derived for coverage probability, which is an important performance metric in the classical information-theoretic approach. To characterise the delay QoS, analytical expression for effective capacity is derived based on coverage probability analysis. Henceforth, coverage probability analysis is introduced first, and, subsequently, effective capacity is derived. In summary, the main contributions of the chapter are as follows

- It studies and analyses the coverage probability and effective capacity for MIMO cellular systems employing distance-based fractional power control and no multicell coordination is assumed. Two cases have been considered and analysed; SU-MIMO and MU-MIMO. Analytical expressions are derived for coverage probability, subsequently the effective capacity is derived in terms of coverage probability. Moreover, closed-form expressions are derived for Laplace term accounting for interference for spacial cases power control factors.

- It studies and analyses the coverage probability of MIMO cellular systems employing interference cancellation using multicell MIMO coordination. The coverage probability is defined as a function of coordination range inside which the coordination takes place. Analytical expression is derived for coverage probability of such scenario.

- The locations of BSs are modelled as random PPP model for both scenarios, where we use tools from stochastic geometry to analyse coverage probability and effective capacity.

The remainder of this chapter is organised as follows. Section 3.2 describes the system model of the analysed cellular system. Section 3.3 presents the main results of coverage analysis for SU-MIMO and MU-MIMO with power control and no interference cancellation. In Section 3.4, the analytical result of coverage probability with

interference cancellation is presented. In Section 3.5, analytical expression for effective capacity is introduced. Section 3.6 presents simulation and numerical results. Finally, 3.7 summarises the chapter.

3.2 System Model

Consider a downlink multicell cellular system, where the BSs, each equipped with N_t, are positioned in a two-dimensional horizontal plane as a homogeneous spatial PPP Φ with density λ. In PPP, the number of nodes, e.g. BSs in a given bounded area A is a random variable (r.v.) following Poisson distribution with their positions being uniformly distributed. Thus, the cell boundaries are shown to be Voronoi tessellation [97], as shown in Fig. 3.1. Since a homogeneous PPP is considered, the statistics evaluated for every node in the system will be similar. Hence, the analysis will be performed based on a typical user at the origin. This is justified by Slivnyak's [97], [98], which states that the statistical properties observed by a typical point of the Φ are similar to those observed by a point at the origin in the process $\Phi \cup \{0\}$. The BSs distances from this typical user are given according to the homogeneous PPP, $\Phi = \{r_k, k \in \mathbb{N}\}$, on the two dimensional plane $\mathbb{R}^2$, where r_k denotes the distance from the kth BS. The user is assumed to be associated with the nearest base station denoted as BS_1 and located at distance r_1 from it. While all other BSs ($\text{BS}_k, k \in \Phi$) are regarded as interferers to this user as shown in Fig. 3.1.

Notice that the distance between a typical user and the kth BS is a r.v. following generalised Gamma distribution given by [103]

$$f_{r_k}(r) = \frac{2(\lambda\pi r^2)^k}{r\Gamma(k)} e^{-\lambda\pi r^2} \tag{3.1}$$

It is also assumed that each user is equipped with a single-antenna.

Assuming that each user is able to estimate its downlink channel perfectly and feeds

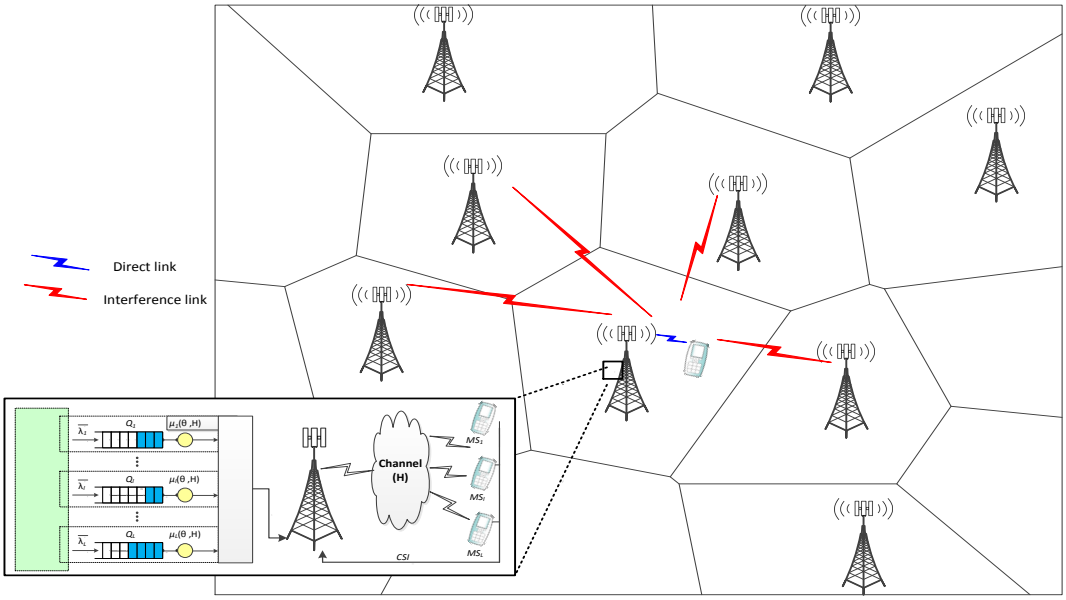

Figure 3.1: An illustration of random network configuration, BSs are distributed randomly in two-dimensional space, and each BS has several queues for packet accumulation. The scheduler serves a user (or multiple users in MU-MIMO) according to a scheduling rule that should incorporate θ of the user.

CSI back to its serving BS by means of dedicated pilot signal. If the user is assumed to be helped through coordination it should also estimate its channels to $K-1$ BSs and feed them back to its serving BS, whereby they are conveyed to the other BSs through delay-free unlimited capacity links.

Denote the downlink small-scale channel vector between the typical user and kth BS as $\mathbf{h}_k = [h_1, ..., h_{N_t}] \in \mathbb{C}^{1\times N_t}$, where each component of $\mathbf{h}_k$ are an independent and identically distributed (i.i.d) complex Gaussian r.v with zero mean and unit variance, i.e. $\mathcal{CN}(0,1)$. Two types of beamforming techniques, i.e. MRT and ZF, are considered for SU-MIMO and MU-MIMO, respectively, which are defined as follows

1- *MRT Beamforming*: MRT beamforming vector is constructed such that it is aligned to the channel direction, i.e. if the channel vector is $\mathbf{h}$, the beamfomer

is constructed as [73].

$$\mathbf{v} = \frac{\mathbf{h}^{\mathsf{H}}}{\| \mathbf{h} \|} \tag{3.2}$$

2- *ZF*: for MU-MIMO, let $\mathbf{H} = \left[\mathbf{h}_1^{\mathsf{H}}, \mathbf{h}_2^{\mathsf{H}}, ...\mathbf{h}_K^{\mathsf{H}}\right]^{\mathsf{H}}$ denote the aggregate channel matrix of K users. The ZF beamforming vectors $\mathbf{v}_1, ..., \mathbf{v}_K$ can be chosen to be the normalised columns of the matrix [73]

$$\mathbf{V} = \mathbf{H}^{\dagger} = \mathbf{H}^{\mathsf{H}}(\mathbf{H}\mathbf{H}^{\mathsf{H}})^{-1} \tag{3.3}$$

For interference cancellation via CBF, a BS with N_t can cancel interference for up to $K = N_t - 1$ users using ZF technique. As an example for a given nth user with channel vector $\mathbf{h}_n$, the beamforming precoder vector can be obtained by projecting the vector $\mathbf{h}_n$ on the null space of $\hat{\mathbf{h}}_n = \left[\mathbf{h}_1^{\mathsf{H}}, ..., \mathbf{h}_{n-1}^{\mathsf{H}}, \mathbf{h}_{n+1}^{\mathsf{H}}, ..., \mathbf{h}_K^{\mathsf{H}}\right]^{\mathsf{H}}$ [106]

$$\mathbf{v}_n = (\mathbf{I} - \mathcal{P}_{\hat{\mathbf{h}}_n})\mathbf{h}_n \tag{3.4}$$

where $\mathcal{P}_{\hat{\mathbf{h}}_n}$ denotes the projection on $\hat{\mathbf{h}}_n$, given as $\mathcal{P}_{\hat{\mathbf{h}}_n} = \hat{\mathbf{h}}_n^{\mathsf{H}}(\hat{\mathbf{h}}_n\hat{\mathbf{h}}_n^{\mathsf{H}})^{-1}\hat{\mathbf{h}}_n$.

The channel distribution of MIMO link is quite different from single antenna link. For single antenna links, the channel is exponentially distributed for both direct and interfering links. While for the link from multi-antenna BS to a single-antenna user the channel distribution depends on the MIMO transmission technique and whether a BS is serving or interfering. This is because when transmitting to a user, the BS precodes its signal for its intended user, hence resulting in different effective channel distribution from the case when it acts as an interferer.

The effective channel of direct and interfering links denoted as g_0 and g_i, respectively, where $g_n = \mid \mathbf{v}_n^{\mathsf{H}}\mathbf{h}_k \mid^2$, are an i.i.d r.v. following gamma distribution, i.e. $\Gamma(\Delta, 1)$ and $\Gamma(\Psi, 1)$, respectively [104]. Δ and Ψ are the shape parameters of gamma distribution.

Now, the main two scenarios studied in this chapter are described as follows

- *Fractional power control and no coordination*: in this scenario, it is assumed that the system does not implement multicell coordination, while employing distance-based fractional power control. Two cases are studied under this scenario; SU-MIMO and MU-MIMO. Each BS makes use of power control to compensate for path-loss attenuation experienced by its served user. More specifically, each ith BS allocates power proportional to the user distance, $X_i^{\alpha\eta}$, where $\eta \in [0, 1]$ is the fractional power control factor, and X_i represents the distance from ith interfering BS to its served user. Likewise, for MU-MIMO each user is allocated power proportional to its distance from the BS. Since $X_1 = r_1$ the desired signal power at the typical user becomes $g_0 r_1^{\alpha(\eta-1)}$. Moreover, the interference power from each interfering BS becomes $(X_i^{\alpha})^{\eta} g_i r_i^{-\alpha}$. Thus, a user closer to its serving BS demands less power than required by a user farther away. Under this system model, the SINR can be written as

$$\text{SINR} = \frac{g_0 r_1^{\alpha(\eta-1)}}{\sigma^2 + I} \tag{3.5}$$

  where $I = \sum_{i \in \Phi/\{\text{BS}_1\}} X_i^{\alpha\eta} g_i r_i^{-\alpha}$ is the aggregate interference experienced at the typical user, and σ^2 represents the additive noise power which is assumed to be constant. Note that for SU-MIMO using MRT, $\Delta = N_t$ and $\Psi = 1$, while for MU-MIMO utilising ZF, we have $\Delta = N_t - \Psi + 1$, where Ψ is the number of users served by MU-MIMO. It is worth noting that for single antenna links, $\Delta = \Psi = 1$, which is equivalent to exponential distribution, the interested reader can refer to [104] for more details.

- *Multicell coordination*: in this scenario, it is assumed that a cluster of BSs denoted by the set $\mathcal{B} = \{\text{BS}_1, ..., \text{BS}_K\}$ are able to coordinate their beamforming to eliminate inter-cell interference at each unintended user. For simplicity in analysis, let use assume SU-MIMO and $\eta = 0$, however the analysis can be straightforwardly generalised to MU-MIMO and any power control strategy.

Thus, SINR for such scenario becomes

$$\text{SINR} = \frac{g_0 P r_1^{-\alpha}}{\sigma^2 + I_c} \tag{3.6}$$

where P is the transmit power, and

$$I_c = \sum_{i \in \Phi / \{\text{BS}_1, \ldots, \text{BS}_K\}} g_i P r_i^{-\alpha} \tag{3.7}$$

is the aggregate inter-cell interference from all BSs except the set $\mathcal{B}$. Recall that $g_0 \sim \Gamma(\Delta, 1)$ and $g_i \sim \Gamma(\Psi, 1)$, with $\Delta = N_t - K + 1$ and $\Psi = 1$ [104].

3.2.1 Effective Capacity

Now, the concept of effective capacity concept (E_c) is briefly introduced. Consider a queuing system of a typical BS with constant arrival rate as shown in Fig. 3.1. The arriving packets are stacked in the buffer for transmission in time slot T_s, over a subband of bandwidth denoted as W. The statistical delay QoS for this system can be defined as the probability for the queue length of the transmitter buffer exceeding a certain threshold x decays exponentially as a function of x, therefore the QoS exponent θ can be defined as [92]-[93]:

$$\theta = -\lim_{x \to \infty} \frac{\ln\big(\mathbb{P}\big(\text{q}(\infty) > x\big)\big)}{x} \tag{3.8}$$

where $\mathbb{P}(x)$ denotes the probability of event x, and $\text{q}(t)$ denotes the buffer length at time t. Notice that $\theta \to 0$ implies no delay constraint required in the system, whereas $\theta \to \infty$ corresponds to system with a strict delay constraint, therefore θ is considered as the delay QoS constraint of the system [16]. Accordingly, the E_c is defined as [16]:

$$E_c = \frac{\Lambda(-\theta)}{-\theta} = -\lim_{n \to \infty} \frac{1}{n\theta} \ln\left(\mathbb{E}\left\{\text{e}^{-\theta \sum_{i=1}^{n} R[i]}\right\}\right), [\text{nats/sec/Hz}] \tag{3.9}$$

where $R[i]$ is the transmission rate in time slot i defined as:

$$R[i] = T_s W \ln\Big(1 + \text{SINR}\Big), [\text{nats/sec/Hz}] \tag{3.10}$$

Hereafter, we assume $T_s\text{W} = 1$ [92]. Assuming that the stochastic service process is independent and identically distributed (i.i.d) process, i.e. stationary and ergodic process, E_c in (3.9) can be simplified to [92]-[95]

$$E_c = -\frac{1}{\theta}\ln\Big(\mathbb{E}\big\{\text{e}^{-\theta R[n]}\big\}\Big) = -\frac{1}{\theta}\ln\Big(\mathbb{E}\Big\{1 + \text{SINR}\Big\}^{-\theta}\Big) \tag{3.11}$$

Thus, QoS can be incorporated in the scheduling process of the system by interpreting θ exponent as the QoS requirement. Thereby, the effective capacity is maximised for a given θ instead of the conventional approach in which the throughput is maximised subject to delay constraint.

3.3 Coverage Probability Analysis: No Interference Cancellation

In this section, analytical expressions are derived for coverage probability for a typical user in MIMO system. The coverage of SU-MIMO with power control is introduced first, then we proceed to analyse the coverage of MU-MIMO. The coverage probability, i.e. the probability of achieving the target SINR $\bar{\gamma}$ at the typical user can be defined as $\mathbb{P}[\text{SINR} > \bar{\gamma}]$, which is equivalent to the complementary cumulative distribution function CCDF of the SINR [102]. Coverage probability can also be interpreted as the average fraction of the network area (users) for which (for whom) SINR is greater than $\bar{\gamma}$.

3.3.1 Coverage Probability with SU-MIMO

Focusing the attention on the coverage probability of SU-MIMO with power control, an upper bound for coverage is introduced in the following proposition.

Proposition 3.1: The upper bound on the coverage probability for SU-MIMO system employing distance-based fractional power control, P_c^{SU}, is given by:

$$P_c^{\mathsf{SU}} \leq \sum_{m=1}^{N_t} \binom{N_t}{m} (-1)^{m+1} \int_0^{\infty} 2\pi\lambda r_1 e^{-(\pi\lambda r_1^2 + \bar{\gamma} m \zeta r_1^{\alpha(1-\eta)} \sigma^2)} \exp(-2\pi\lambda\psi) \mathrm{d}r_1 \quad (3.12)$$

where

$$\psi = \mathbb{E}_X \left\{ \frac{\bar{\gamma} m \zeta r_1^{(2-\alpha\eta)} X^{\alpha\eta}}{\alpha - 2} {}_2F_1\big(1, 1 - \frac{2}{\alpha}; 2 - \frac{2}{\alpha}; -\bar{\gamma} m \zeta r_1^{-\alpha\eta} X^{\alpha\eta}\big) \right\}, \quad (3.13)$$

$\zeta = (N_t!)^{\frac{-1}{N_t}}$, and

$${}_pF_q(a_1, .., a_p; b_1, ...b_q; z) = \sum_{n=0}^{\infty} \frac{(a_1)_n ... (a_p)_n}{(b_1)_n ... (b_q)_n} \frac{z^n}{n!} \quad (3.14)$$

is the hypergeometric function, where $(a)_n$ denotes the Pochhammer symbol representing the falling factorial [105].

Proof: See Appendix A.1.

The lower bound for the coverage probability can be obtained by setting $\kappa = 1$. Furthermore, it can be observed that the bound is closed for single-input single-output (SISO), i.e. $N_t = 1$. The expressions in the above results involve double integrations, however the expectation in (3.13) can be further simplified using the following corollary.

Corollary 3.1: For the (3.13), closed form expressions can be obtained for special cases defined below:

When $\alpha = 4, \eta = 0$, ψ is given by:

$$\psi = \frac{r_1^2 \bar{\gamma} m \zeta}{\alpha - 2} {}_2F_1 \left(1, 0.5; 1.5; -\frac{\bar{\gamma} m \zeta r_1^2}{\pi \lambda}\right) \tag{3.15}$$

Proof: See the Appendix A.2.

Note that this case corresponds to constant power allocation. Furthermore, following the same steps in Appendix A.2, (3.13) can be obtained in closed form for other two special cases. When $\alpha = 4, \eta = 1$, ψ is given by:

$$\psi = \frac{2\bar{\gamma} m \zeta}{(\lambda \pi r_1)^2 (\alpha - 2)} {}_4F_1 \left(1, 0.5, 1.5, 2; 1.5; -\frac{4\bar{\gamma} m \zeta}{(\pi \lambda)^2 r_1^4}\right) \tag{3.16}$$

This case corresponds to full-channel inversion. When $\alpha = 4, \eta = 0.5$, ψ is given by:

$$\psi = \frac{\bar{\gamma} m \zeta}{\lambda \pi (\alpha - 2)} {}_3F_1 \left(1, 0.5, 2; 1.5; -\frac{\bar{\gamma} m \zeta}{\pi \lambda r_1^2}\right) \tag{3.17}$$

This case corresponds to the fractional power control. For the other values of α and η, the integration should be evaluated numerically.

3.3.2 Coverage Probability with MU-MIMO

When the system utilises SDMA to serve multiple users, a number of Ψ users can be served simultaneously over the same frequency band and time slot. Since the users have different positions from the BS, each user will be allocated an amount of power based on its distance from its serving BS. This, however, may lead to more analysis complexity. For tractability of analysis, let us assume that the set of scheduled users served via SDMA are located on equal distances from their serving BS, hence, they will be allocated the same amount of power. Alternatively, it can be also assumed that the users are located at different distances from the serving BS, however, they will be allocated an equal amount of power which is proportional to farthest user distance from its serving BS. These assumptions significantly render the analysis more tractable.

In the following proposition, an exact analytical expression of coverage probability for MU-MIMO is presented.

Proposition 3.2: The coverage probability of a typical user served via full-SDMA in MU-MIMO employing distance-based fractional power control is given by

$$P_c^{\mathsf{MU}} = \int_0^\infty 2\pi\lambda r_1 e^{-(\pi\lambda r_1^2 + \bar{\gamma} r_1^{\alpha(1-\eta)}\sigma^2)} \exp(-2\pi\lambda\psi) \mathrm{d}r_1 \tag{3.18}$$

where

$$\psi = \mathbb{E}_X \left\{ \sum_{m=1}^{\Psi} \binom{\Psi}{m} \frac{r_1^{2-m\alpha\eta} X^{m\alpha\eta} \bar{\gamma}}{m\alpha - 2} {}_2F_1\left(\Psi, m - \frac{2}{\alpha}; m + 1 - \frac{2}{\alpha}; -\frac{\bar{\gamma} r_1^{\alpha(1-\eta)} X^{\alpha\eta}}{r_1^\alpha}\right) \right\} \tag{3.19}$$

Proof: See the Appendix A.3.

It is worth noting that the expectation in (3.19) can be obtained in closed form in special cases as in Corollary 1. Note that the above result is tight for full-SDMA, i.e. the number of users served by each BS is equal to the number of transmit antennas ($\Delta = N_t - \Psi + 1$). Otherwise, an upper bound should be sought for coverage probability in a similar manner to that of SU-MIMO analysis.

3.4 Coverage Probability with Multicell Coordination

In this section, coordinated MIMO is considered, whereby the effect of interference cancellation on coverage probability is studied and analysed. Let us consider a cluster of BSs denoted as $\mathcal{B} = \{\mathrm{BS}_1, ..., \mathrm{BS}_K\}$ that are able to share CSIs of their respective users, and coordinate their transmission beamforing. Since the main focus here is on the interference cancellation and its impact on coverage, only SU-MIMO and constant power allocation $\eta = 0$ are assumed for this case. However, the analysis can be straightforwardly extended to MU-MIMO and general fractional power control

cases.

For the sake of tractability of analysis, a new parameter ρ is introduced to designate the coordination distance ratio, it is defined as the ratio of the user distance to its serving BS_1 over its distance to the first interfering BS_K, i.e. $\rho = \frac{r_1}{r_K}$. This parameter defines the coordination range inside which the interference is to be eliminated using coordinated beamforming technique. Moreover, this parameter sheds light on where the coordination strategy is more beneficial than transmission with no coordination. Although the analysis can be conducted by averaging over all randomness involved in the assumed scenario, the analysis will be set out based on the conditional coverage probability for a given value of ρ. The following proposition gives the conditional probability of coverage.

Proposition 3.3: The upper bound of coverage probability in cellular systems employing interference cancellation using coordinated-MIMO and conditioned on ρ with path-loss $\alpha = 4$, $P_c^{\mathsf{CB}}(\rho)$, is given as

$$P_c^{\mathsf{CB}}(\rho) \leq \frac{(\lambda\pi)}{(2G(\rho,\bar{\gamma})+1)^K} \sum_{m=1}^{\Delta} \binom{\Delta}{m} (-1)^{m+1} \sum_{n=0}^{K-1} \frac{(\lambda\pi)^n (2G(\rho,\bar{\gamma})+1)^n}{n!} \mathcal{G}_n(\bar{\gamma},\rho) \tag{3.20}$$

where:

$$\mathcal{G}_n(\bar{\gamma},\rho) = (2Z)^{-\frac{n+1}{2}} \Gamma(n+1) \exp\left(\frac{\left(\lambda\pi(G(\bar{\gamma},\rho)+1)\right)^2}{4Z} \right) \times D_{-(n+1)}\left(\sqrt{\frac{2}{Z}} \lambda\pi\big(G(\bar{\gamma},\rho)+1\big) \right) \tag{3.21}$$

$$G(\bar{\gamma},\rho) = \frac{m\kappa\bar{\gamma}\rho^{\alpha}}{\alpha-2} {}_2F_1\left(1, 1-\frac{2}{\alpha}; 2-\frac{2}{\alpha}; -m\kappa\bar{\gamma}\rho^{\alpha}\right) \tag{3.22}$$

$$Z = \frac{\sigma^2 m\kappa\bar{\gamma}}{P} \tag{3.23}$$

where $\kappa = (\Delta!)^{(-1/\Delta)}$, and $\Delta = N_t - K + 1$. D_{-v} denote the parabolic cylinder function defined in [105], [107].

Proof: See Appendix A.4

3.5 Effective Capacity Analysis

In this section, analytical expression are introduced for effective capacity. The effective capacity can be expressed in terms of coverage probability, and thus it will be defined as a function of the key system parameters; BSs density, path-loss, power control policy, and antenna number. For multicell setting, the effective capacity quantifies the average of maximum arrival rate supportable by a system with inter-cell interference. It can also be interpreted as (i) the average of the maximum arrival rate that the system can support for a randomly chosen user, (ii) the average fraction of users for whom the maximum arrival rate can be supported, (ii) the average fraction of the network area for which the maximum arrival rate can be supported. The following proposition gives the effective capacity expression.

Proposition 3.4: For a given QoS exponent θ, the upper bound of effective capacity in multicell cellular systems can be approximated by:

$$E_c \approx -\frac{1}{\theta}\ln\left(1-\sum_{n=1}^{N}\omega_n f(x_n)\right) \tag{3.24}$$

where x_n and ω_n are the nth zero of the Hermite polynomial $H_n(x_n)$ of degree N, and the corresponding weight of the function $f(.)$ at the nth abscissa, respectively [105]. The $f(x_n)$ is the coverage probability of the system with $\bar{\gamma} = m\kappa\big(x_n^{\frac{-1}{\theta}} - 1\big)$.

Proof: See Appendix A.5

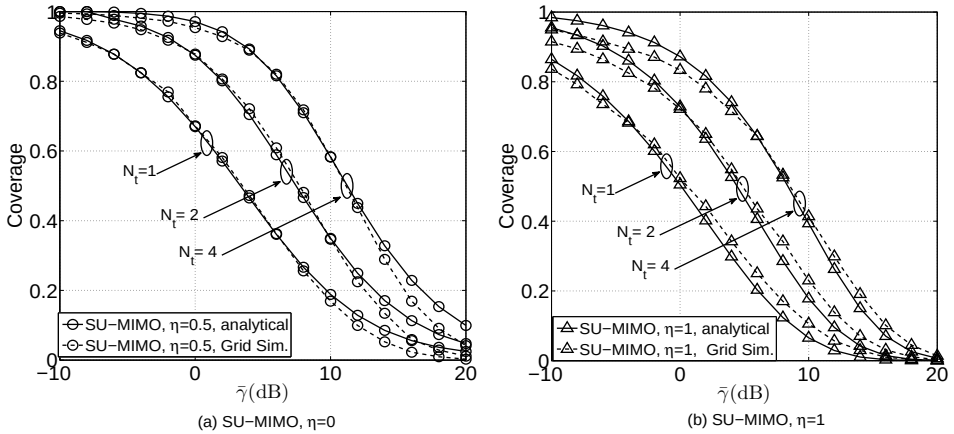

Figure 3.2: Simulation results of coverage probability of SU-MIMO, ($N_t = \{1, 2, 4\}$, $\eta = \{0, 1\}$, $\sigma^2 = 0$).

3.6 Numerical Results

This section provides the simulation and analytical results of coverage probability and effective capacity for both considered scenarios. To simulate PPP model, we first consider a bounded area of 10km^2. The density of BSs in this area is $\lambda = 1/(30000 * \pi^2)$ BS per m^2. The number of BSs follows Poisson distribution. Then, the BSs are distributed uniformly on the bounded area. The points distributed as such represents one realization of point process. Grid model is also considered by assuming uniformly spaced square area of BSs. For simulation purposes, 36 BSs are positioned at regular distance from each other.

In Figs. 3.2(a) and (b), analytical expressions of coverage probability of SU-MIMO are compared with grid simulation for different antenna number for power control factors $\eta = 0, 1$, and assuming interference-limited case, i.e. $\sigma^2 = 0$. It can be clearly observed that the analytical expressions excellently approximate the simulation of coverage probability over the entire range of signal-to-interference ratio (SIR) of interest.

Similar observation can be made about Figs. 3.3 and 3.4 that show the comparison of simulation and analytical results of MU-MIMO system and coordinated MIMO,

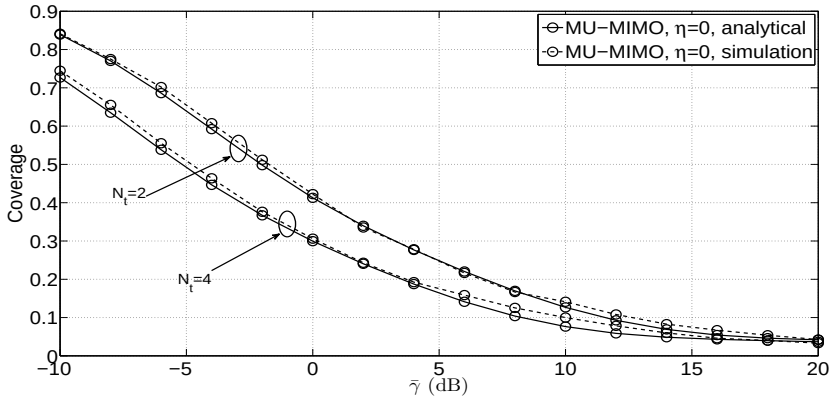

Figure 3.3: Simulation results of coverage probability of MU-MIMO, ($N_t = \{2, 4\}$,$\eta = 0$, $\sigma^2 = 0$).

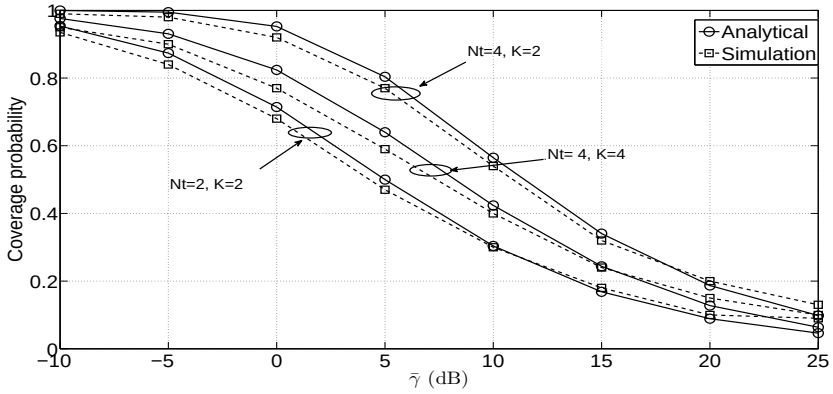

Figure 3.4: Simulation comparison of coverage results for coordinated MIMO system, ($\eta = 0$, $N_t = \{2, 4\}$, $K = \{2, 4\}$, $\sigma^2 = 0$).

respectively, assuming $\sigma^2 = 0$. It can be clearly noticed that for both cases the analytical expressions approximate the coverage probability for different antenna numbers and entire range of (SIR).

The analytical results in Figs. 3.5 and 3.6 compare between the cases of zero and non-zero noise. Small gap can be observed in MU-MIMO between $\sigma^2 = 0.1$ and $\sigma^2 \to 0$ cases over the entire range of (SINR) and slightly larger in SU-MIMO. This confirms the fact that the noise is not a crucial issue in densely-deployed cellular networks, in which the regime is almost interference-limited, and therefore noise can be neglected

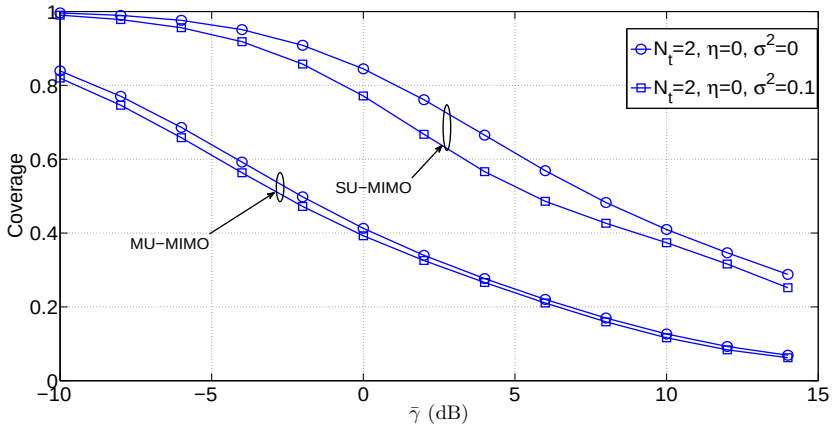

Figure 3.5: Analytical results of coverage with non-zero noise, ($\eta = 0$, $\sigma^2 = \{0, 0.1\}$)

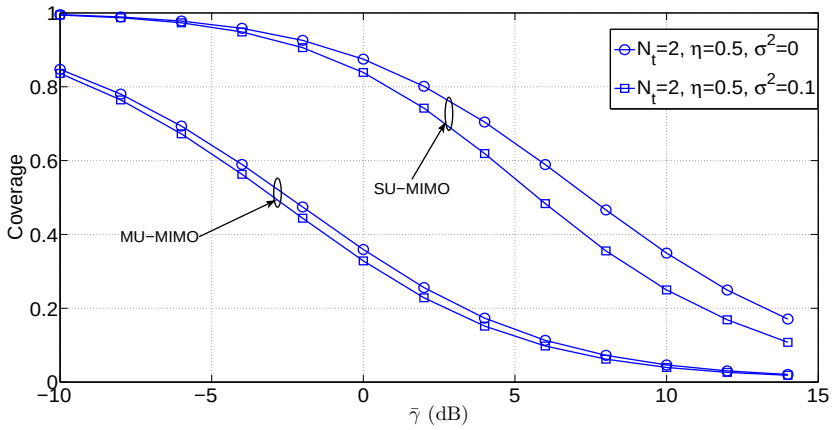

Figure 3.6: Analytical results of coverage with non-zero noise, ($\eta = 0.5$, $\sigma^2 = \{0, 0.1\}$)

in these scenarios.

Figs. 3.7(a) and (b) depict the coverage probability of SU-MIMO and MU-MIMO, respectively, as a function of power control strategies $\eta = 0, 0.25, 0.5, 1$, and antenna number $N_t = 2, 4$. It can be clearly observed the fact that for all η values, the coverage probability decreases with the increase of transmit antenna N_t in MU-MIMO (full SDMA) scheme, while increasing with SU-MIMO as shown more clearly in Fig. 3.8, that compares between both schemes for different power control factors and $N_t = 2$. This is due to two reasons: firstly, ZF utilised in SDMA to cancel intra-user

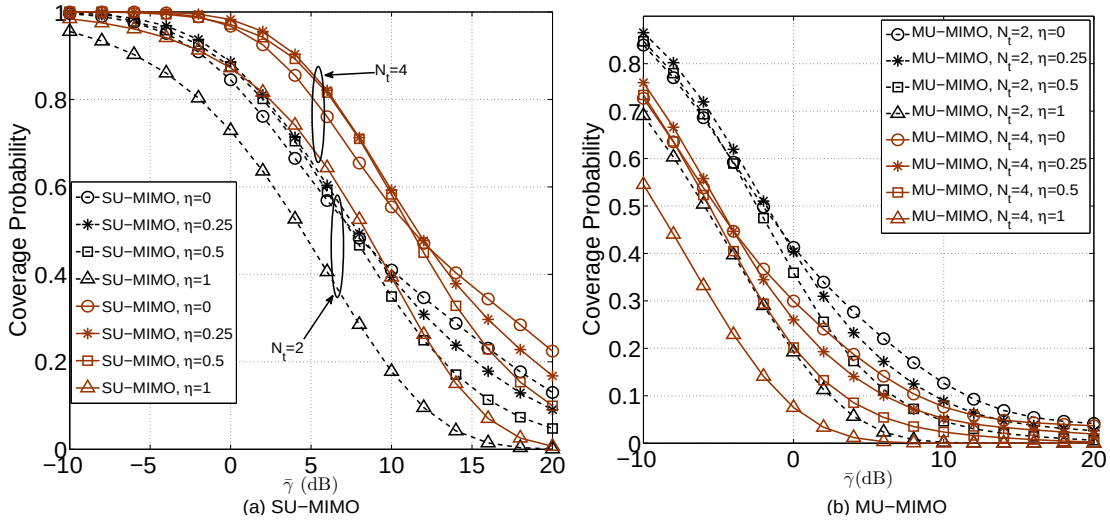

Figure 3.7: The analytical results of coverage probability for SU-MIMO and MU-MIMO, respectively for various fractional power control strategies are shown in both cases. ($\eta = 0, 0.25, 0.5, 1,\ N_t = \{2, 4\},\ \sigma^2 = 0$).

interference causes loss in degrees of freedom, hence degrading the signal quality. Secondly, more interference is generated with the increase in number of users served via SDMA.

Despite the decrease in both coverage and average user rate with MU-MIMO scheme, the scheme serves more users and may results in higher sum rate in the system. This presents another delicate trade-off inherent in wireless systems between area spectral efficiency measured in (bits/sec/Hz/m^2) and user-link spectral efficiency given in (bits/sec/Hz). Noticeably, both SU-MIMO and MU-MIMO have an identical performance in terms of power control strategies; the coverage probability of both is highest with fractional power control in low SIR threshold values, while the constant power allocation provides the best performance in higher SIR values.

Now, the discussion is focused on the impact of power control strategies on coverage probability in both SU-MIMO and MU-MIMO schemes. Constant power $\eta = 0$ is considered as the the reference of comparison. It can be clearly observed that for both SU-MIMO and MU-MIMO cases the constant power allocation almost gives comparable performance (coverage probability) to the cases ($\eta = 0.25, \eta = 0.5$) in low SIR thresh-

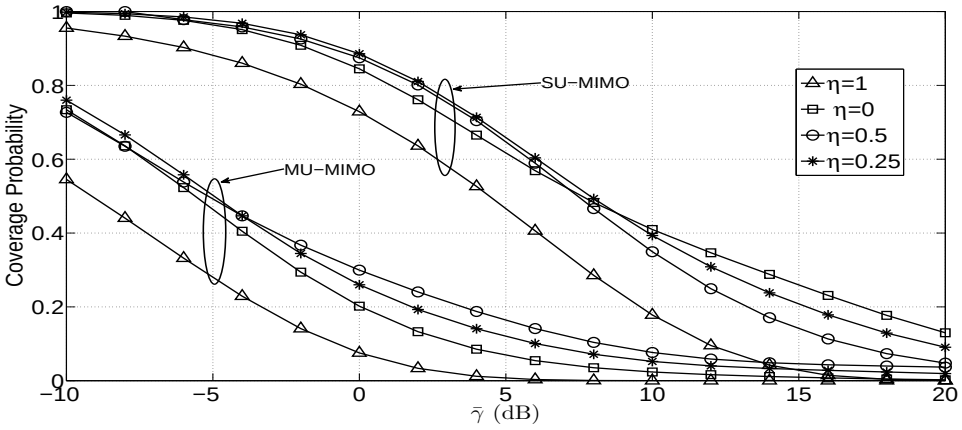

Figure 3.8: Comparison between SU-MIMO and MU-MIMO for different power control strategies; ($\eta = 0, 0.5, 1$, $N_t = 2$, $\sigma^2 = 0$).

olds, while outperforming all other power control strategies in high SIR values.

The largest coverage probability in the lower 50 percentile is provided by $\eta = 0.25$ followed by $\eta = 0.5$ before crossing below $\eta = 0$ case at 8.5 dB and -4 dB for SU-MIMO and MU-MIMO (with $N_t = 2$), respectively. The difference in coverage for $\eta = 0, 0.25, 0.5$ is almost negligible in the low SIR thresholds. As η increases towards 1, the coverage decreases accordingly. The case η provides the lowest coverage across the entire range of SIR thresholds. The effect of power control can be fully explained by concentrating on the performance of cell-edge users relative to the cell-centre and the intrinsic trade-off between their performance. Cell-centre usually enjoy good channel conditions and are not susceptible to strong interference. Thus, they are typically noise-limited, and reducing the transmit power inevitably reduces their SIR. Considering this fact, constant power control is the optimal power strategy.

On the other hand, cell-edge users typically more susceptible to high interference (interference-limited case). Hence, employing high power control factors such as $\eta = 1$ results in an increase in their SIR, while relatively reducing the transmit power of cell-centre users served by neighbouring BSs (interfering BSs). This disparity becomes more noticeable with high η values. Consequently, there is a delicate trade-off between increasing interference experienced by cell-edge users and reducing interference from

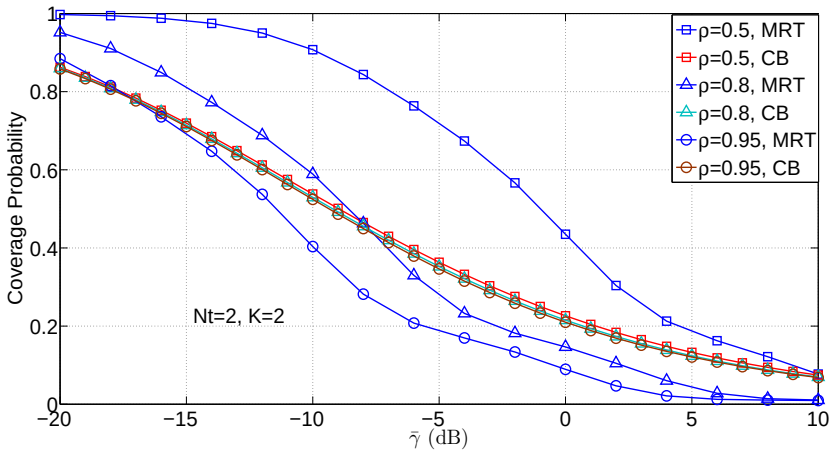

Figure 3.9: Comparison between coordination using CB and no coordination using MRT for different ρ values, ($N_t = 2$, $P = 1$, $\sigma^2 = 0$).

cell-centre users at the neighbouring cells, giving rise to the fact that fractional values of η provides the highest coverage values for the majority of users.

Now, its is assumed that a typical BS serves only one user, i.e. SU-MIMO, but uses the rest of its degrees of freedom to cancel the interference on the users in neighbouring cells. Fig. 3.9 provides the coverage probability of coordinated MIMO as a function of ρ, and compares between no coordination with coordination schemes. As previously discussed, coordination causes loss in degrees of freedom and thereby lowering SIR. This loss of degrees of freedom may be disadvantageous when the nearer interferers are far away from the user, therefore, in this case, no coordination, i.e. transmitting through MRT, is preferable as it exploits the whole degrees of freedom provided by the system. This case corresponds to the lower values of ρ as shown in Fig. 3.9. However, when the interferes get closer, i.e. $\rho = 0.95$, coordination becomes necessary to enhance the coverage for the system. When $\rho = 0.8$, for low SIR thresholds MRT performs better than CB before crossing below CB curve in -6 dB, where CB outperforms MRT.

Fig. 3.10 depicts the performance of E_c for SU-MIMO and MU-MIMO as a function of power control factor. Similar to the coverage probability, the performance of E_c for

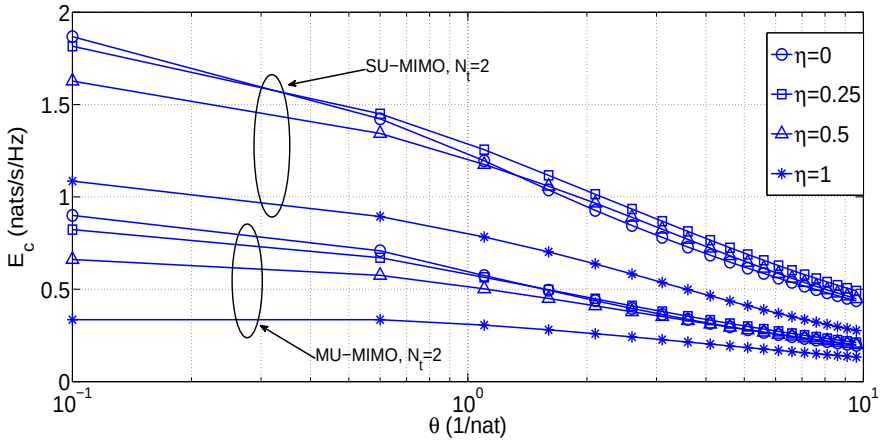

Figure 3.10: Comparison of effective capacity of both SU-MIMO and MU-MIMO systems for different power control strategies; ($\eta = 0, 0.25, 0.5, 1$, $\sigma^2 = 0$).

SU-MIMO scheme is noticeably better than that of MU-MIMO due to the same reason mentioned previously. Notice that when θ gets larger, E_c approaches 0, suggesting that the system is incapable of supporting the arrival rate when the delay constraint is very stringent.

For both schemes, it can also be clearly observed that for low delay constraints i.e. $\theta \to 0$, lower power control factors provide comparable performance with the strategy of $\eta = 0$ being the best over all. When delay constraint gets more stringent $\theta \to \infty$, fractional power control strategy outperforms the others, in particular $\eta = 0.25$ yields the best performance. Note that the strategy of $\eta = 1$ gives the worst performance over the entire range of θ values. When the delay constraint gets looser, i.e. small θ, it might be better to transmit with power control factors less than 0.25. While in case of stringent delay constraint, transmitting with power $\eta = 0.25$ provides the best performance. These observations suggest that fractional power control of $\eta \leq 0.25$ is the best strategy among all others for enhancing E_c in interference-limited scenarios.

The impact of power control factor on E_c can be understood by noticing the behaviour of E_c with respect to θ. When the delay constraints θ becomes more stringent, the

best power policy is to compensate for the path-loss and keep the rate as fixed as possible calling for using power control factor $0.5 > \eta > 0$. Although a strategy with large values of θ keeps a user with fixed SIR (hence fixed rate), it cause strong interference to the cell-edge of neighbouring cells or deprive cell-centre users from high SIR gain that is necessary for QoS guarantee.

3.7 Chapter Summary

This chapter studied and analysed coverage probability and effective capacity in MIMO downlink cellular networks employing distance-based power control. Using spatial PPP model, tractable, analytical expressions for coverage probability and effective capacity are derived for two system scenarios; a scenario of fractional power control and no multicell coordination and a scenario with multicell coordination. The numerical results shows that for coverage probability, the strategy of power control factor $\eta \leq 0.25$ is the best in low thresholds, while constant power allocation outperforms the others in high thresholds. Moreover, for effective capacity the constant power allocation strategy performs better in low QoS constraints, while fractional power control factors, i.e. $\eta \leq 0.25$, outperforms the other strategies in high QoS constraints. Numerical results also reveal that coordination performs better when the interferers are close enough to the served user, while MRT is better when the interferers are far enough from the served user, hence suggesting that suitable adaptive strategy yields better perfromance as will be proved in the next chapter.

Chapter 4

Adaptive Coordination Inter-Cell Interference Cancellation in Cellular Networks

This chapter proposes an adaptive coordination and inter-cell interference cancellation strategy for downlink cellular network. This technique exploits coordination on frequency domain while cancelling interference on space domain using MIMO. Two variant schemes are presented for such an adaptive interference management strategy. Analytical expressions are derived for coverage probability and average rate for both schemes.

4.1 Introduction

Since the inter-cell interference has been regarded as the major challenge facing densely-deployed mobile networks with aggressive spectrum reuse [56], [81], [108], there has been extensive research addressing this problem in the last few years. Var-

ious approaches including scheduling, power control, and multicell coordination have been proposed in [56], [59], [60], [66] to minimise the inter-cell interference. Multicell MIMO is considered as an effective approach to eliminate inter-cell interference, and two variants have been proposed; cooperative MIMO and coordinated MIMO. In the cooperative MIMO, a number of neighbouring cells cooperate to form a cluster and operate as a one giant BS working effectively to manage the interference by utilising spatial domain [56], [59], [60], [66]. With the cooperative MIMO, the system utilises all the degrees of freedom and, thus, all BSs in a cluster transmit to all users. Using cooperative MIMO to manage the interference, however, requires both data and CSI of users in different cells to be exchanged among the BSs within a cluster; thus, a tight synchronization and low latency is required along with overhead signalling [56], [60]. Nevertheless, cooperative MIMO has attracted a great deal of attention, and various techniques and approaches have been proposed [56], [59], [63] in this context.

On the other hand, for coordinated MIMO, a group of BSs exchange only CSIs of their users and coordinate their beamforming strategies accordingly [64], [66], [67]. More specifically, each BS serves only its own users but attempt to cancel interference on the users in other cells. Although coordinated MIMO requires overhead signalling less than that of cooperation, it still consumes significant amount of resources. To overcome the problem of overhead signalling, distributed schemes are proposed in [63], [67]. In [73], a low complexity coordination strategy is proposed to suppress the inter-cell interference. The authors proposed an adaptive strategy where a cluster of BSs jointly select beamforming techniques. Closed-form expressions are derived for two cells scenario for the proposed strategy selection. In [74], the authors extended the work in [73] to user scheduling and proposed a strategy selection to maximise system throughput. Following the same line of reasoning, strategy selection for cooperation scheme is proposed in [111], where different strategy transmission is adopted based on user location.

The cluster of BSs can also use a frequency domain method, instead of spatial domain, to mitigate inter-cell interference using ICIC techniques [81], [109]. In ICIC, each cell allocates its spectrum resources such that interference created is minimised [81], [109].

FFR and SFR are two variants of ICIC techniques [109]. The basic idea of ICIC is to partition the cell area into inner and outer regions and divide the bandwidth used in each cell such that orthogonal resources are allocated for the outer region users in overlapping cell-edge areas, hence reducing the interference experienced by cell-edge users [109]. ICIC techniques can remarkably improve system spectral efficiency and outer region users throughput [109], [110]. It is worth emphasising the difference between two terms used in this thesis, i.e. interference cancellation and interference coordination. The first term is used to refer to the process of cancelling interference on space domain by using coordinated MIMO technique, whereas the later term refers to interference mitigation implemented on frequency domain as mentioned above. It can be noticed from all aforementioned works that no joint interference cancellation and interference coordination is considered. Besides, all were restricted to only specific cellular system geometry. Thus, these works based their analyses on the deterministic grid or lattice cellular models, which is an optimistic and unrealistic assumption. Since deterministic models are unamenable to analysis, and due to the fact the wireless networks are randomly deployed, there has been a growing interest in considering random networks. Stochastic geometry approach provides elegant mathematical tools for dealing with such random systems [29], [112]. Thereby they are effectively utilised for deriving expressions for coverage probability and average rate in cellular systems [98], [97]. This approach is, while being much more tractable, proven to be as accurate as a hexagonal or a lattice based cellular system models. The stochastic geometry has been used to analyse the performance in different network scenarios. Thus, in [113]-[116], multicell cooperation is analysed assuming random system layout. In [116], asymptotic analysis using large deviation results are conducted to study cooperation in cellular networks. In [117], single-antenna multicell coordination is analysed for the asymptotic regimes, but the authors do not consider coordinated MIMO. In [118], successive interference cancellation technique is analysed in heterogeneous networks, but the work does not consider coordinated MIMO as well. In [119], [120], user-centric coordinated MIMO is considered. In [119], quantised channel feed back is analysed and optimised in random clustering. In [120], performance of coordinated beamforming with dynamic clustering is characterised. The authors assume a cluster-

based coordination defined for a given user. However, [119] and [120] only assume interference cancellation strategy which is not necessarily an optimal choice as will be explained in the subsequent sections. Moreover, these works do not consider other approaches such frequency-based coordination strategies.

Unlike the aforementioned works, in this chapter, multicell coordination strategy is proposed for downlink cellular systems to mitigate interference on both frequency and space domain. More specifically, this strategy combines interference cancellation enabled by coordinated MIMO with ICIC on space and frequency domains, respectively. On space domain, the system adaptively switches between MRT and CBF techniques, where the adaptation takes place over different spectrum bands according to the user channel condition. Two schemes for this strategy were proposed; the first scheme considers a priority of enhancing the performance of inner region users, while the second scheme yields better fairness between inner region and outer region users. We use stochastic geometry approach to derive analytical expressions for coverage probability. The numerical results reveal that this strategy can significantly outperform any other strategy with only CBF strategy.

The main contributions of this chapter are summarised as follows:

- Firstly, an adaptive scheme is proposed for multicell coordination in which each cell area is divided into an inner and outer region with different spectrum bands being utilised over these regions. Users in the outer region served via CBF strategy. While users in the inner region are served through MRT only.

- Secondly, another adaptive scheme is proposed where the same cell regions are considered but with different frequency planning and coordination strategies. More specifically, a user in the outer region is served through MRT while being helped by other BSs, i.e. they cancel the interference experienced by the user. Whereas a user in the inner region scarifies some of its degrees of freedom to help outer region users in other cells. However, this inner region user is not helped by other BSs.

- For both proposed schemes, stochastic geometry tools are utilised to model the BSs positions as a homogeneous PPP. Following this approach, a tractable, statistical model is introduced to evaluate the system performance with such adaptive strategies. For a typical user, we derive analytic expressions for SINR distributions in both schemes as a function of the main system parameters, namely path loss, BS density, number of antennas per BS. Then, an expression for average rate is derived in both schemes.

The remainder of this chapter is organised as follows. Section 4.2 describes the proposed system model as well as the proposed adaptive coordination strategy. Section 4.3 presents the proposed adaptive coordination strategy, its two schemes, the main results of coverage analysis for the two proposed schemes, and the analytical expression of average rate. Section 4.4 presents numerical results of the proposed strategy. Finally, 4.5 summarises the chapter.

4.2 System Model

Consider a downlink multi-carrier multicell cellular system. BSs are positioned in a two-dimensional horizontal plane as a homogeneous spatial PPP Φ with density λ. In PPP, the number of nodes, e.g. BSs in a given bounded area A is a random variable (r.v.) following Poisson distribution with their positions being uniformly distributed. Thus, the cell boundaries are shown to be Voronoi tessellation [112], as shown in Fig. 4.1. Since a homogeneous PPP is considered, the statistics evaluated for every node in the system will be similar. Hence, the analysis will be performed based on a typical user at the origin. This is justified by Slivnyak's [29], [112], which states that the statistical properties observed by a typical point of the Φ are similar to those observed by a point at the origin in the process $\Phi \cup \{0\}$. The BSs distances from this typical user are given according to the homogeneous PPP, $\Phi = \{r_k, k \in \mathbb{N}\}$, on the two dimensional plane $\mathbb{R}^2$ [112] where r_k denotes the distance from the kth BS. The user is assumed to be associated with the nearest base station denoted as BS_1 and

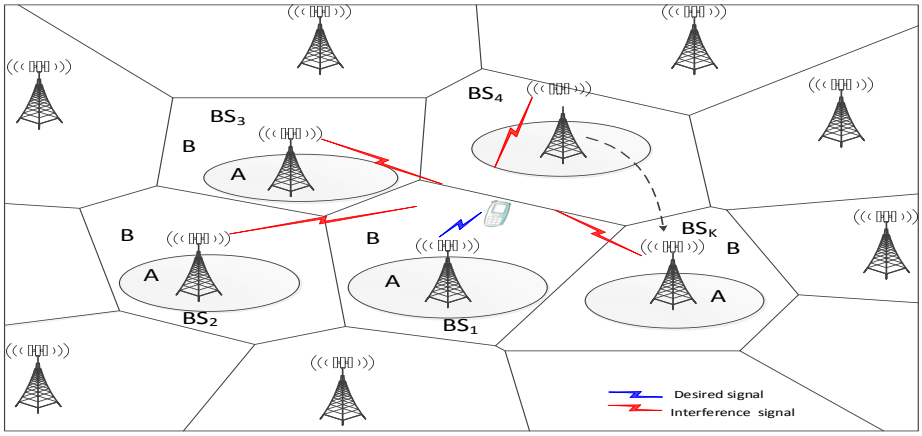

Figure 4.1: Distribution of BSs in a two-dimensional plane with cell boundaries forming a Voronoi tessellation, with each user associated with the nearest BS. Each cell has an inner and outer region where the inner region is illustratively given the shape of a circle.

located at distance r_1 from it. While all other BSs are regarded as interferers to this user as illustrated in Fig. 4.1.

Each BS has N_t antennas, while users are equipped with only single antenna. It is also assumed that a set of K neighbouring of BSs form a cluster and employ coordination over both space and frequency for the sake of interference management. For a cluster, the spectrum is partitioned into two groups of subbands w_c and w_e dedicated for regions A and B, respectively as shown in Fig. 4.1.

Each BS classifies users into inner and outer region user based on signal to noise and interference ratio (SINR) threshold value $\bar{\gamma}_2$. Users with SINR greater than $\bar{\gamma}_2$ are classified as inner region users, and otherwise outer region users.

In this system set up, it is considered that the channel between the user and any BS experiences small-scale fading and path-loss. Although shadowing can also be assumed here, however, it has been proven in [121] that the distribution of SINR for a typical user is invariant with respect to an additional fading distribution with the PPP assumption, given that a network is represented by a sufficiently large ho-

mogeneous point pattern. Thus, the impact of both path loss and small-scale fading on the received signal are sufficient to be considered in the analysis while adding the shadowing is irrelevant in this case.

Assuming that each user is able to estimate its downlink channel perfectly and feeds CSI back to its serving BS by means of dedicated pilot signal. If the user is assumed to be helped through coordination it should also estimate its channels to $K-1$ BSs and feed them back to its serving BS whereby they are conveyed to the other BSs through delay-free unlimited capacity links.

Let us denote the downlink small-scale channel vector between the typical user and kth BS as $\mathbf{h}_k = [h_1, ..., h_{N_t}] \in \mathbb{C}^{1\times N_t}$, where each component of $\mathbf{h}_k$ are an independent and identically distributed (i.i.d) complex Gaussian r.v with zero mean and unit variance, i.e. $\mathcal{CN}(0,1)$. The transmit signal satisfies $\mathbb{E}\{\mid x \mid^2\} \leq P$. While z as the additive Gaussian noise such that $z \sim \mathcal{CN}(0,1)$.

It is considered that each BS uses one of the following two main beamforming techniques.

1- *MRT Beamforming*: as discussed in Chapter 3, if the channel vector is $\mathbf{h}$, the MRT Beamforming is constructed as $\mathbf{v} = \frac{\mathbf{h}^{\mathsf{H}}}{\|\mathbf{h}\|}$.

2- *CBF*: similar to CB discussed in Chapter 3, for a given nth user with channel vector $\mathbf{h}_n$, the CBF vector can be obtained by projecting the vector $\mathbf{h}_n$ on the null space of $\hat{\mathbf{h}}_{\mathrm{n}} = \left[\mathbf{h}_1^{\mathsf{H}}, ..., \mathbf{h}_{n-1}^{\mathsf{H}}, \mathbf{h}_{n+1}^{\mathsf{H}}, ..., \mathbf{h}_{N_t}^{\mathsf{H}}\right]^{\mathsf{H}}$:

$$\mathbf{v}_n = (\mathbf{I} - \mathcal{P}_{\hat{\mathbf{h}}_n})\mathbf{h}_n \tag{4.1}$$

where $\mathcal{P}_{\hat{\mathbf{h}}_n}$ is defined as the projection on $\hat{\mathbf{h}}_n$, given as $\mathcal{P}_{\hat{\mathbf{h}}_n} = \hat{\mathbf{h}}_n^{\mathsf{H}}(\hat{\mathbf{h}}_n\hat{\mathbf{h}}_n^{\mathsf{H}})^{-1}\hat{\mathbf{h}}_n$ [41], [73].

As previously discussed, the multiplication of the channel and beamforming vectors, i.e., $\mid \mathbf{v}_n^{\mathsf{H}}\mathbf{h}_k \mid^2$ is an i.i.d r.v. following gamma distribution, i.e. $\Gamma(\Delta, 1)$, where Δ is a parameter depending on the beamforming strategy and is given by $\Delta = N_t - K + 1$,

where K is the number of BSs participating in coordination [103]. If CBF is used for cancelling interference experienced by $N_t - 1$ users then $\Delta = 1$. The desired received signal for a typical user at the origin is given by $P \mid \mathbf{v}_1^{\mathsf{H}}\mathbf{h}_1 \mid^2 r_1^{-\alpha}$, where α is the path loss exponent. The aggregate interference resulting from the other BSs is given as $I = \sum_{i\in\Phi/\{b_1\}} P \mid \mathbf{v}_i^{\mathsf{H}}\mathbf{h}_i \mid^2 r_i^{-\alpha}$. In [103], it is proven that, for the interfering links, the product of channel and beamforming vectors is gamma r.v., i.e. $\mid \mathbf{v}_i^{\mathsf{H}}\mathbf{h}_i \mid^2 \sim \Gamma(1,1)$. For notational convenience, let $\mid \mathbf{v}_1^{\mathsf{H}}\mathbf{h}_1 \mid^2$ and $\mid \mathbf{v}_i^{\mathsf{H}}\mathbf{h}_i \mid^2$ be denoted as g_o and g_i, respectively. Therefore, the received signal to interference and noise ratio is defined as:

$$\text{SINR} = \frac{P g_o r_1^{-\alpha}}{\sigma^2 + I} \tag{4.2}$$

where $I = \sum_{i\in\Phi/\{b_1\}} P g_i r_i^{-\alpha}$, and σ^2 is the noise power.

4.3 Adaptive Interference Coordination and Cancellation

Now, the proposed schemes of the adaptive strategy are presented. As discussed previously, the strategy is implemented on both frequency and space domain. Suppose that the whole spectrum is partitioned based on reuse factor K into subbands with equal bandwidths, the set of which is given by $\mathcal{F} = \{f_1, ..., f_K\}$. Denote Δ as the number of BSs sharing the same subband in the outer region. Then, the proposed schemes are described as follows:

1- **Inner-MRT Outer-CBF (IMOC)**: In this scheme, cells in a cluster re-utilise the subbands allocated for users in inner and outer regions. Let $w_e \in \{f_1\}$ represent the subband shared by K cells in their outer region, i.e. the BSs in one cluster use the same band in their outer region, thus, $\Delta = K$. Then, $w_c \in \mathcal{F}/\{f_1\}$ will be shared in their inner regions. Depending on the channel quality, CBF and MRT techniques are implemented on subbands w_e and w_c, respectively. Thus, if the user has good channel condition, it will be consid-

ered as an inner region user, and the transmission is performed based on MRT beamforming. Otherwise, if it suffers from high interference (and thereby degraded channel condition), it will be regarded as an outer region user where CBF is implemented in transmission instead. Thus, K BSs coordinate toward each other to eliminate interference from K users.

2- **Inner-CBF Outer-MRT (ICOM)**: In this scheme, the kth cell uses the subbands $w_c \in \mathcal{F}/\{f_k\}$ and $w_e \in \{f_k\}$ for its inner and outer region, respectively, in a similar fashion to that of spectrum partitioning in SFR. For example, when $K = 3$, the BS_1 uses $w_c \in \mathcal{F}/\{f_1\}$ and $w_e \in \{f_1\}$ for its inner and outer regions, respectively. The BS_2 utilises $w_c \in \mathcal{F}/\{f_2\}$ and $w_e \in \{f_2\}$ for its inner and outer regions, respectively. Likewise for BS_3, it uses $w_c \in \mathcal{F}/\{f_3\}$ and $w_e \in \{f_3\}$ for its inner and outer regions, respectively. In this case, $\Delta = 1$, because there is only one BS using single subband in the outer region. There can be also assumed varying degrees of spectrum reuse in the outer region, such as $\Delta = 2$, in which, for example, BS_1 and BS_2 can use $w_e \in \{f_1\}$, while BS_2 uses $w_e \in \{f_3\}$.

   Denote $\mathcal{B}$ as the set of all K BSs, and $\mathcal{B}_i$ as $\mathcal{B}_i = \mathcal{B}/\{\mathrm{BS}_i\}$. For a given subband f_i, define the set of beamforming strategies on subband f_i as $\mathcal{S}_{f_i} = \{\mathrm{MRT}, \mathrm{CBF}(\mathcal{B}_i)\}$, where $\mathrm{CBF}(\mathcal{B}_i)$ is the strategy that all BSs in the set $\mathcal{B}_i$ are doing CBF towards a user associated with BS_i on f_i. Then, an outer region user associated with BS_k is served via MRT on subband w_e. While its inner region user is served via $\mathrm{CBF}(\mathcal{B}_i), i \neq k$. For example, on subband f_1, the BS_1 utilises MRT, i.e. it doesn't coordinate, while other BSs in the set $\mathcal{B}_1$ use $\mathrm{CBF}(\mathcal{B}_1)$, i.e. they coordinate toward it. Thus, in contrast to IMOC, different beamforming strategies can be employed by the BSs on each subband. The justification for this is the fact that the user in the inner region usually enjoys good channel condition, then it is affordable to sacrifice some of its degrees of freedom for the sake of cancelling out interference experienced by an outer region user in a neighboring cell.

4.3.1 Coverage Probability Analysis

Coverage probability is an important metric characterising the system performance. A typical user is said to be covered if the downlink instantaneous signal-to-interference and noise ratio SINR is greater than a threshold value $\bar{\gamma}$. The coverage probability, which is equivalent to the CCDF of the SINR, can be defined as:

$$P_c = \mathbb{P}(\text{SINR} > \bar{\gamma}) \tag{4.3}$$

In general case and regardless of any adaptive coordination and cancellation techniques, the coverage probability of a typical user assuming multiple antenna transmission is given by the following theorem:

Proposition 4.1: The coverage probability, P_c, for a typical user in downlink MIMO channel is given by:

$$P_c = \mathbb{E}_{r_1}\left\{ \sum_{n=0}^{N} \frac{r^{\alpha n}}{n!}(-1)^n \frac{\mathrm{d}^n \mathscr{L}_{\bar{I}}(s)}{\mathrm{d}s^n} \right\} \tag{4.4}$$

where $\mathscr{L}_{\bar{I}}(s)$ represents the Laplace transform of $\bar{I}$, and $\bar{I} = \sigma^2 + I$ which can be obtained as in (B.8), and $s = r_1^{\alpha}$.

Proof: See Appendix B.1.

4.3.2 Coverage Upper Bound With The IMOC Scheme

As previously mentioned, a user is identified as an outer region user if its SINR is smaller than threshold $\bar{\gamma}_2$ on subband w_c, otherwise it is regarded as an inner region user. Therefore, the coverage probability of a typical user in inner region is conditioned on SINR $< \bar{\gamma}_2$, and the conditional probability is expressed as

$$\mathbb{P}\big(\text{SINR}_{inner} > \bar{\gamma}_1 \mid \text{SINR} > \bar{\gamma}_2\big) = \mathbb{P}\left(\frac{P\hat{g}_o r_1^{-\alpha}}{\sigma^2 + I} > \bar{\gamma}_1 \mid \frac{P g_o r_1^{-\alpha}}{\sigma^2 + I} > \bar{\gamma}_2 \right)$$

where $\bar{\gamma}_1$ is the new threshold for inner region user. In the following proposition, the coverage probability for a typical inner region user is introduced.

Proposition 4.2 *(IMOC, inner region user)*: The upper bound of coverage probability of a typical inner region user in the IMOC scheme, $P_{\mathrm{IMOC},i}(\bar{\gamma}_1, \bar{\gamma}_2, \lambda)$, is given by :

$$P_{\mathrm{IMOC},i}(\bar{\gamma}_1, \bar{\gamma}_2, \lambda) \leq \frac{\sum_{n=1}^{N_1} \binom{N_1}{n} (-1)^{n+1} \int_0^\infty r_1 \exp(-\mathcal{A}_o r_1^\alpha - \pi\lambda(1+2\psi(s_o))r_1^2) \mathrm{d}r_1}{\sum_{m=1}^{N_2} \binom{N_2}{m} (-1)^{m+1} \int_0^\infty r_1 \exp(-\mathcal{A}_2 r_1^\alpha - \pi\lambda(1+2\psi(s_2))r_1^2) \mathrm{d}r_1} \tag{4.5}$$

where $\mathcal{A}_o = s_o\sigma^2/P$, $s_o = n\zeta_1 \max\{\bar{\gamma}_1, \bar{\gamma}_2\}$, $\mathcal{A}_2 = s_2\sigma^2/P$, $s_2 = m\zeta_2\bar{\gamma}_2$, and

$$\psi(s_n) = \frac{s_n}{\alpha - 2} {}_2F_1\left(1, 1 - \frac{2}{\alpha}; 2 - \frac{2}{\alpha}; -s_n\right) \tag{4.6}$$

Proof: See Appendix B.2.

The coverage probability given above is a function of the main system parameters. Note that the integral in (4.5) is for de-conditioning with respect to r_1. While the expression in (4.5) holds for any system parameters values, it can be derived in a closed-form expression for the case of $\alpha = 4$ as in the following corollary.

Corollary 4.1: For path-loss value $\alpha = 4$, the upper bound of $P_{\mathrm{IMOC},i}(\bar{\gamma}_1, \bar{\gamma}_2, \lambda)$ can be obtained as:

$$P_{\mathrm{IMOC},i}(\bar{\gamma}_1, \bar{\gamma}_2, \lambda) \leq \frac{\sum_{n=1}^{N_1} \binom{N_1}{n} \frac{(-1)^{n+1}}{\sqrt{\mathcal{A}_o}} \exp\left(\frac{G^2(s_o)}{8\mathcal{A}_o}\right) D_{-1}\left(\frac{G(s_o)}{\sqrt{2\mathcal{A}_o}}\right)}{\sum_{m=1}^{N_2} \binom{N_2}{m} \frac{(-1)^{m+1}}{\sqrt{\mathcal{A}_2}} \exp\left(\frac{G^2(s_2)}{8\mathcal{A}_2}\right) D_{-1}\left(\frac{G(s_2)}{\sqrt{2\mathcal{A}_2}}\right)} \tag{4.7}$$

where $G(x)$ is defined as:

$$G(s_n) = \lambda\pi + \frac{s_n}{\alpha - 2} {}_2F_1\left(1, 1 - \frac{2}{\alpha}; 2 - \frac{2}{\alpha}; -s_n\right) \tag{4.8}$$

$D_{-\nu}(.)$ is the parabolic cylinder function which can be calculated by $D_{-1}(x) = \sqrt{\frac{\pi}{2}} e^{x^2/4} \mathrm{erfc}\left(\frac{x}{\sqrt{2}}\right)$ for $\nu = 1$, where $\mathrm{erfc}(x)$ is the complementary error function and defined as: $\mathrm{erfc}(x) = \frac{2}{\sqrt{\pi}} \int_x^\infty e^{-t^2} \mathrm{d}t$ [107].

Proof: See Appendix B.3.

Now, the attention is turned to the outer region user and proceed to derive the upper bound of coverage probability for this case. As described previously, a user is considered as an outer region user if its SINR is smaller than a predetermined threshold, i.e. $\text{SINR} < \bar{\gamma}_2$, and is therefore allocated a new subband w_e and helped by neighbouring BSs through CBF technique.

$$\mathbb{P}\big(\text{SINR}_{outer} > \bar{\gamma}_1 \mid \text{SINR} < \bar{\gamma}_2\big) = \mathbb{P}\bigg(\frac{P\hat{g}_o r_1^{-\alpha}}{\sigma^2 + I} > \bar{\gamma}_1 \mid \frac{P g_o r_1^{-\alpha}}{\sigma^2 + I} < \bar{\gamma}_2\bigg)$$

Similar to the previous chapter, for the subsequent analysis, the parameter ρ is defined as the ratio of the distance between the typical user and its serving BS_1 over its distance to the BS_K, $\rho = \frac{r_1}{r_K}$. This parameter allows us to incorporate r_K through r_1 and ρ, and, hence, making the analysis more tractable. Now, let us proceed to derive the coverage probability conditioned on ρ, then we de-condition on it. The following proposition gives the coverage probability upper bound.

Proposition 4.3 *(IMOC, outer region user)*: The upper bound of coverage probability for the typical outer region user in the IMOC scheme conditioned on ρ with coordination being employed, $P_{\text{IMOC},e|\rho}(\bar{\gamma}_1, \bar{\gamma}_2, \lambda)$, is given by:

$$P_{\text{IMOC},e|\rho}(\bar{\gamma}_1, \bar{\gamma}_2, \lambda) \leq \frac{\Upsilon_1(\rho, \bar{\gamma}_1) - \Upsilon_2(\rho, \bar{\gamma}_1, \bar{\gamma}_2)}{1 - 2\pi\lambda \sum_{m=1}^{N_2} \binom{N_2}{m} (-1)^{m+1} \int_0^\infty r_1 \exp(-\mathcal{A}_2 r_1^\alpha - \pi\lambda(1 + 2\psi(s_2)) r_1^2) \mathrm{d}r_1} \tag{4.9}$$

where:

$$\Upsilon_1(\rho, \bar{\gamma}_1) = 2\pi\lambda \sum_{n=1}^{N_1} \binom{N_1}{n} (-1)^{n+1} \int_0^\infty r_1 e^{-\mathcal{A}_1 r_1^\alpha - \pi\lambda(1 + 2\psi(s_3)/\rho^2) r_1^2} \mathrm{d}r_1 \tag{4.10}$$

$$\Upsilon_2(\rho, \bar{\gamma}_1, \bar{\gamma}_2) = 2\pi\lambda \sum_{n=1}^{N_1} \sum_{m=1}^{N_2} \binom{N_1}{n} \binom{N_2}{m} (-1)^{n+m} \int_0^\infty r_1 e^{-(\mathcal{A}_1 + \mathcal{A}_2) r_1^\alpha - \pi\lambda r_1^2} \mathcal{Q}(r_1, \rho, s_1, s_2) \mathrm{d}r_1 \tag{4.11}$$

where

$$\mathcal{Q}(r_1,\rho,s_1,s_2)=e^{-2\pi\lambda\int_{r_1}^{r_K}\left(1-\frac{1}{1+s_2r_1^{\alpha}\nu^{-\alpha}}\right)\nu\mathrm{d}\nu}e^{-2\pi\lambda\int_{r_K}^{\infty}\left(1-\frac{1}{1+s_2r_1^{\alpha}\nu^{-\alpha}}\times\frac{1}{1+s_1r_1^{\alpha}\nu^{-\alpha}}\right)\nu\mathrm{d}\nu} \quad (4.12)$$

where $\psi(.)$ is defined in (4.6), and $\mathcal{A}_1 = s_1\sigma^2/P$, $s_1 = n\zeta_1\bar{\gamma}_1$, $s_3 = n\rho^{\alpha}\zeta_1\bar{\gamma}_1$, and $r_K = r_1/\rho$.

Proof: See Appendix B.4.

The integrations in the above expressions can be easily numerically evaluated. Furthermore, for the special case of $\alpha = 4$, the terms $\Upsilon_1(\rho,\bar{\gamma}_1)$ and denominator can be expressed in closed-form expressions similar to Corollary 1. Note that the $\Upsilon_1(\rho,\bar{\gamma}_1)$ represents the conditional coverage probability of coordinated-MIMO with no adaptation. ρ sheds light on the advantage of interference cancellation. The case $\rho \longrightarrow 0$ corresponds to the nearest interferers being far away from the user, in which case no interference cancellation may outperform IMOC. When $\rho \longrightarrow 1$, this implies that the nearest interferers are close to the user, thereby interference cancellation becomes more useful. In contrast to the inner region user case, the outer region user suffers less interference due to employing interference cancellation as can be seen from the Laplace transform in (B.13). However, this comes at the price of losing some of the degree of freedom. Arguably, although interference cancellation may not always lead to better performance with such loss in the degrees of freedom, the simulation and numerical results reveal that the coverage probability of an outer region user in IMOC is worsen with such loss in degrees of freedom.

To de-condition the coverage expression in (4.9) on ρ, we use the following corollary.

Corollary 4.2: The unconditioned $P_{\mathrm{IMOC},e}(\bar{\gamma}_1,\bar{\gamma}_2,\lambda)$ is given by:

$$P_{\mathrm{IMOC},e}(\bar{\gamma}_1,\bar{\gamma}_2,\lambda) \leq \frac{2(K-1)\sum_{i=1}^{N} w_i x_i (1-x_i^2)^{K-2}\big(\Upsilon_1(x_i,\bar{\gamma}_1)-\Upsilon_2(x_i,\bar{\gamma}_1,\bar{\gamma}_2)\big)}{1-2\pi\lambda\sum_{m=1}^{N_2}\binom{N_2}{m}(-1)^{m+1}\int_0^{\infty} r_1\exp(-\mathcal{A}_2 r_1^{\alpha}-\pi\lambda(1+2\psi(s_2))r_1^2)\mathrm{d}r_1} \quad (4.13)$$

where x_n is the nth zero of the Hermite polynomial $\mathrm{H}_n(x)$ of degree N, w_n is the corresponding weight of the function $f(.)$ at the nth abscissa [105], [107].

Proof: See Appendix B.5.

4.3.3 Coverage Upper Bound With The ICOM Scheme

Similar to the IMOC scheme, in ICOM scheme the spectrum is partitioned into two groups of subbands w_c and w_e for inner region and outer region, respectively. Recall that, an inner region user associated with BS_k is served via $\mathrm{CBF}(\mathcal{B}_i), i \neq k$ on subband w_c. While an outer region user is served via MRT on subband $w_e \in \{f_k\}$. Hence, the user sacrifices some of its degrees of freedom to help other cells users, which can be afforded because the inner region user usually enjoys good channel quality. Thus, in contrast to IMOC scheme in which high priority is given to the inner region users, ICOM scheme provides better fairness between inner region and outer region users. The expression of coverage probability can be obtained by following the same previous procedure in subsection 4.3.2 so the discussion will be concise.

Proposition 4.4: The upper bound of coverage probability for a typical inner region user in the ICOM scheme,$P_{\mathrm{ICOM},i}(\bar{\gamma}_1, \bar{\gamma}_2, \lambda)$, is given by

$$P_{\mathrm{ICOM},i}(\bar{\gamma}_1, \bar{\gamma}_2, \lambda) \leq \frac{\sum_{n=1}^{N_1}\sum_{m=1}^{N_2}\binom{N_1}{n}\binom{N_2}{m}(-1)^{n+m}\int_0^\infty r_1 \exp(-(\mathcal{A}_1+\mathcal{A}_2)r_1^\alpha - \pi\lambda(1+2\psi(s_1))r_1^2)\mathrm{d}r_1}{\sum_{m=1}^{N_2}\binom{N_2}{m}(-1)^{m+1}\int_0^\infty r_1 \exp(-\mathcal{A}_2 r_1^\alpha - \pi\lambda(1+2\psi(s_2))r_1^2)\mathrm{d}r_1} \tag{4.14}$$

where $N_1 = N_t - \Delta$, and $\psi(s_n)$ is given by (4.6)

Proof: See Appendix B.6.

Obviously, in ICOM scheme the received power of inner region user will be less than that of IMOC scheme due to loss in degrees of freedom required for coordination while benefiting the outer region user as in the following theorem. The upper bound of the coverage probability for the outer region user in the second scheme is given by the following proposition.

Proposition 4.5: The upper bound of coverage probability for a typical outer region user in the ICOM scheme, $P_{\mathrm{ICOM},e}(\bar{\gamma}_1, \bar{\gamma}_2, \lambda)$, is given by (4.13) with $N_1 = N_t - \Delta + 1$.
Proof: See Appendix B.7.
Recall that Δ, $1 \leq \Delta < K$, denotes the number of lost degrees of freedom in ICOM. The case of $\Delta = 1$ implies that there is only one BS transmitting by MRT technique in the cluster of coordinating BSs. Hence, the case will be equivalent to the frequency pattern in SFR. The case of $\Delta > 1$ means that the subband w_e is reused in the outer regions of Δ BSs, then the BSs serving outer region users will transmit with partial interference cancellation in which the interference is cancelled from Δ outer region users. ICOM allows adjacent BSs to serve inner region users on the same subbands used by adjacent outer region users, while attempting to coordinate toward them. Thus, the CCDF is similar in structure to $P_{\mathrm{IMOC},e}$, and only N_1 differs in expressions.

4.3.4 Average Rate

In modern cellular mobile networks, the average rate is the most important performance metric. Here, the average user rate is derived using the same technical tools used for deriving coverage probability.

Assuming adaptive modulation and coding such that the a typical user can achieve the data rate given in nats/Hz. The average rate of an outer region user is given by:

$$\widetilde{R} = \mathbb{E}\{\ln(1 + \mathrm{SINR})\} \tag{4.15}$$

The next proposition provides an expression for the average rate of a typical outer region user in the IMOC scheme. For the other cases, the same procedure can be followed.
Proposition 4.6: The upper bound of the average ergodic rate of a typical outer

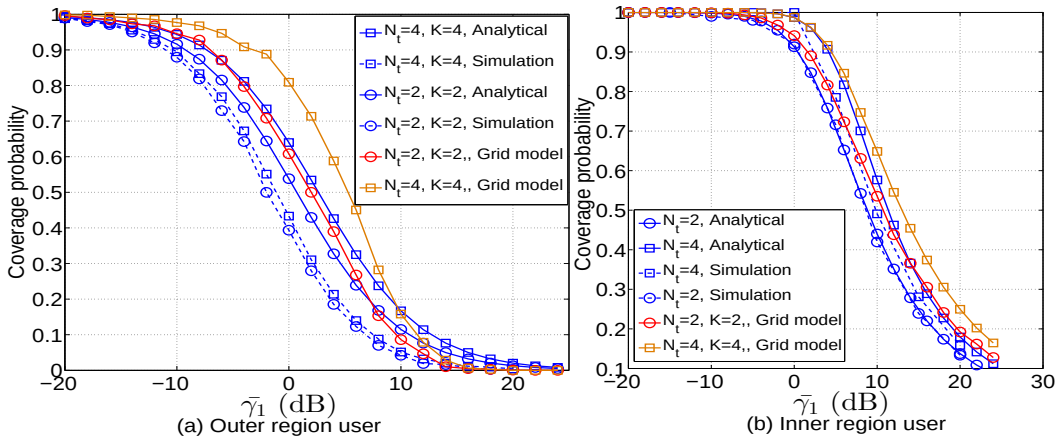

Figure 4.2: Comparison between simulation results and derived analytical results for a typical outer region user and an inner region user in IMOC scheme, respectively ($P = 1, \alpha = 4, \bar{\gamma}_2 = 1$ dB).

region user in IMOC scheme, $\widetilde{R}_{\mathrm{IMOC},e}$, is given by:

$$\widetilde{R}_{\mathrm{IMOC},e} \leq \int_{t>0}^{\infty} P_{\mathrm{IMOC},e}(e^t - 1, \bar{\gamma}_2, \lambda)\mathrm{d}t \tag{4.16}$$

where $P_{\mathrm{IMOC},e}(e^t - 1, \bar{\gamma}_2, \lambda)$ is given by (4.9).

Proof: See Appendix B.8.

4.4 Numerical Results and Discussion

In this section, the analytical results of coverage obtained based on PPP model are compared with the simulation of both PPP and grid models. The system performance and the influence of the key system parameters on system performance on coverage probability will be discussed thoroughly. While the results presented in Section 4.3 hold true for general system parameters, i.e. path-loss exponent and noise power, the cases, $\alpha = 4$ and $\bar{\gamma}_2 = 1$ dB, are considered in the simulation and numerical results. The transmission power is assumed to be constant in all cases and normalised to $P = 1$.

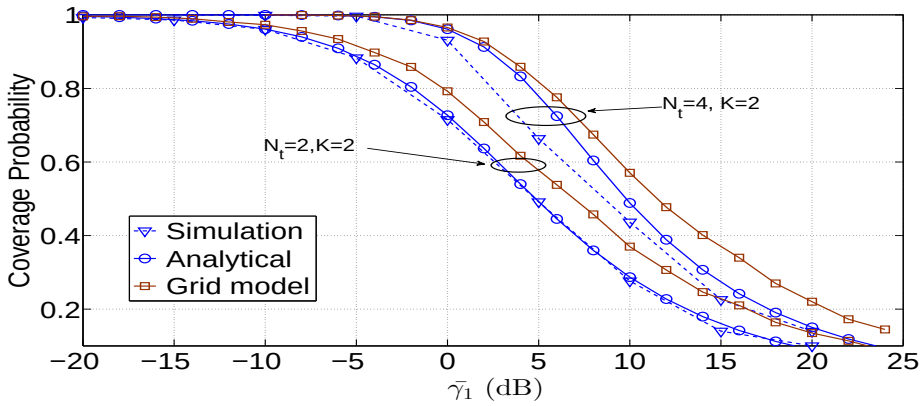

Figure 4.3: Comparison between simulation results and derived upper bounds analytical results for inner region in ICOM scheme for different number of transmit antennas ($P = 1, \alpha = 4, \bar{\gamma}_2 = 1$ dB).

To simulate PPP model, a bounded area of 10km^2 is considered. The density of BSs in this area is $\lambda = 1/(30000 * \pi^2)$ BS per m^2. The number of BSs follows Poisson distribution. Then, the BSs are distributed uniformly on the bounded area. The points distributed as such represents one realization of point process, then a single value of coverage probability is obtained by averaging over 10^5 iterations. A grid model is also considered in the simulation assuming uniformly spaced square area of BSs. For simulation purposes, 36 BSs are positioned at regular distance from each other.

In Figs. 4.2(a) and (b), a comparison is made between the CCDFs of SINR of inner region user and outer region user in the proposed IMOC scheme, respectively with PPP and grid models. It is assumed that $\sigma^2 = 0$, parameters setting $\zeta_1 = 1$ and $\zeta_2 = 1$ for inner region user and $\zeta_1 = 1$ and $\zeta_2 = (N_2!)^{-1/N_2}$ for outer region user. It can be clearly observed that the grid model is more optimistic and gives the upper bound on coverage probability. This is due to the regular layout of BSs in grid model and the restriction of minimum distance between BSs, resulting in an optimal geometry from coverage perspective. While PPP model, on the other hand, is indeed a lower on the achievable coverage. The reason is that in PPP model the BSs number and distances between BSs are both random, and therefore strong interference can be generated

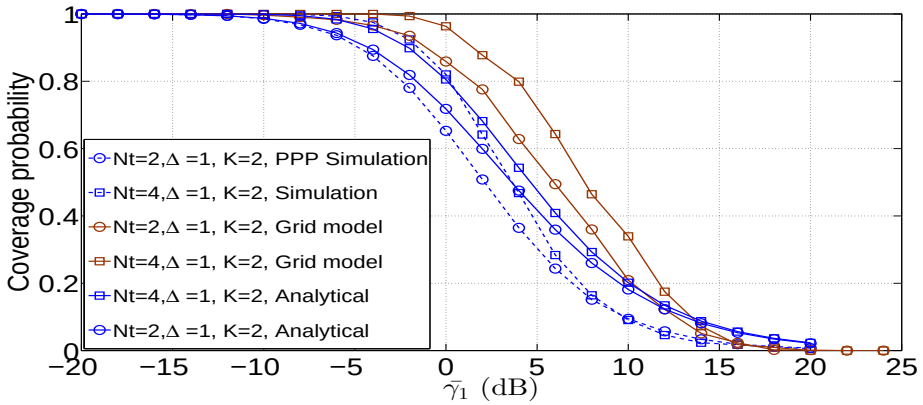

Figure 4.4: Comparison between simulation results and derived analytical results for outer region in ICOM scheme for different number of transmit antennas ($P = 1, \alpha = 4, \bar{\gamma}_2 = 1$ dB).

from nearby BSs. The analytical expressions give an excellent approximation results in between for the entire range of $\bar{\gamma}_2$.

Similarly, in Figs. 4.3 and 4.4, a comparison is shown between the CCDFs of the SINR of the inner and outer region users in the proposed ICOM scheme with PPP simulation model assuming $\sigma^2 = 0$ and setting the parameters values $\zeta_1 = (N_1!)^{-1/N_1}$ and $\zeta_2 = 1$ for inner region user and $\zeta_1 = 1$ and $\zeta_2 = (N_2!)^{-1/N_2}$ for outer region user.

Fig. 4.5 depicts the coverage probability of a typical inner region users in both schemes. While the coverage in the ICOM scheme is shown to be less than that of the IMOC scheme due to loss in degrees of freedom, this, however, leads to an additional improvement in the coverage probability of outer region users in other cells, and, thus, reflecting the trade-off between outer region and inner region system performance. This point will be explained further in the discussion related to Fig. 4.6.

Fig. 4.6 depicts the coverage probability of a typical outer region user in both schemes. It can be clearly seen that noticeable improvement in coverage probability by about 7 dB or more can be achieved with ICOM scheme, while less coverage can be achieved

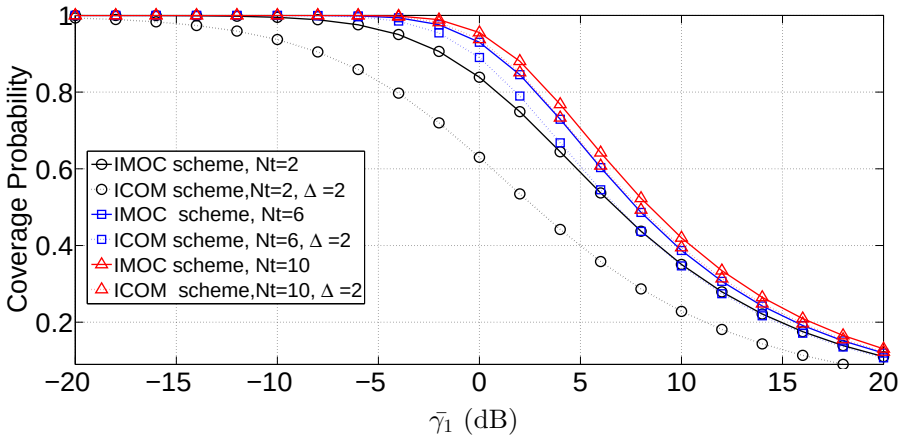

Figure 4.5: CCDF of typical inner region user in IMOC and ICOM schemes for different number of transmit antennas ($P = 1, \alpha = 4, \bar{\gamma}_2 = 1$ dB, $\sigma^2 = 1$).

with the IMOC scheme. The improvement in coverage stems from the fact that the outer region user in the ICOM scheme now enjoys two advantages; better quality in the desired signal due to exploitation of most degrees of freedom by using MRT technique and substantial interference reduction offered by neighbouring BSs. Reducing interference, however, comes at the price of losing degrees of freedom, thereby causing reduction in the inner region user coverage and average rate. If the inner region user enjoys good channel condition, it may yet have high coverage, though less than that of IMOC scheme. That is to say the coverage of inner region user in a cell is decreased for the sake of improving the coverage of outer region users in other cells.

Considering the aforementioned observation, the system may have different objectives and priorities. If the desired goal is to maximise total system rate, then IMOC scheme may be a better choice. However, when its is assumed that the system presumes minimum rate for each user including those on the cell boundaries, ICOM scheme may fit well this purpose.

Fig. 4.7 shows the trade off between inner region user rate and the outer region user rate in IMOC and ICOM schemes, respectively. As can obviously noticed, better trade off is the one in which most outer region user rate can be obtained as a return

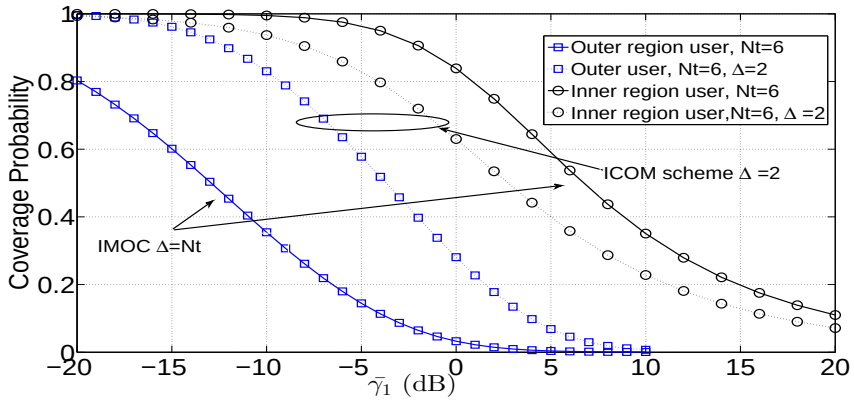

Figure 4.6: Comparison between inner region and outer region users in IMOC and ICOM schemes. The gap between CCDFs of SINR of inner region and outer region users is smaller in ICOM ($P = 1, \alpha = 4, \bar{\gamma}_2 = 1$ dB).

for least loss in the inner region user rate. When N_t increases, better trade off can be achieved for a given number of coordinated BSs K, where less rate of inner region user is lost.

Generally interference cancellation does not always play an important role in enhancing system performance, even though it plays significant part in enhancing system performance at the cell edges. More specifically, it could worsen the signal of outer region users when the interference reduction does not outweigh the signal quality reduction due to loss in degrees of freedom.

Now, a comparison is made between the proposed schemes of adaptive-CIIC and non adaptive coordination strategy introduced in [120]. In [120], a non adaptive coordinated beamforming is analysed wherein a cluster of BSs coordinate regardless of other cell's users positions without any adaptation in implementing coordination.

In Fig. 4.8, the coverage probability of a outer region user are plotted for three strategies; IMOC scheme, ICOM scheme, and non adaptive coordination. It can be noticed that the ICOM scheme leads to better coverage amongst the others for thresholds less than 2 dB. Intuitively, this can be inferred from the fact that the IMOC

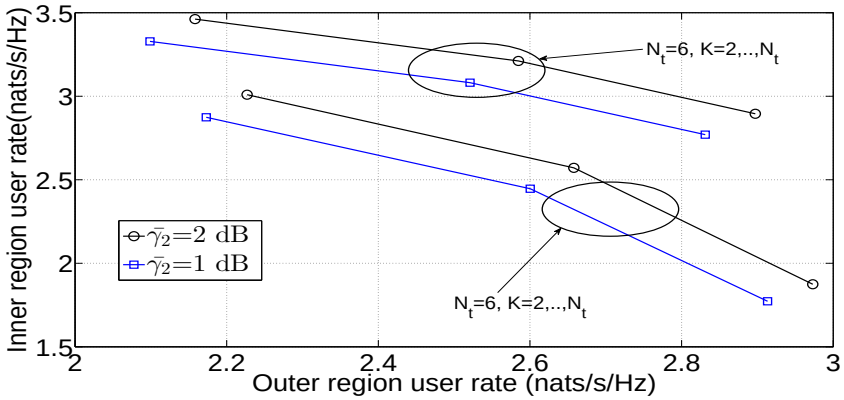

Figure 4.7: Trade off between average rates of inner region and outer region user in IMOC and ICOM schemes, respectively ($P = 1, \alpha = 4$).

scheme and non adaptive strategy causes unnecessary lose in the degrees of freedom, particularly when the network is more sparse or when the user enjoys very good channel condition. While, in the ICOM scheme, via suitable spectrum management and adaptation, the degrees of freedom can be better utilised, since losing degrees of freedom for one user in a cell can be allowed if that user is located in the inner region of the cell where the users naturally have good channel quality, therefore they can afford losing some of their degrees of freedom. On the other hand, when the user is on the cell boundaries where its channel quality usually is not good enough, it may be more helpful to exploit all degrees of freedom in the transmission toward him. It is worth mentioning that in the IMOC scheme implementing coordination is conditioned on a threshold value, which is assumed 1dB in the simulation. However, the larger the chosen threshold value is, the greater coverage probability becomes.

The impact of threshold values $\bar{\gamma}_2$ on coverage can be noticed from Figs. 4.9 and 4.10. It can be observed that low threshold values result in lower coverage and high values leads to higher coverage. As an effect, $\bar{\gamma}_2$ can be set as a system design parameter, and may be chosen based on traffic load distribution, i.e. low $\bar{\gamma}_2$ for low outer-region users traffic and high $\bar{\gamma}_2$ for high traffic load. It can be also observed that the impact of $\bar{\gamma}_2$ on coverage is diminishing for higher $\bar{\gamma}_2$, i.e. the increase in coverage for low $\bar{\gamma}_2$ is higher than that with high $\bar{\gamma}_2$ values.

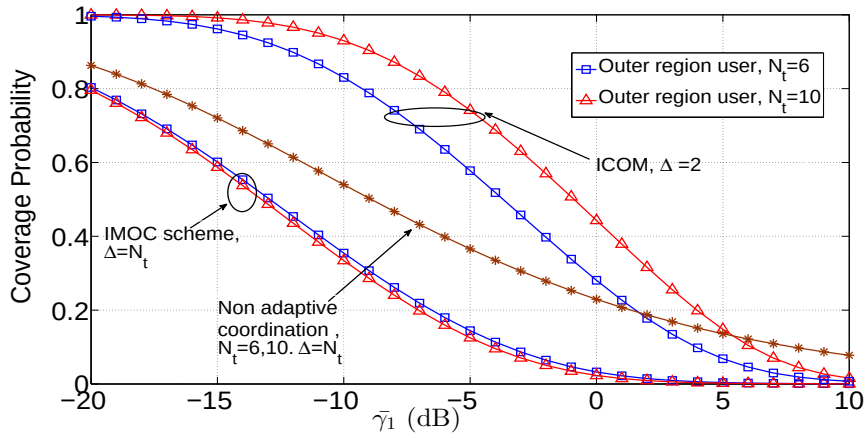

Figure 4.8: Comparison between the proposed schemes of adaptive-CIIC and non adaptive coordination using only CBF for a typical outer region user ($N_t = K \in \{6, 10\}, P = 1, \alpha = 4, \bar{\gamma}_2 = 1$ dB, $\sigma^2 = 1$).

4.5 Chapter Summary

In this chapter, an adaptive strategy is introduced based on frequency space domains to mitigate and cancel inter-cell interference, respectively. Using PPP model, two scheme are developed and analysed for this purpose. Tractable expressions for upper bound of coverage probability are derived for both schemes, which can be easily utilised for deriving average user rate. The numerical results confirm that a strategy based on the ICOM scheme can yield better coverage; consequently it results in better system performance while achieving better fairness between outer region and inner region in a cell. In short, the best choice is to allow only those users enjoying good channel conditions to scarify some of their degrees of freedom, while letting the users at the cell edges to enjoy full diversity with interference being perfectly eliminated. Furthermore, this strategy has low overhead requirements since CSI is required only at the serving BS and the neighbouring BSs that are involved in the process of cancelling the interference toward the user.

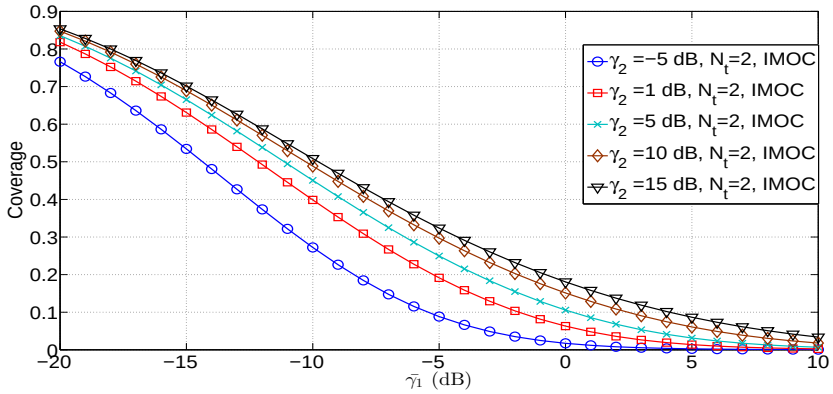

Figure 4.9: The impact of thresold values on coverage probability of outer-region user in IMOC ($N_t = 2, P = 1, \alpha = 4, \sigma^2 = 1$).

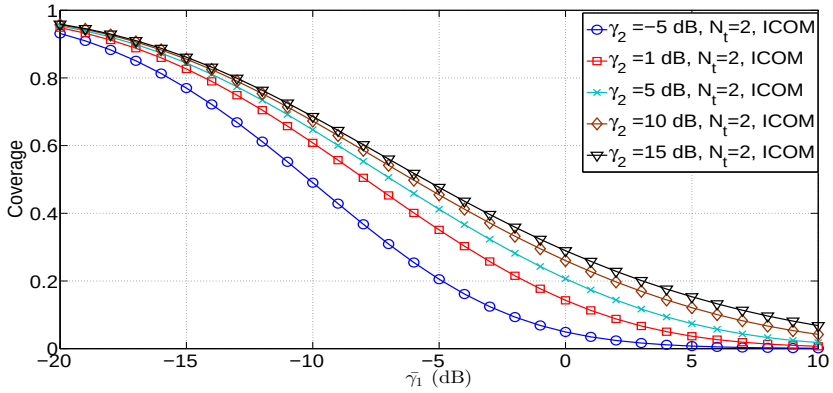

Figure 4.10: The impact of thresold values on coverage probability of outer-region user in ICOM ($N_t = 2, P = 1, \alpha = 4, \sigma^2 = 1$).

Chapter 5

User and Multimode Selection in Multicell MIMO Cellular Networks

This chapter investigates multicell scheduling for coordinated MIMO cellular networks. Low complexity algorithms are proposed for user scheduling. In addition, multimode scheduling scheme is developed. The proposed algorithms are analysed and compared with optimal solution obtained by exhaustive search.

5.1 Introduction

Alongside with spectrum reuse, MU-MIMO has the potential of increasing system capacity by exploiting extra degrees of freedom offered by space domain. Multiple users can be served simultaneously on the same frequency band through spatial multiplexing and precoding techniques. The channel can be decomposed into multiple parallel spatial subchannels to transmit multiple spatial data streams [126].

The number of users that can be served by MU-MIMO is constrained by the transmit

antennas. Hence, user selection needs to be implemented to choose the best spatially compatible users (their channels are uncorrelated) so that inter-user interference can be efficiently eliminated.

Various algorithms are developed for user selection [41], [127]-[134]. For ZF, greedy user selection algorithms based on null-space successive projection and capacity-based metric are proposed in [41] and [127], respectively. For BD, capacity-based and Frobenius-based greedy algorithms are developed in [128]. However, these algorithms incur high complexity due to using frequent singular value decomposition (SVD) and waterfilling. To overcome this limitation and avoid the unreliability caused by dealing with large concatenated matrix, a novel algorithm to iteratively select users is introduced in [130]. The algorithm is based on the idea of null spaces intersection where the precoder matrix of each user is obtained iteratively and sequentially to eliminate the inter-user interference and thereby incorporating it in user selection. Strategies based on angle between subspaces are proposed in [131]-[133]. This approach accounts for the spatial compatibility between users and relatively incurs less computational complexity. The authors of [133] utilise the iterative procedure in [130] to introduce an algorithm for user selection based on principal angle between subspaces. The idea of principal angle is further utilised with a different selection criteria based on capacity bound in [132]. These works assume that users utilise all their receive antennas. However, when the user has more antennas than can be served, a set of user antennas must be selected for transmission. Antenna selection combined with user selection is addressed in [134], [135]. In [134], a simplified scheduling for antennas and user selection is proposed MU-MIMO systems. While in [135], an adaptive strategy (multimode selection) for allocating varying number of spatial streams among users is developed employing capacity-based metric. More specifically, antennas and user selection are jointly performed so that an optimal subset of users and receive antennas are selected to maximise the sum capacity thereby it can better exploit multiuser diversity.

In the aforementioned works, the focus has been mainly on single-cell scenario and, therefore, losing practicality where the interference can not be ignored. As previously discussed, MIMO can be utilised on multicell level to combat inter-cell inter-

ference [56], whereby coordinated MIMO and network MIMO [56] have been widely considered. In the first scheme, a cluster of BSs coordinate their beamforming transmission such that the interference is cancelled at the users served by neighbouring cells [67], [136]-[137]. In this strategy, global CSIs of users in neighbouring cells must be exchanged among BSs. Whereas, in the later, a cluster of BSs act as a one giant BS jointly transmitting to their users so that the system can be viewed as a MU-MIMO [62], [138]-[141]. In this case, data as well as CSIs must be exchanged among the cells. Obviously network MIMO comes at the price of high cost in terms of control and data signals exchange [56].

Unlike the aforementioned works, in this chapter, the problem of user scheduling in multicell setting is addressed. Assuming the number of users in each cell is larger than that can be served, the problem considered here is how to select users in the cells with the best spatially separated channels such that the sum rate of the system is maximised. Furthermore, in addition to user selection, multimode selection problem is considered, where users may not all have the same number of spatial streams, thereby the user selection is implemented across spatial modes. In both cases, solving multicell scheduling problem brings about high complexity in terms of computations and overhead signalling. To overcome these limitations, a two-stage distributed multicell scheduling algorithm is proposed; multicell user scheduling stage and precoding stage.

In the first stage, the algorithm works on sequential manner such that in each cell, a BS selects its users based on CSIs of already selected users in other cells. In the second stage, after selecting the sets of users by BSs, the precoding matrices are designed for the selected users in each cell. In both stages, each BS works separately from other BSs, thus no centralised action is required. Furthermore, two algorithm are proposed for the scheduling stage; in the first algorithm, named as distributed sequential user scheduling (DSUS), each BS schedules its set of users in its turn, where in each turn, users are selected such that the space spanned by users channels lies almost in the null space of the interference channels of already selected users in the previous cells. The reason for doing so is to suppress the interference more efficiently.

The process continues until all BSs select their users. In the other algorithm, named as distributed circular user scheduling (DCUS), users are iteratively scheduled across the cells. Unlike, the algorithm DSUS, in this algorithm only one user is selected by the cell in each turn. Having all BSs selected one user per each, in the next round the process is repeated for selecting one user by each BSs. In each user selection, the BS takes CSIs of the so far selected users so that it can select another user in the null space of all users interference channels.

In the first algorithm, the cells have noticeable disparity in the sum rate, where the last cell in selection order has better performance among the others. While, in the second algorithm, better fairness among cells can be achieved compared to the first algorithm. This point will be further illustrated and justified in the subsequent sections.

In the procedure of multi-cell users selection described above, the order of BS sequence can be dictated by the system through central unit. Furthermore, no need to exchange all CSIs of all users among the cells but only of those selected users.

The main contribution of this chapter are summarised as follows:

- Low complexity user scheduling scheme is proposed for multicell setting with MIMO coordination. The proposed algorithm works on sequential distributive manner and consists of two stages: multicell scheduling and precoding stage. Thus, the proposed algorithm can greatly reduce overhead signalling by allowing only selected users to feedback their CSIs.

- Two variants of multicell scheduling are proposed. The first algorithm has less complexity but leads to more difference in sum rate among cells. While the second algorithm results in better fairness in terms of system performance though with more signalling iteration among the cells.

- The algorithm is extended to multimode selection in addition to the user selection, whereby the spatial modes are adaptively selected in each cell.

The remainder of the chapter is organised as follows. Section 5.2 describes the proposed system model and the concept of BD and principal angle. Section 5.3 presents the problem of multicell scheduling and introduces the proposed algorithms and its two variants and how theproposed algorithm is extended to multimode selection. In Section 5.4, fair scheduling is introduced for the proposed algorithm. Section 5.5 presents the simulation results of the proposed algorithm. Finally, conclusions are drawn in Section 5.6.

5.2 System model

5.2.1 Signal Model and Block Diagonalization

Consider a downlink cellular network consisting of a set of $\mathcal{B}$ BSs, where $\mathcal{B} = \{1, ..., \mid \mathcal{B} \mid\}$. Each BS is equipped with N_t antennas and serves users equipped with N_r antennas as shown in Fig. 5.1. Suppose that the active set of users to be selected and served in the BS b is $\mathcal{K}_b \in \mathcal{U}_b$ where $\mathcal{U}_b$ is the set of all users in cell b, and denote k_b as an index of a user served by BS b such that $k_b \in \mathcal{K}_b = \{1, ..., \mid \mathcal{K}_b \mid\}$.

The downlink channel matrix from set of $\mathcal{B}$ BSs to user k_b in cell b is given by:

$$\mathbf{H}_{k_b} = \left[\sqrt{\beta^1_{k_b}}\mathbf{H}^{(1)}_{k_b}, \sqrt{\beta^2_{k_b}}\mathbf{H}^{(2)}_{k_b} ... \sqrt{\beta^B_{k_b}}\mathbf{H}^{(B)}_{k_b}\right] \tag{5.1}$$

where $\mathbf{H}^{(i)}_{k_b} \in \mathbb{C}^{N_r \times N_t}$ is the downlink channel matrix from BS i to UE k_b located at BS b. Each component of $\mathbf{H}^{(i)}_{k_b}$ is an independent identically distributed (i.i.d) complex Gaussian random variable (r.v.) with zero-mean and unit-variance. $\beta^i_{k_b} = \varrho^i_{k_b}\varsigma^i_{k_b}$ where $\varsigma^i_{k_b}$ and $\varrho^i_{k_b}$ denotes path-loss and lognormal shadowing coefficient with standard deviation $\hat{\varrho}_s$ between ith BS and k_b user, respectively. The transmit data vector of user k_b is given by $\mathbf{x}_{k_b} \in \mathbb{C}^{L_{k_b} \times 1}$, where L_{k_b} denotes the number of spatial streams allocated for user k_b. The data vector $\mathbf{x}_{k_b}$ is multiplied by $N_t \times L_{k_b}$ precoding matrix $\mathbf{P}_{k_b}$ and the resultant signal is transmitted through N_t antenna from BS b.

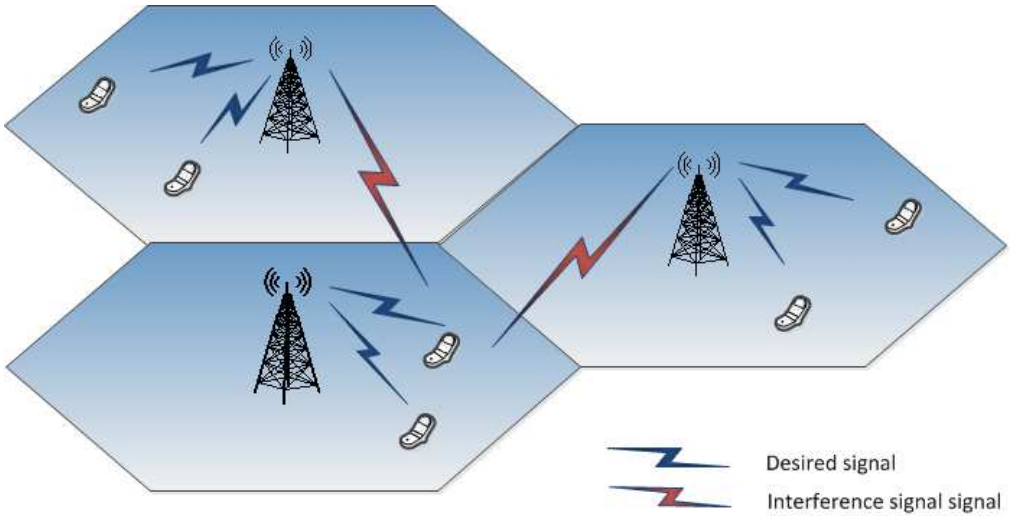

Figure 5.1: Illustration of coordinated MIMO cellular network, each BS serves multiple users equipped with multiple antennas

At the receiver side k_b, a post-processing matrix $\mathbf{W}_{k_b} \in \mathbb{C}^{N_r \times L_{k_b}}$ is employed to decode the spatial streams at the receiver. Hence, the received signal $\mathbf{y}_{k_b} \in \mathbb{C}^{L_{k_b} \times 1}$ after post-processing is given by:

$$\mathbf{y}_{k_b} = \underbrace{\mathbf{W}_{k_b}^{\mathsf{H}} \mathbf{H}_{k_b}^{(b)} \mathbf{P}_{k_b} \mathbf{x}_{k_b}}_{\text{desired signal}} + \underbrace{\mathbf{W}_{k_b}^{\mathsf{H}} \mathbf{H}_{k_b}^{(b)} \sum_{i_b=1, i_b \neq k_b}^{|\mathcal{K}_b|} \mathbf{P}_{i_b} \mathbf{x}_{i_b}}_{\text{intra-cell interference}} + \underbrace{\mathbf{W}_{k_b}^{\mathsf{H}} \sum_{s=1, s \neq b} \mathbf{H}_{k_b}^{(s)} \sum_{n_s=1}^{|\mathcal{K}_s|} \mathbf{P}_{n_s} \mathbf{x}_{n_s}}_{\text{inter-cell interference}} + \mathbf{W}_{k_b}^{\mathsf{H}} \mathbf{n}_{k_b} \quad (5.2)$$

where $\mathbf{n}$ is the additive white Gaussian noise (AWGN) such that $\mathbb{E}\{\mathbf{n}_{k_b} \mathbf{n}_{k_b}^{\mathsf{H}}\} = \sigma^2 \mathbf{I}$. The second term is the intra-cell interference that comes from transmission to the users served by the same BS. The third term is the inter-cell interference that comes from other BSs. To cancel the intra-cell interference, the following should be satisfied:

$$\mathbf{H}_{k_b}^{(b)} \mathbf{P}_{i_b} = 0, \qquad \forall k_b \neq i_b, \forall k_b, i_b \in \mathcal{K}_b \quad (5.3)$$

for cancelling inter-cell interference, the following should also be satisfied:

$$\mathbf{H}_{k_b}^{(s)}\mathbf{P}_{n_s} = 0, \qquad \forall k_b \in \mathcal{K}_b, n_s \in \mathcal{K}_s, b \neq s \in \mathcal{B} \tag{5.4}$$

To satisfy the above constraints, firstly the precoding matrix $\mathbf{P}_{k_b}$ should lie in the null space of $\tilde{\mathbf{H}}_{k_b}^{b}$ which is defined as:

$$\tilde{\mathbf{H}}_{k_b}^{(b)} = [\mathbf{H}_1^{(b)^{\mathsf{H}}}, ..., \mathbf{H}_{k_b-1}^{(b)^{\mathsf{H}}}, \mathbf{H}_{k_b+1}^{(b)^{\mathsf{H}}}, ..., \mathbf{H}_{|\mathcal{K}_b|}^{(b)^{\mathsf{H}}}]^{\mathsf{H}} \tag{5.5}$$

whereas, to cancel out the inter-cell, the precoding matrix $\mathbf{P}_{k_b}$ should lie in the null space of $\hat{\mathbf{H}}_{k_b}^{(b)}$ which is defined as:

$$\hat{\mathbf{H}}_{k_b}^{(b)} = [\bar{\mathbf{H}}_1^{(b)^{\mathsf{H}}}, ..., \bar{\mathbf{H}}_{s-1}^{(b)^{\mathsf{H}}}, \bar{\mathbf{H}}_{s+1}^{(b)^{\mathsf{H}}}, ..., \bar{\mathbf{H}}_{B}^{(b)^{\mathsf{H}}}]^{\mathsf{H}}, \qquad \forall b \neq s \in \mathcal{B} \tag{5.6}$$

where we define $\bar{\mathbf{H}}_s^{(b)}$ as:

$$\bar{\mathbf{H}}_s^{(b)} = [\mathbf{H}_1^{(b)^{\mathsf{H}}}, ..., \mathbf{H}_{|\mathcal{K}_s|}^{(b)^{\mathsf{H}}}]^{\mathsf{H}} \tag{5.7}$$

To obtain the precoders that satisfy the conditions in (5.3) and (5.4), each BS b concatenates channel matrices of its own users along with interference channels to the users in other cells as follows: Denote $\widehat{\mathbf{H}}_{k_b}^{(b)}$ as $\widehat{\mathbf{H}}_{k_b}^{(b)} = [\tilde{\mathbf{H}}_{k_b}^{(b)^{\mathsf{H}}}, \hat{\mathbf{H}}^{(b)^{\mathsf{H}}}]^{\mathsf{H}}$. Thus, to nullify both inter-cell and intra-cell interference using BD, the precoder $\mathbf{P}_{k_b}$ must be constructed such that:

$$\widehat{\mathbf{H}}_{k_b}^{(b)}\mathbf{P}_{k_b} = 0, \qquad \forall b \neq s \in B \tag{5.8}$$

Let $\widehat{l}_{k_b} = \mathsf{Rank}(\widehat{\mathbf{H}}_{k_b}^{(b)})$, the (5.8) can only be satisfied when $\mathsf{Rank}(\widehat{\mathbf{H}}_{k_b}^{(b)}) < N_t$. Let the singular value decomposition (SVD) of $\widehat{\mathbf{H}}_{k_b}^{(b)}$ as $\widehat{\mathbf{H}}_{k_b}^{(b)} = \widehat{\mathbf{U}}_{k_b}^{(b)}\widehat{\mathbf{\Lambda}}_{k_b}^{(b)}\big[\widehat{\mathbf{V}}_{k_b,1}^{(b)}\widehat{\mathbf{V}}_{k_b,0}^{(b)}\big]^{\mathsf{H}}$.
where $\widehat{\mathbf{\Lambda}}_{k_b}^{(b)}$ is the $\widehat{l}_{k_b} \times \widehat{l}_{k_b}$ diagonal matrix, i.e. $\widehat{\mathbf{\Lambda}}_{k_b}^{(b)} = \mathrm{diag}(\lambda_{1,k_b}, ..., \lambda_{\widehat{l}_{k_b},k_b})$, $\widehat{\mathbf{V}}_{k_b,1}^{(b)}$ contains the first $\widehat{l}_{k_b}$ right singular vectors, and $\widehat{\mathbf{V}}_{k_b,0}^{(b)}$ contains the last $N_t - \widehat{l}_{k_b}$ right singular vectors. Therefore, the columns of $\widehat{\mathbf{V}}_{k_b,0}^{(b)}$ forms the null space basis of $\widehat{\mathbf{H}}_{k_b}^{(b)}$.

From $\widehat{\mathbf{V}}_{k_b,0}^{(b)}$, the precoding matrix $\mathbf{P}_{k_b}$ can be constructed such that both intra-cell and inter-cell interference can be eliminated.

The precoding matrix $\mathbf{P}_{k_b}$ can be decomposed into three matrices $\mathbf{Z}_{k_b}^1$, $\mathbf{Z}_{k_b}^2$, and $\mathbf{B}_{k_b}$, i.e. $\mathbf{P}_{k_b} = \mathbf{Z}_{k_b}^1 \mathbf{Z}_{k_b}^2 \mathbf{B}_{k_b}$, where $\mathbf{Z}_{k_b}^1$ is designed to eliminate intra-cell interference, therefore it should lie in $\mathcal{N}(\tilde{\mathbf{H}}_{k_b}^{(b)})$. While $\mathbf{Z}_{k_b}^2$ is designed to eliminate inter-cell interference, thus it should lie in $\mathcal{N}(\hat{\mathbf{H}}_{k_b}^{(b)})$. $\mathbf{B}_{k_b}$ is the matrix holding singular vectors that maximise data rate. Let $\ddot{\mathbf{H}}_{k_b}^{(b)}$ denote the effective channel matrix for user k_b, i.e. $\ddot{\mathbf{H}}_{k_b}^{(b)} = \mathbf{H}_{k_b}^{(b)} \mathbf{Z}_{k_b}^1 \mathbf{Z}_{k_b}^2$. To obtain $\mathbf{B}_{k_b}$ that maximise data rate, we find SVD of $\ddot{\mathbf{H}}_{k_b}^{(b)}$ as:

$$\ddot{\mathbf{H}}_{k_b}^{(b)} = \ddot{\mathbf{U}}_{k_b}^{(b)} \left[\ddot{\mathbf{\Lambda}}_{k_b}^{(b)}, \mathbf{0} \right] \left[\ddot{\mathbf{V}}_{k_b,1}^{(b)} \ddot{\mathbf{V}}_{k_b,0}^{(b)} \right]^{\mathsf{H}} \tag{5.9}$$

where $\ddot{\mathbf{V}}_{k_b,1}^{(b)}$ contains the first right singular vectors, and the columns of which correspond to the orthonormal basis of $\mathcal{R}(\ddot{\mathbf{H}}_{k_b}^{(b)})$. Thus, by setting $\mathbf{B}_{k_b} = \ddot{\mathbf{V}}_{k_b,1}^{(b)}$, the data rate is maximised. The method to design precoding matrices mentioned above utilises SVD to find the null space for each user. The issue with this method is that it incurs costly computations. Motivated by the iterative method introduced in [130], the null space matrices can be obtained iteratively by utilising the idea of null space intersection [142]. More specifically, consider the matrix that nullifies the intra-cell interference of user 1, i.e. $\mathbf{Z}_1^1$. Let $\mathbf{Z}_1^{1^{(i)}}$ be precoding matrix $\mathbf{Z}_1^1$ after ith iteration, $\mathbf{Z}_1^{1^{(i)}}$ should satisfy that $\mathbf{H}_{k_b}^{(b)} \mathbf{Z}_1^{1^{(i)}} = 0$ for all $1 < k_b \leq i$. Then, $\mathbf{Z}_1^{1^{(i+1)}}$ can be found as:

$$\mathbf{Z}_1^{1^{(i+1)}} = \mathbf{Z}_1^{1^{(i)}} \mathbf{G} \tag{5.10}$$

where columns of $\mathbf{G}$ lie in the null space of $\mathbf{H}_{i+1}^{(b)} \mathbf{Z}_1^{1^{(i)}}$, i.e. $\mathcal{N}(\mathbf{H}_{i+1}^{(b)} \mathbf{Z}_1^{1^{(i)}})$. In the same manner, the precoding matrices of other users can be obtained iteratively. In each iteration, the number of columns of $\mathbf{Z}_1^{1^{(i)}}$ is reduced by N_r. Algorithm 1 summarises the aforementioned procedure [130].

Algorithm 1 Iterative precoder design algorithm

1: $i = 1$, $\mathbf{P}_1^1 = \mathbf{I}_{N_t}$.
2: **while** $i <\mid \mathcal{K}_{max} \mid$ **do**
3: $\quad \mathbf{P}_{i+1}^{i+1} = \mathbf{P}_i^i \times \text{null}(\mathbf{H}_i \mathbf{P}_i^i)$.
4: $\quad$ **for** $m = 1$ to i **do**
5: $\quad\quad$ Update $\mathbf{P}_m^{i+1} = \mathbf{P}_m^i \times \text{null}(\mathbf{H}_{i+1} \mathbf{P}_m^i)$
6: $\quad$ **end for**
7: **end while**

5.2.2 Principal Angle Between Subspaces

To utilise the iterative procedure for user selection, an approach based on the angle between subspaces of users channels is followed. Here, we review the concepts of principal angle and geometrical angle utilised in this chapter. Assume that $\mathcal{U}$, $\mathcal{V} \subset \mathbb{C}^n$ are two nonzero subspaces, the principal angles $\delta_i \in [0, \pi/2]$ between $\mathcal{U}$ and $\mathcal{V}$ are recursively defined such that [143]:

$$\begin{aligned} \cos \delta_i &= \max_{\mathbf{u} \in \mathcal{U}, \mathbf{v} \in \mathcal{V}} \mathbf{u}^{\mathsf{H}} \mathbf{v} \\ &= \mathbf{u}_i^{\mathsf{H}} \mathbf{v}_i \qquad i = 1, ..., m \\ &\text{s.t. } \| \mathbf{u} \| = \| \mathbf{v} \| = 1 \end{aligned} \tag{5.11}$$

where $m = \min\{\dim(\mathcal{U}), \dim(\mathcal{V})\}$, $\mathbf{u}$ and $\mathbf{v}$ are the vectors that forms the ith principal angle.

$\cos(\delta_i)$ can be defined in terms of the eigenvalues as follows [143], [144]:

$$\cos^2(\delta_i) = \lambda_i \tag{5.12}$$

where λ_i $(i = 1, ..., m)$ are the eigenvalues of $\widehat{\mathbf{P}}_1^{\mathsf{H}} \widehat{\mathbf{P}}_2 \widehat{\mathbf{P}}_2^{\mathsf{H}} \widehat{\mathbf{P}}_1$ where $\widehat{\mathbf{P}}_1$ and $\widehat{\mathbf{P}}_2$ are orthonormal basis matrices of subspaces $\mathcal{U}$ and $\mathcal{V}$, respectively.

Principal angles can be used as an indication of the degree of spatial correlation. That is, the larger the principal angel is, the more uncorrelated subspaces are. Thus, principal angles can be utilised to measure the orthogonality between users channels.

To fully characterise the spatial correlation between two subspaces, it is beneficial to consider the concept of geometrical angle. In the following the definition of geometric angle and its relation to singular values will be given.

Geometrical Angle: For the given subspace $\mathcal{U}$ and $\mathcal{V}$, the geometrical angle, i.e. the angle $\Theta = \measuredangle(\mathcal{U}, \mathcal{V})$ between the two subspaces, is defined as [143], [144].

$$\begin{aligned} \cos^2(\Theta) &= \prod_{i=1}^{m} \cos^2(\delta_i) \\ &= \det(\widehat{\mathbf{P}}_1^{\mathsf{H}} \widehat{\mathbf{P}}_2 \widehat{\mathbf{P}}_2^{\mathsf{H}} \widehat{\mathbf{P}}_1) \end{aligned} \tag{5.13}$$

$\cos^2(\Theta)$ represents the ratio between the volumes of the parallelepiped spanned by the projection of the basis vectors of the lower dimension subspace on the higher dimension subspace and the one spanned by the basis vectors of the lower dimension subspace [145].

Based on both principal angle and the previously described iterative procedure, the authors of [133] propose low complexity algorithm for user selection in single cell scenario. In the next section, the algorithm is subtly modified and utilised in the proposed multicell scheduling.

5.3 Multicell User Scheduling Algorithms

In this section, the problem of multicell scheduling that maximise sum rate of the system is defined. In order to make the analysis more consistent, let us start first with single cell scheduling and then, subsequently, proceed to define multicell scheduling problem. The reason behind this can be clarified in the next discussions.

5.3.1 Single Cell scheduling

In a single cell scenario, inter-cell interference is not accounted for. Hence, as described previously, scheduling users can be either implemented with fixed number of spatial modes being allocated for each user, which corresponds to the conventional BD, or with varying number of spatial modes per each user, which corresponds to the multimode selection. In the later case, the selected users may have different number of spatial modes. One way to implement multimode scheduling is by the way of antenna selection. In antenna selection, the scheduler should select the best set of antennas that maximises the sum rate in the system. Multimode scheduling allows more flexibility in allocating the spatial modes and can substantially improve data rate by exploiting multimode diversity [135]. Even though throughput of user k_b can be decreased, nevertheless, it frees up the resources so that they can be used by other users with better spatial channel separation. Hence, in general, the sum rate of conventional BD/multimode scheme in single cell is written as

$$R_b = \max_{\mathcal{K}_b \in \mathcal{U}_b, L_{k_b}, \mathbf{P}_{k_b}, \mathbf{Q}_{k_b}} \sum_{k_b \in \mathcal{K}_b} \log_2 \det \left(\mathbf{I} + \frac{1}{\sigma^2} \mathbf{H}_{k_b}^{(b)} \mathbf{P}_{k_b} \mathbf{Q}_{k_b} \mathbf{P}_{k_b}^{\mathsf{H}} \mathbf{H}_{k_b}^{(b)\mathsf{H}} \right) \tag{5.14}$$

s.t.

$$\sum_{k_b}^{|\mathcal{K}_b|} L_{b_k} \leq N_t \qquad \forall b \in \mathcal{B} \tag{5.15}$$

$$\sum_{k_b=1}^{|\mathcal{K}_b|} \mathsf{tr}(\mathbf{Q}_{k_b}) \leq P \qquad \forall b \in \mathcal{B} \tag{5.16}$$

Where $\mid \mathcal{K}_b \mid$ and L_{b_k} are the maximum supportable number of users served by each BS and the number of spatial modes allocated to user k_b, respectively. For conventional BD, L_{b_k} is fixed, i.e. $L_{b_k} \leq N_r$, and for mulimode selection it can take the values $0 \leq L_{b_k} \leq N_r$ for each user at each scheduling instant. $\mathbf{Q}_{k_b}$ and P are the transmit covariance matrix of size L_{k_b} and the total transmit power allowed for each BS, respectively. Note that the covariance matrix $\mathbf{Q}_{k_b}$ can be determined by waterfilling over the non zero eigen modes of the effective channel. However, it is

well known that equal power allocation performs as good as waterfilling in high SNR regime. Thus, we will consider equal power allocation and for the rest of analysis, then we have $\mathbf{Q}_{k_b} = (P/\sum_i^{|\mathcal{K}_b|} L_{b_k})\mathbf{I}_{L_{b_k}\times L_{b_k}}$.

In general, only exhaustive search can solve this problem by searching over all possible sets of users/spatial modes, which is, however, highly computationally costly. Therefore, suboptimal low complexity algorithms 2 and 3 are proposed for both conventional BD and multimode user scheduling schemes, respectively. In the following discussion we briefly explain the algorithms and how they work.

a) *Scheduling with fixed number of spatial modes (conventional BD)*: when the transmission from the BS to each user utilises all available receive antennas at the users, no antenna (or multimode) selection is needed and $L_{b_k} = N_r$. Hence, the channel matrix between BS b and the user k_b is $\mathbf{H}_{k_b}^b \in \mathbb{C}^{N_r\times N_t}$. Accordingly, scheduling can be implemented to choose the best highly uncorrelated users channels.

   In [133], a greedy user selection algorithm based on principal angle is proposed for single cell setting. The algorithm introduces a metric for user selection based on iterative procedure used in [130]. We modify the algorithm so that it can be easily utilised as a part of the proposed multicell scheduling algorithm. Consider a cell b, at the initialisation step, the algorithm computes the null space of other cells users interference channels denoted as $\mathbf{N}$, and uses it to compute $\mu_{k_b}^{(1)}$ for all users in the cell. Then it selects the first user $\hat{k}_b$ in cell b satisfying (5.17), and the precoding matrices $\mathbf{W}$ and $\mathbf{Z}_{\hat{k}_b}^{(1)}$ are initialised according to step (4). Our modifications primarily lie in two steps; firstly in the metric selection in (5.17), whereby the null space of interference channels $\mathbf{N}$ is included in product of eigenvalues, and secondly in step (4) of the algorithm to update the null space of selected user's matrices $\mathbf{W}$, which will subsequently affect the selection metric given by (5.18). The inclusion of $\mathbf{N}$ yields further intersection with null space of other users interference channels. Note that $\mathcal{Z}_b$ and $\mathcal{W}_b$ are the sets of selected users and unselected users, respectively. At the ith iteration,

the algorithm selects the ith user satisfying (5.18). After the user is selected, the $\mathcal{Z}_b$, $\mathcal{W}_b$, and $\mathbf{W}$ are updated accordingly. The modified algorithm is detailed in **Algorithm 2**.

Algorithm 2 Iterative greedy user selection algorithm

Initialisation: $\mathcal{W}_b = \{1, ..., \mid \mathcal{W}_b \mid\}$, $\mathcal{Z}_b = \phi$, matrix of interference channels null space $\mathbf{N}$.

$\mathbf{G}_{k_b} = \text{row}(\mathbf{H}_{k_b}^{(b)})$, $\mu_{k_b}^{(1)} = \det(\mathbf{H}_{k_b}^{(b)}\mathbf{N}\mathbf{N}^{\mathsf{H}}\mathbf{H}_{k_b}^{(b)\mathsf{H}})$ $\quad \forall k_b \in \mathcal{W}_b$.

Select the best user $\hat{k}_b$ as

$$\hat{k}_b = \arg\max_{k_b \in \mathcal{W}_b} \mu_{k_b}^{(1)} \tag{5.17}$$

$\mathbf{W} = \mathbf{N} \times \text{null}(\mathbf{H}_{\hat{k}_b}^{(b)})$, $\mathbf{Z}_{\hat{k}_b}^{(1)} = \mathbf{I}$.

Update users sets: $\mathcal{W}_b = \mathcal{W}_b - \{\hat{k}_b\}$, $\mathcal{Z}_b = \mathcal{Z}_b + \{\hat{k}_b\}$

for $i = 2$ to $\mid \mathcal{K}_b \mid$ **do**

  for $m \in \mathcal{Z}_b$ **do**

    $\mathbf{Z}_m^{(i)} = \mathbf{W}$, $\bar{\mathbf{H}}_m^{(b)} = \mathbf{H}_m^{(b)}\mathbf{Z}_m^{(i)}$.

    $\mu_m^{(i)} = \det(\bar{\mathbf{H}}_m^{(b)}\bar{\mathbf{H}}_m^{(b)\mathsf{H}})$.

    $\cos^2\psi_m = \det\big(\mathbf{G}_m\mathbf{W}\mathbf{W}^{\mathsf{H}}\mathbf{G}_m^{\mathsf{H}}\big)$.

  end for

  Select the next user according to.

$$\hat{k}_b = \arg\max_{m \in \mathcal{W}_b} \mu_m^{(i)} \prod_{k \in \mathcal{Z}_b} \mu_k^{(i-1)} \cos^2\psi_m \tag{5.18}$$

  Update $\mathcal{Z}_b = \mathcal{Z}_b + \{\hat{k}_b\}$, $\mathcal{W}_b = \mathcal{W}_b - \{\hat{k}_b\}$.

  Update $\mathbf{Z}_{k_b}^{(i)}$ and $\mu_{k_b}^{(i)}$ $\quad \forall k_b \in \mathcal{Z}_b$.

  Update $\mathbf{W} = \mathbf{W} \times \text{null}(\mathbf{H}_{\hat{k}_b}^{(b)}\mathbf{W})$

end for

b) *Scheduling with multimode selection*: when the number of spatial modes are adaptively allocated for each user, both user and spatial mode selection need to be implemented. In **Algorithm 3**, **Algorithm 2** is further modified to incorporate spatial multimode selection. The algorithm works by checking the best antenna of a user that has maximum space angle with the subspace spanned by already selected antennas. Accordingly, the channel matrix between BS b and antenna l at user k_b is represented by $\mathbf{h}_{k_b,l}^{(b)} \in \mathbb{C}^{1\times N_t}$. Denote the $\mathcal{A}_{k_b}$ and

$\mathcal{S}_{k_b}$ as the sets of remaining antennas and selected antennas for user k_b in a cell b, respectively. $\mathcal{W}_b$ is the set of users in cell b that have some antennas still unselected. While $\mathcal{Z}_b$ is the set of users that have antennas selected.

The **Algorithms 2,3** will be used for multicell scheduling algorithms presented in the next section. They can be used by each cell to select its own users/spatial modes such that the selected users channel directions have maximum subspace angle with interference channels of the previous users cells. Further elaboration will be made to describe this process in the next section.

5.3.2 Multicell Scheduling Problem Formulation

When considering multicell scenario, the problem of finding the best users set for each cell $\mathcal{K}_b \in \mathcal{U}_b,\ \forall b \in \{1, ..., \mid \mathcal{B} \mid\}$, gets coupled with precoding design due to inter-cell interference. Hence, scheduling users across multiple cells becomes more complicated since we have to jointly schedule users/ spatial modes sets across all cells. Thus, multicell scheduling that maximises the sum rate for $\mid \mathcal{B} \mid$ cells is mathematically expressed as

$$R_{sum} = \max_{\mathcal{K}_b \in \mathcal{U}_b, L_{k_b}, \mathbf{P}_{k_b}, \mathbf{Q}_{k_b}} \sum_{b=1}^{|\mathcal{B}|} \sum_{k_b \in \mathcal{K}_b} \log_2 \det\left(\mathbf{I} + \mathbf{H}_{k_b}^{(b)} \mathbf{P}_{k_b} \big(\sum_{s \neq b} \mathbf{H}_{k_b}^{(s)} \mathbf{P}_{k_s} \mathbf{Q}_{k_s} \mathbf{P}_{k_s}^{\mathsf{H}} \mathbf{H}_{k_b}^{(s)\mathsf{H}} + \sigma^2 \mathbf{I} \big)^{-1} \mathbf{Q}_{k_b} \mathbf{P}_{k_b}^{\mathsf{H}} \mathbf{H}_{k_b}^{(b)\mathsf{H}} \right) \quad (5.19)$$

s.t.

$$\sum_{k_b}^{|\mathcal{K}_b|} L_{b_k} \leq N_t - \mid \mathcal{B} \mid\mid \mathcal{K}_b \mid \qquad \forall b \in \mathcal{B} \quad (5.20)$$

$$0 \leq L_{b_k} \leq N_r \quad (5.21)$$

$$\sum_{k_b=1}^{|\mathcal{K}_b|} \mathsf{tr}(\mathbf{Q}_{k_b}) \leq P \qquad \forall b \in \mathcal{B} \quad (5.22)$$

Algorithm 3 Iterative greedy multimode selection algorithm

Initialisation: $\mathcal{A}_1 = ...\mathcal{A}_{k_b} = \{1, ..., N_r\}$, $\mathcal{W}_b = \{1, ..., \mid \mathcal{W}_b \mid\}$, $\mathcal{S}_1 = ... = \mathcal{S}_{k_b} = \phi$, $\mathcal{Z}_b = \phi$, matrix of interference channels null space $\mathbf{N}$.

$\mathbf{G}_{k_b,l} = \text{row}(\mathbf{h}_{k_b,l}^{(b)})$, $\mu_{k_b,l}^{(1)} = \det(\mathbf{h}_{k_b,l}^{(b)} \mathbf{N}\mathbf{N}^{\mathsf{H}} \mathbf{h}_{k_b,l}^{(b)\mathsf{H}})$ $\quad \forall k_b \in \mathcal{W}_b,\ l \in \mathcal{A}_{k_b}$.

Select the best antenna $\hat{l}$ of the best user $\hat{k}_b$ as

$$(\hat{k}_b, \hat{l}) = \arg \max_{k_b \in \mathcal{W}_b; l \in \mathcal{A}_{k_b}} \mu_{k_b,l}^{(1)}$$

$\mathbf{W} = \mathbf{N} \times \text{null}(\mathbf{h}_{\hat{k}_b,\hat{l}}^{(b)})$, $\mathbf{Z}_{\hat{k}_b,\hat{l}}^{(1)} = 1$.

Update antenna and users sets: $\mathcal{A}_{\hat{k}_b} = \mathcal{A}_{\hat{k}_b} - \{\hat{l}\}$, $\mathcal{S}_{\hat{k}_b} = \mathcal{S}_{\hat{k}_b} + \{\hat{l}\}$, $\mathcal{Z}_b = \mathcal{Z}_b + \{\hat{k}_b\}$

for $i = 2$ to $\mid \mathcal{K}_b \mid$ **do**

  for $m \in \mathcal{Z}_b$ **do**

    for $l \in \mathcal{S}_{k_b}$ **do**

      $\mathbf{Z}_{m,l}^{(i)} = \mathbf{W}$, $\bar{\mathbf{h}}_{m,l}^{(b)} = \mathbf{h}_{m,l}^{(b)} \mathbf{Z}_{m,l}^{(i)}$.

      $\mu_{m,l}^{(i)} = \det(\bar{\mathbf{h}}_{m,l}^{(b)} \bar{\mathbf{h}}_{m,l}^{(b)\mathsf{H}})$.

      $\cos^2\psi_j(l) = \det\big(\mathbf{G}_{m,l} \mathbf{W}\mathbf{W}^{\mathsf{H}} \mathbf{G}_{m,l}^{\mathsf{H}}\big)$.

    end for

  end for

  Select the next antenna according

$$(\hat{k}_b, \hat{l}) = \arg \max_{m \in \mathcal{W}_b; l \in \mathcal{A}_{k_b}} \mu_{m,l}^{(i)} \prod_{k \in \mathcal{Z}_b; j \in \mathcal{S}_{k_b}} \mu_{k,j}^{(i-1)} \cos^2\psi_j(l)$$

  Update $\mathcal{A}_{\hat{k}_b} = \mathcal{A}_{\hat{k}_b} - \{\hat{l}\}$, $\mathcal{S}_{\hat{k}_b} = \mathcal{S}_{\hat{k}_b} + \{\hat{l}\}$, $\mathcal{Z}_b = \mathcal{Z}_b + \{\hat{k}_b\}$

  if $\mathcal{A}_{\hat{k}_b} = \phi$ **then** $\mathcal{W}_b = \mathcal{W}_b - \{\hat{k}_b\}$

  end if

  Update $\mathbf{Z}_{k_b,l}^{(i)}$ and $\mu_{k_b,l}^{(i)}$ $\quad \forall k_b \in \mathcal{Z}_b, l \in \mathcal{S}_{k_b}$.

  Update $\mathbf{W} = \mathbf{W} \times \text{null}(\mathbf{h}_{\hat{k}_b,\hat{l}}^{(b)} \mathbf{W})$

end for

$$\mathbf{H}_{k_b}^{(b)}\mathbf{P}_{i_b} = 0, \qquad \forall k_b \neq i_b \tag{5.23}$$

$$\mathbf{H}_{k_b}^{(s)}\mathbf{P}_{n_s} = 0, \qquad \forall k_b \in \mathcal{K}_b, n_s \in \mathcal{K}_s, b \neq s \in \mathcal{B} \tag{5.24}$$

Evidently, solving the problem (5.19) in realistic systems faces three major challenges summarised as follow:

- *Inter-cell interference:* the first challenge is the inter-cell interference coming from neighbouring BSs. To overcome this challenge, BSs can coordinate their beamforming or precoding matrices so that the interference is eliminated at all users. To better utilise coordinated MIMO technique, the set of users in the cells should be selected such that each set of users in a cell have maximum spatial separation with interference channels of users in the other cells.

- *Computational complexity:* the second challenge is how to find an optimal set of users in each cell such that the inter-cell interference is perfectly eliminated, while maximising the sum rate of all cells. To clarify this point, without loss of generality consider two cells; b_1 and b_2 serving users k_{b_1} and k_{b_2}, respectively. For the the b_1 to perfectly eliminate the interference to user k_{b_2} while serving its user k_{b_1}, the channel direction of b_1 from its served user k_{b_1}, i.e. $\mathbf{H}_{k_{b_1}}^{b_1}$ and its interference channel to the user k_{b_2}, i.e. $\mathbf{H}_{k_{b_2}}^{b_1}$ must have perfect orthogonality. When there are more users than that can be served, only exhaustive search can find the optimal solution for this problem by searching over all possible subsets of users and spatial modes given by $\sum_{i=1}^{\lceil |\mathcal{B}|N_t/N_r \rceil} C_i^{|\mathcal{B}||\mathcal{U}_b|}$ and $\sum_{i=1}^{\lceil |\mathcal{B}|N_t \rceil} C_i^{|\mathcal{B}||\mathcal{U}_b|N_r}$, respectively. This induces complexity given by

$$\varphi_{us} \approx \mathcal{O}\left(\mid \mathcal{K}_b \mid (\mid \mathcal{B} \mid N_t)^3 C_{|\mathcal{K}_b|}^{|\mathcal{B}||\mathcal{U}_b|} \right) \tag{5.25}$$

$$\varphi_{mm} \approx \mathcal{O}\left(\frac{(\mid \mathcal{B} \mid N_t)^5}{N_r} C_{|\mathcal{B}|N_t}^{|\mathcal{B}||\mathcal{U}_b|N_r} \right) \tag{5.26}$$

  which becomes prohibitive as the total number of users in the cell $\mid \mathcal{U}_b \mid$ grows large. It can be observed that the problem becomes even more harder due to the coupling in user selection among cells. Consequently, the computational

complexity of exhaustive search becomes even more higher than that of a single cell user selection.

- *CSIs feedback cost:* assuming perfect CSIs feedback and centralised processing for selecting users across cells, the BSs should exchange the global CSI of all users at each scheduling period, which put too much burden to be permitted on the limited-capacity backhaul links. Moreover, when the number of users in each cells gets larger, CSIs cost increases accordingly. This holds true even when no exhaustive search but centralised processing is implemented.

Motivated by the previous discussion, suboptimal low complexity algorithm is necessary from the practical point of view for user selection in multicell setting to avoid complexity involved in (5.19), while requiring less CSIs sharing among cells. To decouple the joint problem (5.19) into two subproblems, two stages procedure are proposed; scheduling stage and precoding stage. In the scheduling stage, BSs progressively and sequentially select their users in their coverage region such that each cell selects its users separately from all other cells. At each step, each BS, say b, takes a limited amount of information from the previous BSs from 1 to $b-1$ based on which the BS b greedily selects users in its region. Two types of algorithms are proposed to implement this procedure; DSUS and DCUS. In the following discussion, each algorithm will be described thoroughly. Without loss of generality, let us assume fixed spatial stream case, i.e. conventional BD, when discussing the multicell algorithms; nevertheless, the algorithms are also applicable to multimode case.

a) ***DSUS algorithm***: in DSUS algorithm, multicell scheduling is implemented in sequential distributed manner. At the initialization, the first BS $b = 1$ schedules its users according to **Algorithm 2**, and conveys the interference channels from all other BSs to all of them. At the ith step, a BS b, where $b = i$, selects its own users such that the channel directions of selected users have maximum spatial separation with interference channels between BS b and the users already selected by BSs 1 to $b-1$. To achieve this, the BS b selects its users with maximum effective channels lying in the null space of all interference channels

to the already selected users in the previous cells. It does so by incorporating the input matrix $\mathbf{N}$ which represents the space allowed for use by its own users. To select users in each cell, an iterative algorithm determining the best users group using principal angle between subspaces is employed. Once the users are selected, the BS b passes the CSIs of channels between its selected users and all other BSs. The process continues until the last BS involved in coordination selects its users.

The second stage of algorithm is implemented distributively by each BS, where each BS, after selecting its own users, designs the transmission precoding matrices separately.

With this algorithm, no need to estimate the interference channels by all users in a cell. But only the set of selected users can estimate the CSIs and feed them back to its serving BS. Thus, this algorithm, while reducing the complexity of user selection, can significantly reduce the overhead signalling and feedback cost.

Simulation results reveal that DSUS algorithm results in disparity in performance among cells. More specifically, while the first cell, i.e. BS $b = 1$, obtains lower throughput compared with other cells, the last cell, i.e. BS $b =\mid \mathcal{B} \mid$ enjoys best performance compared to others. This stems from the fact that the first cell in the sequence, when selecting its own users, does not take into account the interference channels to users in other cells as they are not yet selected. In contrast, the last cell knows all interference channels to the already selected users in other cells so that the BS, $b =\mid \mathcal{B} \mid$, can select users in a subspace which is an intersection of null spaces of all interference channels.

b) ***DCUS algorithm***: in DCUS algorithm, the process of user selection is implemented circularly among the cells. More specifically, while in DSUS algorithm, each BS selects its set of users in the one round and then the next BS does the same and the process continues until the last cell, in DCUS algorithm, however, each BS selects one user in its round and the next BS does the same and so on.

When the next round comes the process repeated from the first BS to the last one to select another single user by each cell. Thus, the process is implemented circularly among the cells. The detailed process of circular multicell scheduling is presented in **Algorithm 5**. The DCUS algorithm brings about more delay and frequent signalling, since each BS has to wait for other BSs to select one user per each so that it can select another single user again. However, with DCUS the disparity in sum rates among the cells is significantly reduced, especially when users have the same average SNR, as will be evident by simulation results. Further comment will be made regarding this point in simulation results.

Algorithm 4 DSUS scheduling algorithm

1: Initialisation step: $\mathcal{W}_b = \{1, ..., \mid \mathcal{W}_b \mid\}$, $\mathcal{Z}_b = \phi$. $\mid \mathcal{K}_b \mid = \frac{N_t}{\mid \mathcal{B} \mid N_r}$, $\forall b \in \{1, ..., \mid \mathcal{B} \mid\}$.

2: Scheduling step

- BS $b = 1$ independently selects $\mid \mathcal{K}_b \mid$ users using algorithm 2, updates $\mathcal{W}_b$ and $\mathcal{Z}_b$. Then, it conveys the interference channels of selected users by other BSs to all BSs.
- **for** $b = 2$ to $\mid \mathcal{B} \mid$ **do**
  - Each BS b conveys the interference channels $\mathbf{H}_{k_b}^{(s)}$ to each BS s, $\forall k_b \in \mathcal{Z}_b, s \in \{b+1, ..., \mid \mathcal{B} \mid\}$.
  - BS b constructs $\hat{\mathbf{H}}^{(b)} = [\bar{\mathbf{H}}_1^{(b)^{\mathsf{H}}}, ..., \bar{\mathbf{H}}_s^{(b)^{\mathsf{H}}}]^{\mathsf{H}}, \forall b > s \in \{1, .., \mid \mathcal{B} \mid\}$ and $\bar{\mathbf{H}}_s^{(b)} = [\mathbf{H}_1^{(b)^{\mathsf{H}}}, ..., \mathbf{H}_{|\mathcal{K}_s|}^{(b)^{\mathsf{H}}}]^{\mathsf{H}}$.
  - BS b calculates the matrix $\mathbf{N}_b$ as $\mathbf{N}_b = \text{null}(\hat{\mathbf{H}}^{(b)})$ and uses it as an input in the iterative algorithm.
  - BS b selects its users based on $\mathbf{N}_b$.
  - BS b updates $\mathcal{W}_b$ and $\mathcal{Z}_b$.
  - Each BS b conveys the $\bar{\mathbf{H}}_b^{(n)}$ to each BS n, $\forall n < s$.
- **end for**

3: Precoding step: After scheduling step and exchanging the interference channels of all selected users by all BSs, each BS b distributively designs the precoders for their own users by considering a new input matrix $\mathbf{N}_b = \text{null}(\hat{\mathbf{H}}^{(b)})$ where $\hat{\mathbf{H}}^{(b)} = [\bar{\mathbf{H}}_1^{(b)^{\mathsf{H}}}, ..., \bar{\mathbf{H}}_{s-1}^{(b)^{\mathsf{H}}}, \bar{\mathbf{H}}_{s+1}^{(b)^{\mathsf{H}}}, ..., \bar{\mathbf{H}}_{|\mathcal{B}|}^{(b)^{\mathsf{H}}}]^{\mathsf{H}}, \forall b \neq s \in \mathcal{B}$

Algorithm 5 DCUS scheduling algorithm

1: Initialisation step: $\mathcal{W}_b = \{1, ..., \mid \mathcal{W}_b \mid\}$, $\mathcal{Z}_b = \phi$. $\mid \mathcal{K}_b \mid = \frac{N_t}{\mid \mathcal{B} \mid N_r}$, $\forall b \in \{1, ..., \mid \mathcal{B} \mid\}$.
2: Scheduling step
3: **for** $b = 1$ to $\mid \mathcal{B} \mid$ **do**
3.1) Each BS b selects one user based on the following metric

$$\hat{k}_b = \arg \max_{k_b \in \mathcal{W}_b} \mu_{k_b}^{(1)}$$

3.2) Each BS b conveys the interference channels $\mathbf{H}_{k_b}^{(s)}$ to each BS s, $\forall k_b \in \mathcal{Z}_b, s \in \{b+1, ..., \mid \mathcal{B} \mid\}$.
3.3) BS b constructs $\hat{\mathbf{H}}^{(b)} = [\bar{\mathbf{H}}_1^{(b)^{\mathsf{H}}}, ..., \bar{\mathbf{H}}_s^{(b)^{\mathsf{H}}}]^{\mathsf{H}}, \forall b > s \in \{1, .., \mid \mathcal{B} \mid\}$ and $\bar{\mathbf{H}}_s^{(b)} = [\mathbf{H}_1^{(b)^{\mathsf{H}}}, ..., \mathbf{H}_i^{(b)^{\mathsf{H}}}]^{\mathsf{H}}$.
3.4) BS b updates the matrices $\mathbf{N}_b$, $\mathcal{W}_b$, and $\mathcal{Z}_b$.
3.5) Each BS b conveys the $\bar{\mathbf{H}}_b^{(n)}$ to each BS n, $\forall n < s$.
4: **end for**
5: **for** $i = 2$ to $\mid \mathcal{K}_b \mid$ **do**
6: **for** $b = 1$ to $\mid \mathcal{B} \mid$ **do**
- BS b independently selects one user using the following metric

$$\hat{k}_b = \arg \max_{m \in \mathcal{W}_b} \mu_m^{(i)} \prod_{k \in \mathcal{Z}_b} \mu_k^{(i-1)} \cos^2 \psi_m$$

- Do the (3.2-3.5) in step 3 for updating $\mathbf{N}_b$.

7: **end for**
8: **end for**
9: Precoding step: After scheduling step and exchanging the interference channels of all selected users by all BSs, each BS b distributively designs the precoders for their own users by considering a new input matrix $\mathbf{N}_b = \text{null}(\hat{\mathbf{H}}^{(b)})$ where $\hat{\mathbf{H}}^{(b)} = [\bar{\mathbf{H}}_1^{(b)^{\mathsf{H}}}, ..., \bar{\mathbf{H}}_{s-1}^{(b)^{\mathsf{H}}}, \bar{\mathbf{H}}_{s+1}^{(b)^{\mathsf{H}}}, ..., \bar{\mathbf{H}}_B^{(b)^{\mathsf{H}}}]^{\mathsf{H}}, \forall b \neq s \in \mathcal{B}$

5.3.3 Computational Complexity Analysis

Here, a comparison is made between the complexity of the proposed multicell user and multimode scheduling algorithm to that of brute-force search. Computational complexity is usually measured in terms of the number of flops φ required to accomplish the whole process of calculation. A flop is defined as a real floating point point operation, thus, a real addition and multiplication operation have one flop. While a complex addition and multiplication have two flops and six flops, respectively.

Consider a complex matrix $\mathbf{H} \in \mathbb{C}^{m \times n}$, the complexity of the following matrix operations is given as [128]

- Multiplication of an $m \times r$ complex matrix with a $r \times n$ complex matrix has $8mrn$ flops.
- Gram-Schmidt orthogonalisation (GSO) has $8m^2n - 2mn$ flops.
- SVD has approximately $24mn^2 + 48m^2n + 54m^3$.
- $\det(\mathbf{HH})$ takes $8m^2n + \frac{4}{3}m^3 - \frac{3}{2}m^2 + \frac{13}{6}m$ flops.

In the optimal multicell user/multimode scheduling, it is assumed that a central unit conducts an exhaustive search over all possible users and spatial modes combinations of which the complexity are given by (5.25) and (5.26), respectively. To find the complexity of the proposed multicell scheduling algorithm, only the first stage, i.e. user scheduling will be considered, and the precoding stage is neglected. For simple notation, let K denote the total number of users in each cell, i.e. $K = \mid \mathcal{U}_b \mid$. Then, the complexity of the proposed algorithms assuming only user selection (no multimode selection) can be counted for each cell as follows:

- $i = 1$: calculating both $\mu_{k_b}^{(1)}$ and GSO requires $K(16N_r^2N_t - 2N_rN_t + \frac{4}{3}N_r^3 - \frac{3}{2}N_r^2 + \frac{13}{6}N_r)$ flops.
- $i \geq 2$ calculating $\mu_{k_b}^{(i)}$, $\cos^2(\psi_m)$, and $\mathbf{H}_{k_b}^{(b)}$ needs approximately $(8N_r^2N_t + \frac{4}{3}N_r^3 - \frac{3}{2}N_r^2 + \frac{13}{6}N_r)$, $8N_rN_t^2 + 8N_r^2N_t + \frac{4}{3}N_r^3 - \frac{3}{2}N_r^2 + \frac{13}{6}N_r$, and $(8N_t^2N_r)$, respectively.

For cell $b \geq 1$, it requires to calculate the null space of interference channels which takes $8(b-1) \mid \mathcal{K}_b \mid^2 N_r$ flops. Hence, the complexity is given by

$$\begin{aligned}\varphi_{us}^{pro.} \approx & \sum_{b=1}^{|\mathcal{B}|} \Bigg(K(16N_r^2N_t - 2N_rN_t + \frac{4}{3}N_r^3 - \frac{3}{2}N_r^2 + \frac{13}{6}N_r) \\ & + \sum_{i=2}^{|\mathcal{K}_b|}(K-i+1) \times \Bigg\{ 8N_r^2N_t + \frac{4}{3}N_r^3 - \frac{3}{2}N_r^2 \\ & + \frac{13}{6}N_r + 8N_t^2N_r \Bigg\} + (b-1) \mid \mathcal{K}_b \mid^2 N_r \Bigg) \\ & \approx \mathcal{O}\Bigg(\mid \mathcal{B} \mid K \mid \mathcal{K}_b \mid N_t^2 N_r \Bigg) \end{aligned} \tag{5.27}$$

The complexity ratio of two methods:exhaustive search and the proposed algorithm is approximately given by

$$\xi \approx \frac{KN_r}{\mid \mathcal{B} \mid^2 N_t C_{\lceil BN_t/N_r \rceil}^{BK}} \tag{5.28}$$

(5.28) shows dramatic reduction in computational complexity for multicell scheduling.

5.4 Proportional Fair Scheduling

While **Algorithms 4, 5** described in Section 5.3 aim at maximising system throughput, however, they will always favour users with better channel conditions. Under practical situations, when users may stay at the cell edge for a long time, this gives rise to fairness issue, i.e. cell-edge users may not get scheduled for long time as long as they stay on cell boundaries. Fair scheduling is proposed to guarantee a certain degree of fairness among the users in the system. Various fair scheduling are proposed in literature, however in this work we consider proportional fairness scheduler. To keep space limited, multimode selection is considered with proportional fairness (PF)

scheduler problem in the following discussion, which can be defined as

$$R^{PF} = \arg \max_{\mathcal{K}_b \in \mathcal{U}_b, L_{k_b}, \mathbf{P}_{k_b}, \mathbf{Q}_{k_b}} \sum_{b=1}^{|\mathcal{B}|} \sum_{k_b \in \mathcal{K}_b} \frac{R_{k_b}(t)}{\overline{R}_{k_b}(t)} \tag{5.29}$$

with the same constraints in (5.20)-(5.24). In this problem, $R_{k_b}(t)$ is the rate of the user k_b at time instant t. While $\overline{R}_{k_b}(t)$ is the average rate of user k_b. When setting $\overline{R}_{k_b}(t)$ to 1 the problem is reduced to that of (5.19) which is identical to maximising the sum rate. In PF, $\overline{R}_{k_b}(t)$ is updated as

$$\overline{R}_{k_b}(t+1) = \begin{cases} (1 - 1/t_c)\overline{R}_{k_b}(t) + (1/t_c)R_{k_b}(t) & \text{if selected} \\ (1 - 1/t_c)\overline{R}_{k_b}(t) & \text{if not selected} \end{cases} \tag{5.30}$$

where t_c is window time. The PF scheduler ensures the fairness by giving priority to the users with sufficiently large value of $\frac{R_{k_b}(t)}{\overline{R}_{k_b}(t)}$. Thus, users with low average rate $\overline{R}_{k_b}(t)$ are more likely to be served in the subsequent scheduling intervals. The problem of PF with user selection lies in the fact that the exact rate R_{k_b} of user k_b is unknown before completion of user selection process. However, similar to [41], this problem can be overcome by assuming constant power allocation which is near optimal in high SINR regime. Let $L^i_{k_b}$ be the number of spatial modes at ith iteration for the user k_b including the stream to be scheduled next, denoted as $\hat{l}$. The rate of user k_b in the ith iteration step can be approximated as:

$$R^i_{k_b} \approx \sum_{l=1}^{L_{k_b}} \log_2\big(1 + \frac{P}{iL^i_{k_b}} g^i_{k_b}\big) \tag{5.31}$$

where

$$g^i_{k_b} = \prod_{l \in \mathcal{S}_{k_b} \cup \{\hat{l}\}} \mu^i_{k_b,l} \tag{5.32}$$

$g^i_{k_b}$ represents the product of of squared row norms of the effective channels. The above metric can be further simplified assuming high SINR regime as

$$R^i_{k_b} \approx \log_2\big(\big(\frac{P}{iL^i_{k_b}}\big)^{L^i_{k_b}} g^i_{k_b}\big) \tag{5.33}$$

The multimode selection metric for PF scheduler at the ith iteration is replaced by:

$$(\hat{k}_b, \hat{l}) = \arg \max_{m \in \mathcal{W}_b; l \in \mathcal{A}_{k_b}} \frac{R^i_{k_b}}{\overline{R}_{k_b}} + \sum_{k \in \mathcal{Z}_b} \sum_{j \in \mathcal{S}_{k_b}} \frac{R^i_{k_b}}{\overline{R}_{k_b}} \tag{5.34}$$

5.5 Simulation Results

A multicell system consisting of three hexagonal cells ($\mid \mathcal{B} \mid = 3$) with radius of $R = 1$km is considered for simulation. Each BS is equipped with $N_t = 12$ and employs BD or multimode selection while coordinating toward users served by other cells. Multiple antenna users are randomly and uniformly distributed within the cell area. The users are always assumed to have data for transmission (full buffer assumption). Although the proposed scheme can accommodate multi-carrier systems, only consider single subchannel with bandwidth of 15 kHz is considered. The channel is assumed to be subjected to three components; path-loss, lognormal shadowing, and small-scale Rayleigh fading. The coefficients of Rayleigh fading are assumed to be flat and spatially uncorrelated. The path-loss with shadowing of standard deviation $\varrho_s = 8$ dB is given by:

$$\beta^i_{k_b}(\text{dB}) = 136 + 40 \log_{10}(d^i_{kb}) \tag{5.35}$$

where d is the distance given in km between the user k_b and a BS i. The noise spectral density is given by N_o = -174 dBm/Hz.

Fig. 5.2 depicts the total sum rate in bit/s/Hz versus the total number of users, for $N_t = 12, N_r = 2$ and various power values, averaged over 10^5 channel realisations. It can be clearly observed that the proposed algorithm DSUS achieves most of the

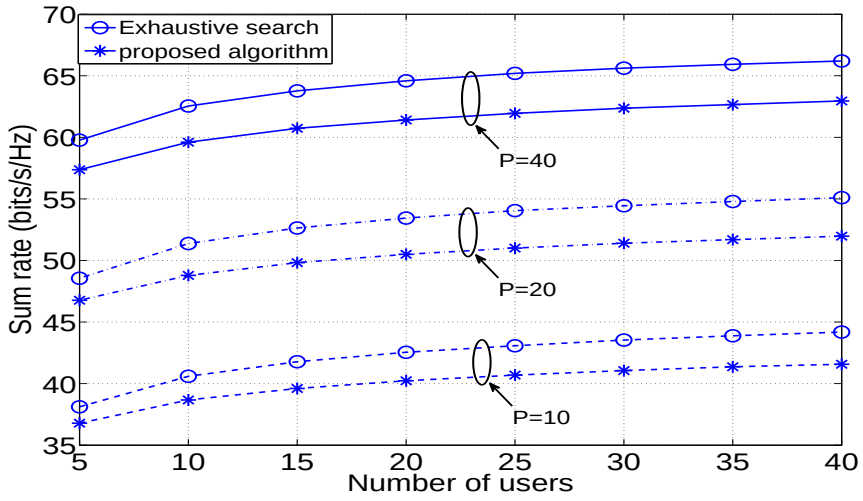

Figure 5.2: Comparison between an optmial solution obtained by exhaustive search and the proposed algorithm for different power values. ($N_t = 12, N_r = 2$)

sum rate achievable by exhaustive search. It can be also noticed that the sum rate is increased with the increase of total number of users, which is due to multiuser diversity.

In Fig. 5.3, comparison between DSUS and DCUS algorithms assuming user pairing in which the users are assumed to have the same SNR so that only small-scale fading is taken into account. As expected, we figure out that the gap in performance among cells in sequential algorithm is larger than that of circular algorithm. This comes in an agreement with our expectation that the order in which the process of multicell scheduling is accomplished allows the latest cells to select users whose channels directions lie almost in the null space of interference channels of all other users belonging to other cells. In contrast, the previous cells in the sequence of algorithm have no knowledge at their turn about other next cells user selection; consequently they may select users whose channels directions may not lie in the null space of interference channels to other cells users. Furthermore, it is expected that the gap diverges with the increase in the number of cells involved in coordination accordingly. On the other hand, in DCUS, since one user is selected by each cell in its turn, this allows the first cells in sequence to have knowledge about more interference channels to other

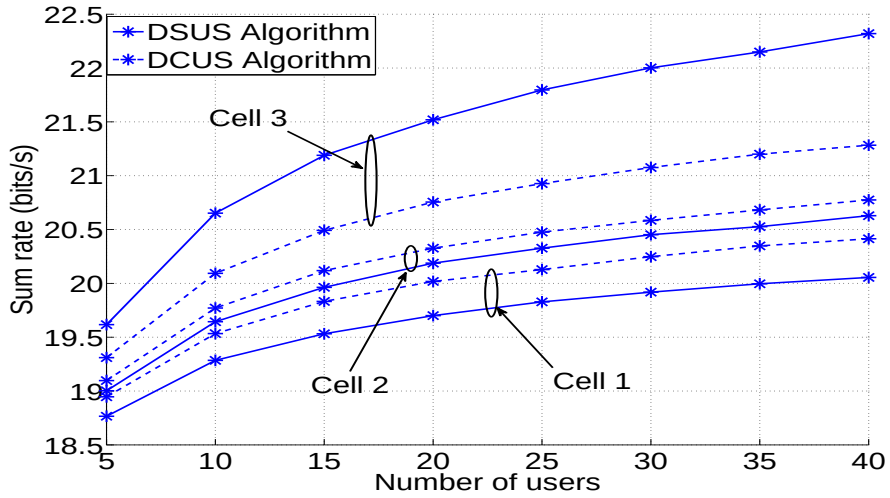

Figure 5.3: Comparison between rates of the cells obatined by the two proposed algorithms DSUS and DCUS. ($N_t = 12, N_r = 2, P = 40$ W)

cells users, while making the latest cells to have knowledge about fewer interference channels, hence yielding more fairness among the cells in terms of sum rate.

However, when the users suffer heterogeneous channel conditions, the gap tends to disappear and both algorithm will then have the same performance due to higher multiuser diversity gain provided by heterogeneity of users channels.

Fig. 5.4 compares between fixed spatial mode (conventional BD) and multimode selection. The figure depicts the sum rate versus number of users, with $N_t = 12$ and $N_r = 2$. As can be clearly observed, multimode selection outperforms the fixed spatial mode scheme with only user selection. The gain comes from the flexibility offered by multimode selection to choose the best set of channel direction on the level of antennas, thereby exploiting the spatial diversity more efficiently.

Figs. 5.5,5.6 compare between PF and MAX. Rate scheduling schemes. The total rates of the system and the sum rate of cells are depicted versus number of users, respectively. The observed decrease in sum rate in PF as compared with MAX. Rate comes from the fact that PF attempts to guarantee fairness as described previously.

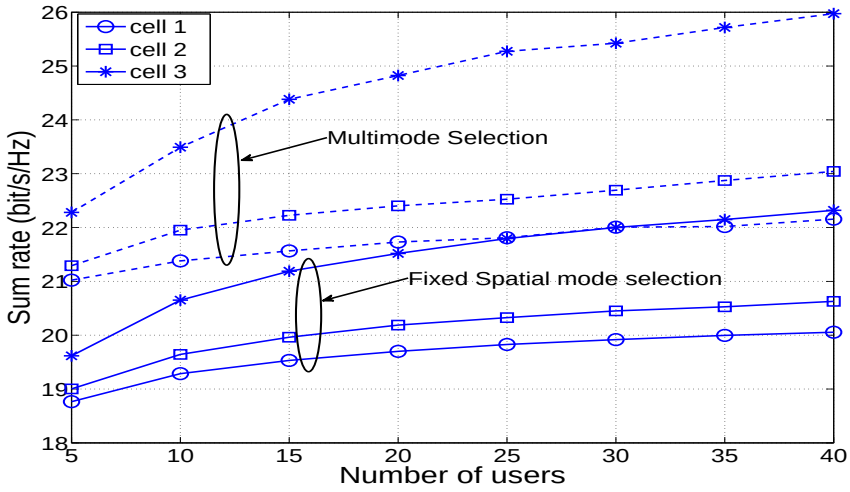

Figure 5.4: Comparison between rates of the cells obatined by conventional BD and multimode selection scheme. ($N_t = 12, N_r = 2, P = 40$ W)

5.6 Chpater Summary

In this chapter, multicell scheduling for coordinated MIMO cellular network is investigated and analysed. Low complexity algorithms are proposed for user scheduling with conventional BD and multimode scheduling schemes. The algorithms are based on two stages progressive sequential distributed multicell scheduling. The simulation results show high percentage of sum rate achievable via exhaustive search can be achieved by these algorithms.

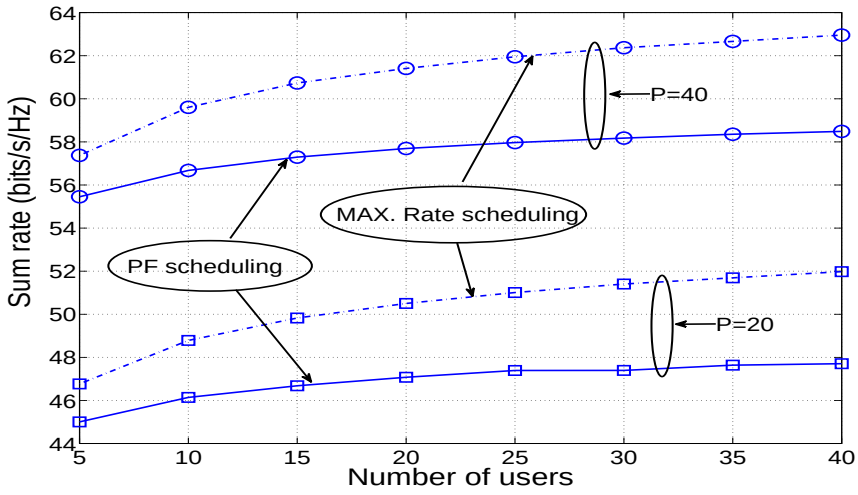

Figure 5.5: The figure compares between MAX. Rate and PF scheduling schemes in terms of sum of rates of the cells in the system versus number of users. ($N_t = 12, N_r = 2$)

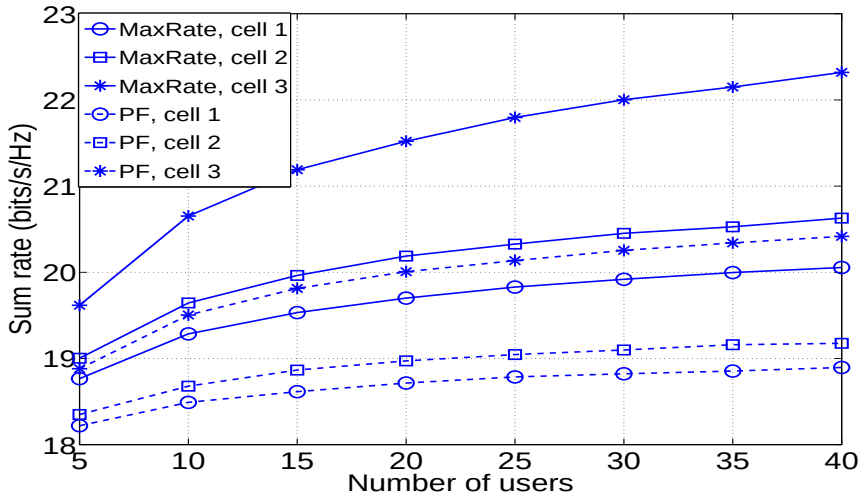

Figure 5.6: Compartsion between MAX. Rate and PF scheduling schemes in terms of sum rates of indivitual cells. ($N_t = 12, N_r = 2, P = 40$ W)

Chapter 6

Energy-Spectral Efficiency Trade-off in Coordinated OFDMA Systems

This chapter considers the network energy efficiency in multicell OFDMA downlink systems. A dynamic resource allocation scheme with limited coordination is proposed to optimise the network energy efficiency and satisfy user requirement. The proposed scheme has two steps; centralized and distributed. The simulation results shows that, for a given spectral efficiency, dramatic reduction in energy consumption can be achieved by such a dynamic coordination scheme.

6.1 Introduction

Most of the work on coordination or cooperation have mainly focused on improving spectral efficiency aspect but neglected the energy efficiency which was not considered in the design of the most cellular systems [18], [149]. Nowadays, energy consumption in industry and technological systems occupies a global concern for its great effect on

environmental on one hand and its economical cost on the other hand [19]. In both industry and operation in cellular networks, the energy consumption shows dramatic increase, particularly with explosive growth in the number of mobile subscribers that demand high bit rate applications. Recent surveys on energy consumption of cellular systems have shown that BSs consume around 70 percent of the energy required for operating the cellular systems [18]. For this reason several projects have been funded in Europe to achieve the goal of energy reduction in cellular systems. Many aspects have been researched to achieve this goal such as deployment, sleep BSs, new energy-efficient signal processing [19], [149]. However, one of the main aspects that could play an important role in energy reduction is multicell scheduling and resource management [150]-[152], [155].

Energy-efficiency is analysed for multicell uplink in [152], an interference-aware scheme to enhance the energy-efficiency is proposed using game theory analysis. In [153], co-operative idling scheme is proposed for enhancing energy efficiency in MIMO multicell systems where some BSs are switched into sleep mode while activating the other BSs. In [154], coordinated beamforming is assumed and lower complexity algorithm is proposed to solve the nonconvex problem. Most of the previous work assume single subcarrier, however, in this chapter a different approach is followed, as the main focus will be on OFDMA system with discrete power allocation and dynamic frequency planning. An adaptive scheme of two level solution is proposed for energy-efficient resource allocation fulfilling the minimum spectral efficiency in the the whole system. The main idea is to propose a dynamic frequency planning to allocate resources in two stages. In the first stage, referred to as the central optimization level, a central unit takes the responsibility of allocating the resources for the outer region users based on best channel quality for the users. The central unit assigns orthogonal subchannels and powers for the outer region users based on their CSIs conveyed by the BSs involved in coordination. While, in the second stage, named as distributed optimization level, each cell allocates the rest resources to the inner region users with an objective of minimizing the total power consumption. In the first stage, the optimisation problem is formulated as a fractional integer programming to allocate the

resources to the cell-edge users with an objective of enhancing energy efficiency. In the second stage, which is implemented distributively by each cell, the optimisation problem is formulated as an integer programming to allocate the remaining resources to the cell-centre users, with an objective of power minimisation to decrease the interference level. Thus, only limited coordination is required by BSs, in which the CSIs of cell-edge users are exchanged among BSs. Based on this proposed scheme, we analyse energy-spectral efficiency trade-off, and compare the simulation results of both dynamic and static frequency planning, in which the resources are fixed for cell-edge and cell centre users.

The rest of this chapter is organised as follows. In Section 6.2, the system model adopted in this chapter is described. In Section 6.3, optimisation problems of both centralised level and distributed level stages are formulated and solved. In Section 6.4, the evaluation of proposed resource allocation scheme and simulation results are introduced. Finally, Section 6.5 summarises the chapter.

6.2 System Model

Consider an OFDMA cellular system with the set of BSs denoted as $\mathcal{B} = \{1, ..., B\}$, each equipped with single-antenna as shown in Fig. 6.1. Each BS serves a set of users denoted as $\mathcal{U}_b$ single-antenna users where $b \in \mathcal{B}$ denotes the index of BS. The total number of resource blocks (RB) in the system is N, where each resource block consists of 12 subcarriers which are supposed to have the same channel response in frequency domain, and 14 OFDM symbols in time domain (1 ms). Frequency reuse of one factor, i.e. FRF=1, is assumed, where all cells share the same spectrum. The instantaneous CSI on all RBs is assumed to be perfectly estimated at each user u_b in cell b and fed back to their serving BS.

Assuming that the channel fading is flat over every RB, i.e. the bandwidth of every RB is less than the coherence bandwidth of the channel, and the channel state doesn't change in OFDM frame duration, i.e. the OFDM system duration is less than

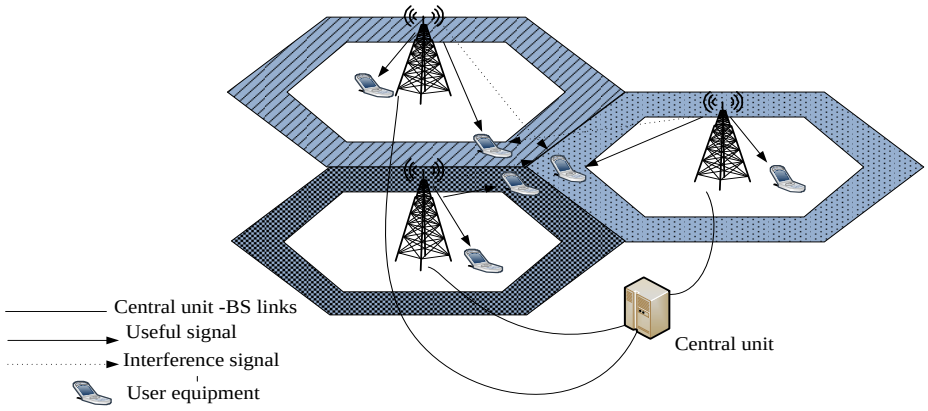

Figure 6.1: An illustration of a hexagonal multicell OFDMA network with the BSs being connected through backhaul links to a central unit. Every cell has outer and inner region users, which are to be served by centralised stage and distributed stage, respectively.

time coherence; then the SINR for user u in cell b estimated over nth RB denoted by $\text{SINR}_{m,n,u}$ can be expressed as follows:

$$\text{SINR}_{b,n,u} = \frac{p_{b,n,u} g_{b,n,u}}{\sigma^2 + \sum_{j=1, j\neq b}^{B} p_{j,n,u} g_{j,n,u}} \tag{6.1}$$

where $p_{b,n,u}$ is the power transmitted by bth BS to user u on RB n, $g_{b,n,u}$ captures both slow fading (due to path-loss and shadowing) and fast fading (due to Rayleigh fading) effects on the subcarriers in RB n for user u in cell b. The denominator represents the noise, σ^2, on the sets of subcarriers in each RB n, added to the interference caused by other base stations in neighbouring cells. In this system set up, we consider only the average interference which can be obtained by averaging the instantaneous channel states over fast fading and shadowing effects. This reduces the feedback signalling required for acquiring the instantaneous channels of all interfering BSs.

6.2.1 Adaptive Modulation and Discrete Power Allocation

Denote $P_r(\texttt{BER}, c)$ as the minimum $\text{SINR}_{b,n,u}$ required to be received in any RB for a given bit error rate (BER) and modulation scheme (c), where c denotes the number of loaded bits taken from the set of possible values $d = \{0, d_1, d_2, ..., d_{\text{C}}\}$ with C denoting the number of possible modulation schemes, for example for QAM modulation schemes,$P_r(\texttt{BER}, c)$ can be represented as [11]:

$$P_r(\texttt{BER}, c) = \frac{N_o}{3}(Q^{-1}(\texttt{BER}))^2(2^c - 1) \tag{6.2}$$

where N_o is the single-sided noise power spectral density ,and $Q^{-1}(x)$ is the inverse Q-function that is given by $Q^{-1}(\texttt{BER}) = \frac{1}{\sqrt{2\pi}} \int_x^\infty \text{e}^{-\frac{t^2}{2}}\, \text{d}t$ [156], therefore for the transmitter to satisfy the requirement of minimum received power for a given BER, the minimum transmission power that should be allocated to the RB n for the user u in cell b must be:

$$p_{b,n,u} \quad = \quad \frac{P_r(\texttt{BER}, c_{b,n,u}) \times (N_{noise} + I)}{g_{b,n,u}} \tag{6.3}$$

where $N_{noise} = N_o W$ represents the amount of noise power in RB n, where W is the bandwidth of RB, and I is the average interference measured within nth RB.

6.2.2 Dynamic Frequency Planning

It is assumed that *dynamic frequency planing* (DFP) wherein the cell area is divided into two regions, inner and outer according to the user proximity to the BS. The users can be classified as inner or outer region users based on threshold value of signal to interference and noise ratio ($\gamma_{\texttt{th}}$). More specifically, for each user if $\frac{\sum_{i=1}^{N} \text{SINR}_{b,n,u}}{N} > \gamma_{\texttt{th}}$, then the user is considered as an inner region user, otherwise an outer region user. BS can do so by using reported measurements of users reference signal. Alternatively, a user can be determined as an inner or outer region user based on its distance from

the BS, if its location is no farther than r_{th}, the user is considered as an inner region and otherwise outer region user, where r_{th} is a threshold distance which can be set by the system. In the proposed DFP the spectrum resources is divided between the outer and inner region, where the spectrum subbands allocated for outer region users should be orthogonal, and the rest of the spectrum subbands are shared by cell centre users.

6.3 Energy Efficient Resource Allocation

In general, it is very well known that the joint optimization of subcarriers and powers allocation in multicell scenarios with interference is non-convex problem due to power coupling among the cells. Hence, from practical perspective, it is necessary to seek for practical approaches that could reduce the complexity of the problem. In multicell scenarios, the main issue is to reduce the interference which has ,in particular, severe effect on the cell-edge users. Therefore a strategy of allocating orthogonal subcarriers can help reduce the interference effect. In order to do so, the BSs must jointly coordinate their resource allocation strategy on the cell-edges such that orthogonal resources are allocated for different cell-edge users. In this context, it is proposed to decompose the problem of joint optimization for enhancing energy efficiency into two subproblems; centralised and distributed levels. Next, each step will be discussed, whereby the optimisation problem is formulated.

6.3.1 Centralised Optimisation Level

In this level the objective is to allocate orthogonal RBs among the outer region users belonging to different cells. There is assumed that there exist error-free, high speed links connecting all BSs to a central unit as shown in Fig. 6.1, wherein the central optimization is carried out to allocate different resource blocks to different outer region users served by different BSs.

First, each cell b determines the number of its own outer region users based on either way described previously. In this thesis, we adopt the second approach which is based on threshold distance r_{th}. Denote the set of outer-region and inner-region users as $\mathcal{U}_o$ and $\mathcal{U}_i$, respectively, where $\mid \mathcal{U}_o \cup \mathcal{U}_i \mid = \mid \mathcal{U}_b \mid$ for every cell (b). Each cell b sends the necessary information of its own outer region users to the central unit which in turn allocates the resources among outer region users with the objective of enhancing the energy efficiency of the whole system. We define the energy efficiency metric (EE) as the ratio of the total power consumption over spectral efficiency (SE) (the unit: joule/bit). SE can be defined as total loaded bits per OFDM symbol (bits/symbol) or equivalently (bps/Hz). Hence, EE can be defined as the ratio of total power consumption over the total transmitted bit rate. We also assume that the total power in a cell is partitioned between outer and inner region users according to a power ratio α, such that $\alpha{=}\frac{P_o}{P_i}$, where P_o and P_i are the total power allocated to outer and inner region users respectively. α can be adjusted by the operator according to the traffic variation, and usually takes values larger than one as the outer region users usually needs more power than the inner region users assuming the same number of users. Let us denote $x_{b,n,u}$ as the assignment variable which has a value of one if the RB n is assigned to the user u in cell b, and zero otherwise [157]. Assuming discrete power allocation and bit loading, the energy efficient resource allocation can be defined as an integer linear optimization problem [158] as follows:

$$\min_{c_{b,n,u},x_{b,n,u}} \quad \mathrm{EE} \quad = \frac{P_{\mathsf{C}} + \sum_{b=1}^{|\mathcal{B}|}\sum_{n=1}^{N}\sum_{u\in\mathcal{U}_o} p_{b,n,u}x_{b,n,u}}{\sum_{b=1}^{|\mathcal{B}|}\sum_{n=1}^{N}\sum_{u\in\mathcal{U}_o} c_{b,n,u}x_{b,n,u}} \tag{6.4}$$

$$\text{s.t.} \quad \sum_{b=1}^{|\mathcal{B}|}\sum_{n=1}^{N}\sum_{u\in\mathcal{U}_o} c_{b,n,u}x_{b,n,u} \geq \mathrm{R}_{sys}^{outer} \tag{6.5}$$

$$\sum_{n=1}^{N} c_{b,n,u}x_{b,n,u} \geq \mathrm{R}_{u}^{\min}, \forall u \in \mathcal{U}_o \tag{6.6}$$

$$\sum_{n=1}^{N}\sum_{u\in\mathcal{U}_o} p_{b,n,u}x_{b,n,u} \leq P_{\mathrm{o}}, \forall b \tag{6.7}$$

$$\sum_{n=1}^{N} x_{b,n,u} = 1 \tag{6.8}$$

$$x_{b,n,u} \in \{0,1\} \tag{6.9}$$

The first constraint (6.5) ensures the target system throughput R_{sys}^{outer}, which is equivalent to system spectral efficiency SE for all outer-region users in the whole system. Constraint(6.6) guarantees the fairness among users by allowing each user having minimum bit rate. Constraint (6.7) is to impose per-cell maximum allowable power constraints. The constraint (6.8) ensures the exclusivity of RBs assignment among the users and cells. where $P_{\mathtt{C}}$ is a circuit power dissipation which is assumed to be static in this paper. Lastly, (6.9) is the optimisation variable that can take only two possible values 0,1. For such an optimisation problem, the central unit decides which RBs to assign to which user so that the EE metric in the whole system is minimized. In this central step, the priority of RBs assignment is given for the outer region users first. Having the outer region users allocated the required resources, the central unit passes the assignment vector for the outer region to all involved BSs, then each BS can distributively allocate the rest of resources to the inner region users. The above formulated problem is a fractional integer optimisation problem [159], which can be iteratively solved using the parametric approach suggested by Dinkelbach in [160]. The basic idea of this algorithm is to transform the fractional objective function into a difference function which can be parametrized by a parameter δ which in turn can be updated by generating sequences of iteration until convergence. The proof of convergence is given in [160]. The steps of the algorithm are shown below:

Algorithm 6 Dinkelbach algorithm

Choose $x^0 \in \{0,1\}$, Compute $\delta^1 = \frac{P(x^0)}{T(x^0)}, k = k+1$.
Find x^k by solving problem x^k=arg $\max_{x\in\{0,1\}} \{P(x) - \delta^k T(x)\}$.
if $Q(\delta^k)$=$\max_{x} \{P(x) - \delta^k T(x)\} < \epsilon$ **then**
  $\delta^* \Leftarrow \delta^k$, $x^* \Leftarrow x^k$, **Stop**.
end if
δ^{k+1}=$\frac{P(x^k)}{T(x^k)}$, $k = k+1$, **go to Step 2.**

6.3.2 Distributed Optimisation Level

At this level, each BS allocate the remaining resources (RBs and power) to the rest of users in distributed manner. Denote the set of RBs allocated for outer-region users and that of the remaining RBs to be allocated for inner-region users as Ω_o and Ω_i respectively, such that $\mid \Omega_o \cup \Omega_i \mid = N$. Now in order to reduce the interference on the other cells, each BS minimises the total transmit power such that each user gets minimum QoS, in short each BS solves the following margin adaptive optimization problem:

$$\min_{c_{b,n,u}, y_{b,n,u}} \mathrm{P} = \sum_{n \in \Omega_i} \sum_{u \in \mathcal{U}_i} p_{b,n,u} y_{b,n,u} \tag{6.10}$$

$$\text{s.t.} \quad \sum_{n \in \Omega_i} \sum_{u \in \mathcal{U}_i} c_{b,n,u} y_{b,n,u} \geq \mathrm{R}_{sys}^{inner} \tag{6.11}$$

$$\sum_{n \in \Omega_i} c_{b,n,u} y_{b,n,u} \geq \mathrm{R}_u^{\min}, \forall u \in \mathcal{U}_i \tag{6.12}$$

$$\sum_{n \in \Omega_i} \sum_{u \in \mathcal{U}_i} p_{b,n,u} y_{b,n,u} \leq P_{\mathrm{i}}, \tag{6.13}$$

$$\sum_{n \in \Omega_i} y_{b,n,u} = 1 \tag{6.14}$$

$$y_{b,n,u} \in \{0, 1\} \tag{6.15}$$

Recall that $\mathcal{U}_i$ denotes the set of inner region users. The constraints have the same meaning as previous optimization problem but for inner-region users. Although margin adaptive optimization may not necessarily be an energy efficient,the justification for adopting it, however, is the fact that minimizing the power reduces the amount of interference on the other cells, which is the crucial factor that deteriorate the throughput as well as the energy efficiency. Furthermore, enhancing the energy efficiency for the inner region users may bring about an extra interference on the outer region users in other cells [152].

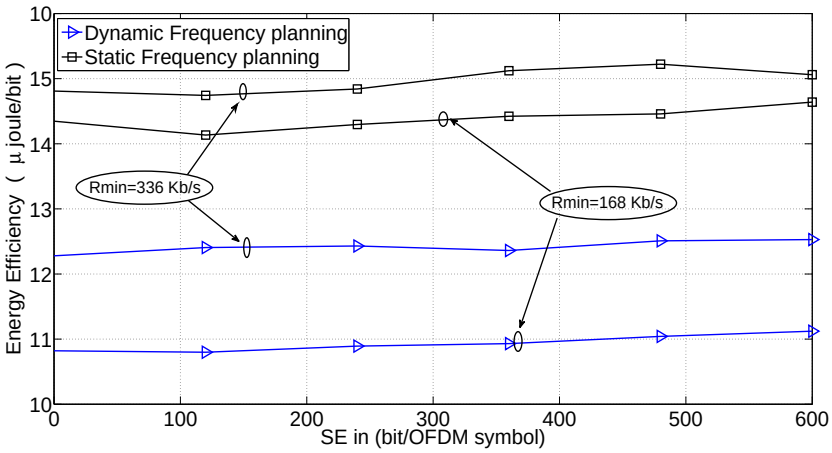

Figure 6.2: System spectral-energy efficiency trade-off.

6.4 Simulation Results and Discussions

Consider three hexagonal cells with a radius of 1 Km, the users are distributed randomly in the cells, with full-buffer for each user. Long Term Evolution (LTE) system parameters are assumed in the our simulation. The resource block structure consists of 12 subcarriers in frequency domain, and 14 symbols in time domain, the frame duration is 1 ms, which is the time period of every new scheduling. The bandwidth of 12 contiguous subcarriers in one RB is 180 KHz. The channel is considered to be subjected to path-loss and shadowing with standard deviation of 8 dB. The path-loss can be calculated as [161]

$$L[\text{dB}] = 136 + 37.6 \log_{10}(d) \tag{6.16}$$

where d is the distance between a user and the its serving BS in km. The static power is assumed to be constant and equal to 100 W, P_{total} = 43 W, , α = 3, N_o = -174 dB/Hz. The BER is fixed to 10^{-4} in all examples.

Fig. 6.2 presents the spectral-energy trade-off for the two scenarios; dynamic and

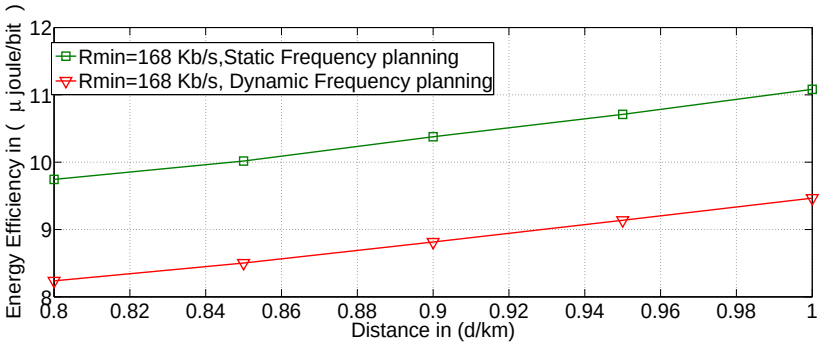

Figure 6.3: Energy efficiency vs. the distance between the BS and users.

static frequency planning, assuming the number of RB is $N = 20$, and transmit power 43 per each BS, the number of users 2 at the cell edge. It can be clearly observed that DFP significantly outperforms the static frequency planning where the spectrum allocation is fixed for outer and inner regions. This indicates that the coordination and adaptation can enhance not only the spectral efficiency as indicated by previous works, but also enhances energy efficiency. This can be arguably reasoned by the fact that enhancing the link quality of outer region users can be more energy efficient if we allocate the RBs with best channel quality instead of increasing power, as the increase of power results in an additional interference which, consequently, deteriorates the links of inner region users in other cells. It can be also noticed that more energy consumption will be required as the QoS (represented by minimum bit rate)for each user is increased.

However, DFP requires frequent CSIs feedback to the serving BS as well as frequent signalling between BSs to convey CSIs to both serving and neighbouring BSs. This gives rise to a trade-off between system performance and cost in uplink resources. Fig. 6.3 depicts the energy consumption for both static and dynamic frequency planning with distance, assuming 20 RB, 6 users, the maximum required system spectral efficiency is 600 bit/symbol, and $\mathrm{R}_u^{\min}$ for each user is fixed at 168 Kb/s, the users are positioned at gradually different positions on cell boundaries. It can be clearly ob-

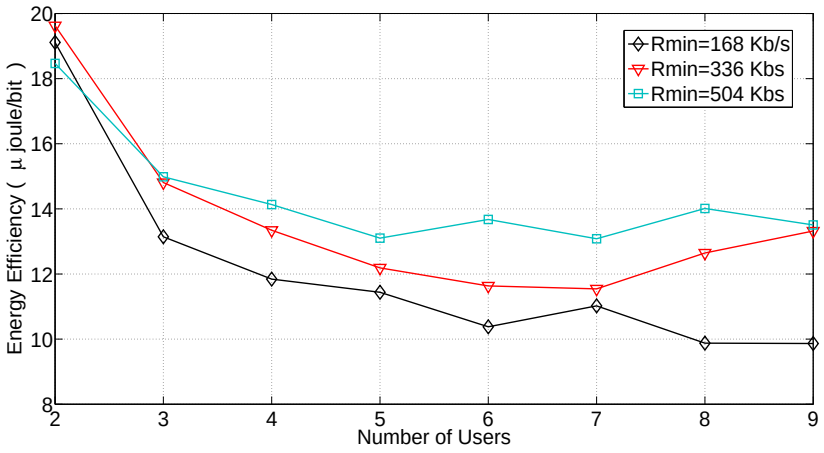

Figure 6.4: Energy efficiency vs. number of users.

served that the energy consumption increases with distance, the reduction in energy consumption in coordinated-cells can be interpreted as a decrease in distance which gives insight on the importance of coordination between small cells in the future generation cellular systems. Fig. 6.4 shows the effect of multiuser diversity on energy reduction, multiuser diversity is the gain obtained by the system when the number of users gets larger and larger, which means there is more likely to find a set of users with high channel quality to be scheduled at every time instance. Hence, scheduling users with better channel quality leads to an increase in system throughput, as the bit rate increases in proportion to the channel gain.

6.5 Chapter Summary

In this chapter, the energy efficiency in multicell scenario is investigated and analysed. An adaptive resource allocation scheme for coordinated multicell is proposed. The simulation results show big reduction in energy consumption as compared with statically coordinated scheme in which the spectrum is fixed for each cell on the boundaries. As a result, this emphasizes the importance of coordination in enhancing both spectral and energy efficiencies. In future research work, it may considerable to

design low complexity suboptimal algorithms for resource allocation and scheduling for coordinated-small cells scenarios.

Chapter 7

Conclusions and Future Work

The tremendous growth of smartphone devices has led to unprecedented demand for high volume of data traffic. To address this challenge, wireless networks tend to be more densified and the spectrum should be very efficiently utilised. In addition, an innovative cellular technology is required to flexibly manage the traffic demands. However, dense deployment and aggressive frequency reuse creates strong inter-cell interference that degrades users perfromance, especially at the cell-edges. Thus, it is important to develop interference management strategies that work alongside with network densification strategy. Multicell coordination is one of the promising techniques in this context.

In this thesis, multicell coordination has been analysed from different perspectives. In this concluding chapter, we summarise the key findings of the thesis and suggest new directions for future research.

7.1 Summary of Results

Chapter 3 has studied coverage probability and effective capacity for multicell downlink random cellular networks. Two main scenarios have been investigated and anal-

ysed. In the first scenario, distance-based power control strategies are analysed for two cases; SU-MIMO and MU-MIMO, and no multicell coordination is assumed to be implemented. In the second scenario, multicell coordination using coordinated beamforming is analysed. The BSs locations are modelled as a PPP, and mathematical tools from stochastic geometry are used to derive analytical expressions for coverage probability and effective capacity. Using the analytical results, the impact of power control and multicell coordination on both coverage and effective capacity is analysed and explained, showing that fractional power control factor is the best strategy in most cases. Interestingly, the analysis shows that in order to make use of coordination strategy, it should be adaptively implemented according to the network layout.

Chapter 4 has proposed an adaptive multicell coordination strategy for multi-carrier downlink cellular networks. The proposed adaptive strategy employs coordination and interference cancellation over frequency and space domains, respectively. Two variant schemes for the adaptive strategy have been proposed and analysed. The BSs location are modelled as a PPP, and stochastic geometry approach is adopted once again to derive analytical expressions for coverage probability of both cell-centre and cell-edge users in both schemes. Moreover, analytical expression for average rate is derived based on coverage probability analysis. It is confirmed through this analysis that such an adaptive strategy yields the best performance among others coordination without adaptation. An interesting observation is that the second scheme in which mixture of coordinated beamforming and no coordination, i.e. MRT are employed over the same frequency band (the second proposed scheme) gives an excellent performance for the cell-edge users, while guaranteeing an acceptable fairness between cell-edge and cell-centre users.

Chapter 5 has investigated joint user selection and scheduling in multicell coordinated MIMO downlink cellular network. Low complexity algorithms based on the idea of principal angle and the intersection of null spaces are proposed for user scheduling in multicell scenario. The algorithms consist of scheduling and precoding stages and work in sequential distributed fashion. Furthermore, multimode selection algorithm is developed to adaptively allocate spatial modes for the users. The algorithms re-

duces the overhead signalling required for CSIs while achieving most of the sum rate achievable by optimal exhaustive search as well dispense with the need for centralised processing. Simulation results show that multimode scheduling in multicell setting yields higher system rate due to exploitation of spatial diversity.

Chapter 6 has investigated the subchannel allocation and bit loading in multicell downlink OFDMA network. An adaptive coordinated multicell resource allocation is proposed to allocate orthogonal resources for the cell-edge and cell centre users. The proposed scheme consists of two stages. In the first stage, in which part of the resource are allocated for cell-edge users, the optimisation problem is formulated as a fractional integer linear programming with an energy efficiency objective function subject to system spectral efficiency and user QoS constraints. While, in the second stage, in which the rest of resource are allocated for cell-edge users, the optimisation problem is formulated as an integer linear programming subject to the same constraints. The first stage is implemented in a centralised manner, while the second is implemented distributively. The spectral-energy efficiency trade-off is analysed under this scheme, and simulation results highlights the improvement attained by such adaptive coordination scheme in reducing energy consumption.

7.2 Future Work

For the effective capacity in multicell scenario, this thesis has only focused on analytical approach to evaluate the performance of power control and coordination. However, it is worth extending the investigation to multicell scheduling approach with the objective of guaranteeing QoS constraints imposed by QoS exponent θ. The focus would be on finding a sub-optimal algorithm that gives best performance while keeping the complexity as low as possible. It is also important to consider fractional power control to combat the effect of small-scale fading in random cellular networks. For adaptive coordination strategies, this thesis considers only analytical approach for system evaluation. It is worth investigating how to apply large-scale MIMO (massive MIMO) and 3D beamforming techniques with such adaptation strategies. Another

interesting future research is how to design adaptive multicell resource allocation or scheduling scheme providing near-optimal performance whilst keeping the complexity as low as possible. The work in the thesis can also motivate a research direction toward using adaptive inter-cell interference cancellation in heterogeneous networks where different types of BSs of different capabilities are deployed. Additionally, a comprehensive framework can also include other important network aspects such as handover issues and traffic dynamics in heterogeneous networks.

For the multicell user scheduling, the thesis presents two algorithm for user and multimode selection, and the main focus was on spectral efficiency. It is also worth considering another objectives such as QoS guarantee or energy efficiency. Another interesting future research is to integrate OFDMA system with coordinated MIMO and investigate low complexity algorithm working in both dimensions; frequency and space, in coordinated multicell network. Also, one of the main challenges is CSIs feedback, thus it is worth investigating how to adaptively utilising limited feedback technique with such adaptive multimode selection in multicell setting.

For the investigation on multicell coordination in OFDMA systems, the thesis presents a general adaptive scheme for resource allocation consisting of two stages. However, the optimisation problems are based on integer programming, which is known to have high complexity. Thus, an interesting future research is to investigate low complexity algorithm giving near-optimal solution. It is also worth considering the integration of coordinated beamforming into OFDMA framework. Another promising future research is to consider adaptive coordination strategies for heterogeneous networks with the objective of seeking an optimal spectral-energy efficiency trade-off.

Appendix A

Proofs for Chapter 3

A.1 Proof of Proposition 3.1

Since $g_0 \sim \Gamma(N_t, 1)$, and its CCDF is the regularized gamma function given by $\frac{\gamma(N_t,x)}{\Gamma(N_t)} = \int_0^x \frac{t^{N_t-1}\mathrm{e}^{-t}}{\Gamma(N_t)}\mathrm{d}t$, bound on the CCDF is used as given in the following lemma [106].

Lemma 1: Suppose g_o is gamma r.v. with N shape parameter, i.e. $\Gamma(N, 1)$, then we have $\mathbb{P}(g_o < x) = \frac{\gamma(N,x)}{\Gamma(N)}$, which can be upper and lower bounded as [106]

$$(1 - e^{-\zeta x})^N \leq \frac{\gamma(N, x)}{\Gamma(N)} \leq (1 - e^{-x})^N \tag{A.1}$$

where $\zeta = (N!)^{-1/N}$.
Thus, using lemma and applying binomial expansion yields

$$\sum_{m=1}^{N_t} \binom{N_t}{m} (-1)^{m+1} \mathrm{e}^{-\zeta m x} \geq \frac{\gamma(N_t, x)}{\Gamma(N_t)} \geq \sum_{m=1}^{N_t} \binom{N_t}{m} (-1)^{m+1} \mathrm{e}^{-mx} \tag{A.2}$$

where $\zeta = (N_t!)^{-1/N_t}$, then the coverage probability can be written as:

$$
\begin{aligned}
P_c^{\mathsf{SU}} &= \int_{r_1\geq 0}^{\infty} \mathbb{P}\bigg(\frac{g_0 r_1^{\alpha(\eta-1)}}{(\sigma^2+I)} \geq \bar{\gamma}|r_1\bigg) f_{r_1}(r_1)\mathrm{d}r_1 \\
&= \int_{r_1\geq 0}^{\infty} \mathbb{P}\bigg(g_0 \geq r_1^{\alpha(1-\eta)}\bar{\gamma}(\sigma^2+I)|r_1\bigg) f_{r_1}(r_1)\mathrm{d}r_1 \\
&\overset{a}{\leq} \int_{r_1\geq 0}^{\infty} \sum_{m=1}^{N_t} \binom{N_t}{m} (-1)^{m+1} e^{-\bar{\gamma} m \zeta r_1^{\alpha(1-\eta)}\sigma^2} \mathbb{E}\big\{e^{-sI}|r_1\big\} f_{r_1}(r_1)\mathrm{d}r_1 \qquad \text{(A.3)}
\end{aligned}
$$

where $s = \bar{\gamma} m \zeta r_1^{\alpha(1-\eta)}$, the inequality in (a) stems from substituting the upper bound of $\frac{\gamma(N_t,x)}{\Gamma(N_t)}$ given by (A.2). The Laplace term, i.e., $\mathbb{E}\{e^{-sI} \mid r_1\}$ conditioned on r_1, can be obtained following the same approach in [98]:

$$
\begin{aligned}
\mathbb{E}\{e^{-sI} \mid r_1\} &= \mathbb{E}_{\Phi,\mathrm{g_i},X_i}\Big\{e^{-s\sum_{i\in\Phi/\{\mathrm{BS}_1\}} g_i X_i^{\alpha\eta} r_i^{-\alpha}}\Big\} \\
&= \mathbb{E}_{\Phi,X_i,\{\mathrm{g_i}\}}\Big\{\Big(\prod_{i\in\Phi/\{b_1\}} e^{-s g_i X_i^{\alpha\eta} r_i^{-\alpha}}\Big)\Big\} \\
&= \mathbb{E}_{\Phi}\Big\{\Big(\prod_{i\in\Phi/\{b_1\}} \mathbb{E}_{g_i,X_i}\Big\{e^{-s g_i X_i^{\alpha\eta} r_i^{-\alpha}}\Big\}\Big)\Big\} \\
&\overset{a}{=} \exp\bigg(-2\pi\lambda\int_{r_1}^{\infty}\Big(1-\mathbb{E}_{g,X}\Big\{e^{-sgX^{\alpha\eta}\upsilon^{-\alpha}}\Big\}\Big)\upsilon\mathrm{d}\upsilon\bigg) \\
&\overset{b}{=} \exp\bigg(-2\pi\lambda\mathbb{E}_X\Big\{\int_{r_1}^{\infty}\frac{(1+sX^{\alpha\eta}\upsilon^{-\alpha})^{\Psi}-1}{(1+sX^{\alpha\eta}\upsilon^{-\alpha})^{\Psi}}\upsilon\mathrm{d}\upsilon\Big\}\bigg) \\
&\overset{c}{=} \exp\bigg(-2\pi\lambda\mathbb{E}_X\Big\{\int_{r_1}^{\infty}\frac{\sum_{m=1}^{\Psi}\binom{\Psi}{m}(sX^{\alpha\eta}\upsilon^{-\alpha})^m}{(1+sX^{\alpha\eta}\upsilon^{-\alpha})^{\Psi}}\upsilon\mathrm{d}\upsilon\Big\}\bigg)
\end{aligned}
$$

where (a) follows from the probability generating functional (PGFL) property of a PPP [98]. (b) stems from the independence between Φ and both channel fading g and X, and evaluating the expectation over g, i.e. $\Gamma(\Psi,1)$. (c) yields from binomial expansion. For SU-MIMO, we have $\Psi = 1$, by substituting in Ψ, and eval-

uating the inner integration as

$$\int_{r_1}^{\infty} \frac{\upsilon}{1+s^{-1}X^{-\alpha\eta}\upsilon^{\alpha}}\mathrm{d}\upsilon = sX^{\alpha\eta}\frac{r_1^{\frac{2-\alpha}{\alpha}}}{\alpha-2}{}_2F_1\left(1,1-\frac{2}{\alpha};2-\frac{2}{\alpha};-\frac{sX^{\alpha\eta}}{r_1^{\alpha}}\right) \tag{A.4}$$

we have

$$\mathbb{E}\{e^{-sI} \mid r_1\} = \exp(-2\pi\lambda\psi) \tag{A.5}$$

where ψ is given by (3.13). By plugging (3.1) (for $K=1$) and (A.5) in (A.3), (3.12) follows immediately.

A.2 Proof of Corollary 3.1

Assuming that the distance between each interfering BS and its served user referred to as X is a r.v. following Rayleigh distribution, for given values of $\alpha = 4$ and $\eta = 0$, expressing the hypergeometric function as an infinite series, invoking the relation $\Gamma(a,b) = (a)_b\Gamma(a)$, and implementing integration and some algebraic manipulations [107] yields the following

$$\begin{aligned}
\psi &= \mathbb{E}_X\left\{\frac{\bar{\gamma}r_1^{(2-\alpha\eta)}X^{\alpha\eta}}{\alpha-2}{}_2F_1\big(1,1-\frac{2}{\alpha};2-\frac{2}{\alpha};-\bar{\gamma}r_1^{-\alpha\eta}X^{\alpha\eta}\big)\right\} \\
&\overset{a}{=} \frac{\bar{\gamma}r_1^{(2-\alpha\eta)}}{\alpha-2}\int_0^{\infty} X^{\alpha\eta}{}_2F_1\big(1,1-\frac{2}{\alpha};2-\frac{2}{\alpha};-\bar{\gamma}r_1^{-\alpha\eta}X^{\alpha\eta}\big)(2\pi\lambda Xe^{-\pi\lambda X^2})\mathrm{d}X \\
&\overset{b}{=} \frac{2\pi\lambda\bar{\gamma}r_1^{(2-\alpha\eta)}}{\alpha-2}\int_0^{\infty} X^{\alpha\eta+1}e^{-\pi\lambda X^2}\sum_{n=0}^{\infty}\frac{(1)_n(1-2/\alpha)_n}{(2-2/\alpha)_n n!}(-\bar{\gamma}r_1^{-\alpha\eta}X^{\alpha\eta})^n\mathrm{d}X \\
&\overset{c}{=} \frac{2\pi\lambda\bar{\gamma}r_1^{(2-\alpha\eta)}}{\alpha-2}\sum_{n=0}^{\infty}\frac{(1)_n(1-2/\alpha)_n(-\bar{\gamma}r_1^{-\alpha\eta})^n}{(2-2/\alpha)_n n!}\int_0^{\infty} X^{1+(1+n)\alpha\eta}e^{-\pi\lambda X^2}\mathrm{d}X \\
&\overset{d}{=} \frac{2\pi\lambda\bar{\gamma}r_1^{(2-\alpha\eta)}}{\alpha-2}\sum_{n=0}^{\infty}\frac{(1)_n(1-2/\alpha)_n(-\bar{\gamma}r_1^{-\alpha\eta})^n}{(2-2/\alpha)_n n!}\frac{\Gamma\big(\frac{2+(1+n)\alpha\eta}{2}\big)}{2(\pi\lambda)^{(1+\frac{(1+n)\alpha\eta}{2})}} \\
&\overset{e}{=} \frac{2\pi\lambda\bar{\gamma}r_1^{(2-\alpha\eta)}}{\alpha-2}\sum_{n=0}^{\infty}\frac{(1)_n(1-2/\alpha)_n(-\bar{\gamma}r_1^{-\alpha\eta})^n}{(2-2/\alpha)_n n!}\frac{(\frac{2+\alpha\eta}{2})_{n\alpha\eta/2}\Gamma(\frac{2+\alpha\eta}{2})}{2(\pi\lambda)^{(1+\frac{(1+n)\alpha\eta}{2})}}
\end{aligned}$$

$$\stackrel{f}{=} \frac{2\pi\lambda\bar{\gamma}r_1^{(2-\alpha\eta)}}{\alpha-2}\sum_{n=0}^{\infty}\frac{(-\bar{\gamma}r_1^{-\alpha\eta})^n(1)_n(1/2)_n}{2\pi\lambda(3/2)_n n!}$$
$$\stackrel{g}{=} \frac{\bar{\gamma}r_1^{(2-\alpha\eta)}}{\alpha-2}\,{}_2F_1(1,1/2;3/2;-\bar{\gamma}r_1^{-\alpha\eta}) \tag{A.6}$$

where (a) comes from the assumption that the distance between each interfering BS and its served user referred to as X is a r.v. following Rayleigh distribution. In (b), the hypergeometric function is expressed as an infinite series by invoking the relation $\Gamma(a,b) = (a)_b\Gamma(a)$. In (c) and (d), the integration is inserted inside the summation and integrating with respect to X, respectively. In $(e),(f)$, and (g), an expression yields, which can be expressed once again as a new hypergoemtric function by using the definition in (3.14) and simple mathematical simplifications.

A.3 Proof of Proposition 3.2

Following similar steps of Appendix A.1 and noticing that in full-SDMA $\Delta = 1$ and $\Psi = N_t$; the desired signal link is exponentially distributed, i.e. $g_0 \sim \exp(\mu)$, and $\mu = 1$, the coverage probability can be written as

$$\begin{aligned}
P_c^{\mathsf{MU}} &= \int_{r_1\geq 0}^{\infty}\mathbb{P}\left(\frac{g_0 r_1^{\alpha(\eta-1)}}{(\sigma^2+I)} \geq \bar{\gamma}|r_1\right) f_{r_1}(r_1)\mathrm{d}r_1 \\
&= \int_{r_1\geq 0}^{\infty}\mathbb{P}\left(g_0 \geq r_1^{\alpha(1-\eta)}\bar{\gamma}(\sigma^2+I)|r_1\right) f_{r_1}(r_1)\mathrm{d}r_1 \\
&= \int_{r_1\geq 0}^{\infty}\mathbb{E}_I\left\{\exp(-\bar{\gamma}r_1^{\alpha(1-\eta)}(\sigma^2+I)) \mid r_1\right\} f_{r_1}(r_1)\mathrm{d}r_1 \\
&= \int_{r_1\geq 0}^{\infty} e^{-\bar{\gamma}r_1^{\alpha(1-\eta)}\sigma^2}\mathbb{E}_I\{e^{-\bar{\gamma}r_1^{\alpha(1-\eta)}} \mid r_1\} f_{r_1}(r_1)\mathrm{d}r_1
\end{aligned} \tag{A.7}$$

To evaluate $\mathbb{E}_I\{e^{-\bar{\gamma}r_1^{\alpha(1-\eta)}} \mid r_1\}$, let $s = \bar{\gamma}r_1^{\alpha(1-\eta)}$, by following the same approach in Appendix A.1 for evaluating the Laplace transform, we have

$$\mathbb{E}\{e^{-sI} \mid r_1\} = \exp(-2\pi\lambda\psi) \tag{A.8}$$

where ψ is given by(3.19). By plugging (A.8) in (A.7), (3.18) follows immediately.

A.4 Proof of Proposition 3.3

Similarly, by considering the upper bound of coverage probability as in the Appendix A.1, the following yields

$$\begin{aligned} P_c^{\mathsf{CB}} &= \mathbb{E}_{r_1,r_K}\left\{\mathbb{P}\left(g \geq \frac{r_1^{\alpha}\bar{\gamma}}{P}(\sigma^2 + I_c)|r_1, r_K\right)\right\} \\ &\leq \mathbb{E}_{r_1,r_K}\left\{\sum_{m=1}^{\Delta}\binom{\Delta}{m}(-1)^{m+1}e^{-Zr_1^{\alpha}}\mathbb{E}_{I_c}\left\{e^{-\frac{m\kappa\bar{\gamma}}{P}r_1^{\alpha}I_c}|r_1, r_K\right\}\right\} \end{aligned} \tag{A.9}$$

where $\Delta = N_t - K + 1$, and Z given by (3.23), and I_c is the aggregate interference coming from all BSs in the point process Φ_c, where $\Phi_c = \Phi/\{\mathrm{BS}_1, ..., \mathrm{BS}_K\}$.

It can be noted that since the nearest interferer is located at distance r_K, the Laplace transform in (A.9) is conditioned on both r_1 and r_K. Similarly, the Laplace transform can be obtained following the same approach in Appendix A.1, by denoting $s = \frac{m\kappa\bar{\gamma}}{P}r_1^{\alpha}$, and substituting for ρ as $\rho = \frac{r_1}{r_K}$, the following is obtained

$$\mathbb{E}_{I_c}\{\mathrm{e}^{-sI_c}\} = \exp\big(-2\pi\lambda f(\bar{\gamma}, \alpha)\big) \tag{A.10}$$

where $f(\bar{\gamma}, \alpha) = r_K^2 G(\bar{\gamma}, \rho)$, and $G(\bar{\gamma}, \rho)$ is given by (3.22).
Plugging (A.10) in (A.9) and de-conditioning on both r_1 and r_K yields the following:

$$\begin{aligned} P_c^{\mathsf{CB}} &\leq \int_0^{\infty} f_{r_1}(r_1)\int_{r_1}^{\infty} f_{r_K}(r_K)\sum_{m=1}^{\Delta}\binom{\Delta}{m}(-1)^{m+1}e^{-Zr_1^{\alpha}}\mathbb{E}_{\rho}\left\{e^{-2\pi\lambda G(\bar{\gamma},\rho)r_K^2}|\rho\right\}\mathrm{d}r_K\mathrm{d}r_1 \\ &\leq \mathbb{E}_{\rho}\Bigg\{\overbrace{\int_0^{\infty} f_{r_1}(r_1)\underbrace{\int_{r_1}^{\infty} f_{r_K}(r_K)\sum_{m=1}^{\Delta}\binom{\Delta}{m}(-1)^{m+1}e^{-Zr_1^{\alpha}}e^{-2\pi\lambda G(\bar{\gamma},\rho)r_K^2}\mathrm{d}r_K}_{\mathcal{I}_1}\,\mathrm{d}r_1}^{\mathcal{I}_2}|\rho\Bigg\} \end{aligned} \tag{A.11}$$

Since r_1, r_K and ρ variables are independent of each other, the integration order is interchanged using Fubini's theorem. Accordingly, after substituting (3.1) in (A.11), $\mathcal{I}_1$ is obtained as follows

$$\begin{aligned}
\mathcal{I}_1 &= \sum_{m=1}^{\Delta} \binom{\Delta}{m} (-1)^{m+1} e^{-Zr_1^{\alpha}} \int_{r_1}^{\infty} f_{r_K}(r_K) e^{-2\pi\lambda G(\bar{\gamma},\rho) r_K^2} \mathrm{d}r_K \\
&= \sum_{m=1}^{\Delta} \binom{\Delta}{m} (-1)^{m+1} e^{-Zr_1^{\alpha}} \int_{r_1}^{\infty} e^{-\lambda\pi r_K^2} e^{-2\pi\lambda r_K^2 G(\bar{\gamma},\rho)} \left(\frac{2(\lambda\pi)^K r_K^{(2K-1)}}{\Gamma(K)} \right) \mathrm{d}r_K \\
&= \frac{2(\pi\lambda)^K}{\Gamma(K)} \sum_{m=1}^{\Delta} \binom{\Delta}{m} (-1)^{m+1} e^{-Zr_1^{\alpha}} \frac{\Gamma\Big(K, \lambda\pi(2G(\bar{\gamma},\rho)+1) r_1^2\Big)}{2\Big(2\lambda\pi G(\rho,\bar{\gamma}) + \lambda\pi\Big)^K}
\end{aligned} \tag{A.12}$$

where the last result can be deduced by utilising the integral identity: $\int_u^{\infty} x^m e^{-\beta x^n} \mathrm{d}x = \frac{\Gamma(v, \beta u^n)}{n\beta^v}$.

Plugging (A.12) and (3.1) with $K = 1$ in (A.11) and considering $\mathcal{I}_2$.

$$\begin{aligned}
\mathcal{I}_2 = \frac{2(\pi\lambda)^K}{\Gamma(K)} \sum_{m=1}^{\Delta} \binom{\Delta}{m} & \frac{(-1)^{m+1}}{2\Big(2\lambda\pi G(\bar{\gamma},\rho) + \lambda\pi\Big)^K} \\
& \times \int_0^{\infty} \Gamma\Big(K, \lambda\pi(2G(\bar{\gamma},\rho)+1) r_1^2\Big) e^{-\lambda\pi r_1^2} e^{-Zr_1^{\alpha}} (2\lambda\pi r_1) \mathrm{d}r_1
\end{aligned} \tag{A.13}$$

By expressing the gamma function in (A.13) as $\Gamma(s,x) = (s-1)! e^{-x} \sum_{n=0}^{s-1} \frac{x^n}{n!}$ [107], doing some mathematical manipulations, and conditioning on ρ, the following yields

$$\begin{aligned}
P_c^{\mathsf{CB}}(\rho) \leq \frac{\pi\lambda}{2\Big(2G(\bar{\gamma},\rho)+1\Big)^K} \sum_{m=1}^{\Delta} \binom{\Delta}{m} (-1)^{m+1} \sum_{n=0}^{K-1} \int_0^{\infty} & e^{-\Big(\lambda\pi\Big(2G(\bar{\gamma},\rho)+1\Big)+\lambda\pi\Big) r_1^2 - Zr_1^{\alpha}} \\
& \times \frac{\Big(\lambda\pi\big(2G(\bar{\gamma},\rho)+1\big) r_1^2\Big)^n}{n!} (2\lambda\pi r_1) \mathrm{d}r_1
\end{aligned} \tag{A.14}$$

Notice that the above expression is the conditional probability of coverage represented

as a function of ρ, so the expectation symbol is omitted. This integral can be evaluated numerically, however, it can be obtained in a closed-form for a special case of $\alpha = 4$, and is given by:

$$P_c^{\mathsf{CB}}(\rho) \leq \frac{\pi\lambda}{2\Big(2G(\bar{\gamma},\rho)+1\Big)^K} \sum_{m=1}^{\Delta} \binom{\Delta}{m} (-1)^{m+1} \sum_{n=0}^{K-1} \frac{(\lambda\pi)^n}{n!} \Big(2G(\bar{\gamma},\rho)+1\Big)^n \mathcal{G}_n(\bar{\gamma},\rho) \tag{A.15}$$

where $\mathcal{G}_n(\bar{\gamma},\rho)$ and $G(\bar{\gamma},\rho)$ are given in (3.21) and (3.22), respectively. The above result can be obtained by changing the variable $r_1^2 = x$ and invoking the integral identity $\int_0^\infty x^{v-1} e^{-\beta x^2 - \gamma x} \mathrm{d}x = (2\beta)^{-v/2}\Gamma(v)\exp(\frac{\gamma^2}{8\beta}) D_{-v}(\frac{\gamma}{\sqrt{2\beta}})$.

A.5 Proof of Proposition 3.4

Starting from (3.12), and using the following identity: $\mathbb{E}\{x\} = \int_{t\geq 0}^{\infty} \mathbb{P}(x \geq t)\mathrm{d}t$, where the expectation operation is defined over all randomness involved in the SINR, the expectation term can be written as

$$\mathbb{E}\Big\{1+\mathrm{SINR}\Big\}^{-\theta} = \int_{r_1\geq 0}^{\infty}\int_{t\geq 0}^{1} f_{r_1}(r_1)\mathbb{P}\bigg(\Big(1+\mathrm{SINR}\Big)^{-\theta} > t|r_1\bigg)\mathrm{d}t\mathrm{d}r_1 \tag{A.16}$$

$$= \int_{r_1\geq 0}^{\infty}\int_{t\geq 0}^{1} f_{r_1}(r_1)\mathbb{P}\Big(\mathrm{SINR} < (t^{\frac{-1}{\theta}}-1)|r_1\Big)\mathrm{d}t\mathrm{d}r_1 \tag{A.17}$$

$$= 1 - \int_{r_1\geq 0}^{\infty}\int_{t\geq 0}^{1} f_{r_1}(r_1)\mathbb{P}\Big(\mathrm{SINR} \geqslant t^{\frac{-1}{\theta}}-1|r_1\Big)\mathrm{d}t\mathrm{d}r_1 \tag{A.18}$$

by substituting for the upper bound of coverage probability in the above integration and approximating the integration in (A.18) by Gauss-Hermite quadrature given by [105]:

$$\int_0^1 x^k f(x)\mathrm{d}x \approx \sum_{n=1}^{N} \omega_n f(x_n) \tag{A.19}$$

(3.24) follows immediately.

Appendix B

Proofs for Chapter 4

B.1 Proof of Proposition 4.1

By conditioning on the distance to the nearest BS, the P_c is given by:

$$P_c = \mathbb{E}_{r_1}\{\mathbb{P}\big(\text{SINR} > \bar{\gamma} \mid r\big)\} \tag{B.1}$$

$$= \mathbb{E}_{r_1}\left\{\mathbb{P}\left(\frac{Pg_o r^{-\alpha}}{\sigma^2 + I} > \bar{\gamma} \mid r\right)\right\} \tag{B.2}$$

$$= \mathbb{E}_{r_1}\{\mathbb{P}\big(g_o > \bar{\gamma} r^{\alpha}(\bar{I}) \mid r\big)\} \tag{B.3}$$

$$\stackrel{a}{=} \mathbb{E}_{r_1}\left\{\mathbb{E}\left\{\sum_{n=0}^{N} \frac{r^{\alpha n}}{n!}(\bar{\gamma}\bar{I})^n e^{-r^{\alpha}\bar{\gamma}\hat{I}}\right\} \mid r\right\} \tag{B.4}$$

where the inner expectation is with respect to $\bar{I}$. (a) stems from the fact that g_o is gamma r.v. and its cumulative distribution function is the regularized gamma function, that is $\mathbb{P}(X < x) = \frac{\gamma(N,x)}{\Gamma(N)}$. Thus, its CCDF is expressed as: $\mathbb{P}(X > x) = \sum_{n=0}^{k-1} \frac{x^n}{n!} e^{-x}$. Moving the second expectation inside the sum and using the Laplace derivative property which states that $\mathbb{E}\{X^n e^{-sX}\} = (-1)^n \frac{\mathrm{d}^n \mathscr{L}_X(s)}{\mathrm{d}s^n}$, we finally arrive at (4.4).

B.2 Proof of Proposition 4.2

First, the CCDF of SINR for general MIMO system is needed, which is already given in (4.4). Although Laplace derivative in (4.4) can be calculated using Faa'di Bruno's formula for the composite function [123], however its numerical evaluation is rather difficult. Therefore, similar to [120], an upper bound on the distribution can be easily utilised using the lemma introduced in Appendix A.1, which is given by

$$\mathbb{P}(g_o > x) \leq \sum_{k=1}^{m} \binom{m}{k} (-1)^{k+1} e^{-\zeta k x} \tag{B.5}$$

Thus, in the subsequent derivation the (B.5) is utilised for upper bounding CCDF of SINR. Now, it is proceed to prove Theorem 4.2. When a user has SINR $> \bar{\gamma}_2$ on the subband w_c it is considered as an inner region user and served by MRT, mainly, $N_1 = N_2 = N_t$, experience a new channel fading $\hat{g}_o$, and no interference cancellation is used, i.e. $I = \sum_{i \in \Phi/\{\mathrm{BS}_1\}} P g_i r_i^{-\alpha}$. The upper bound for the CCDF of inner region user $P_{\mathrm{IMOC},i}(\bar{\gamma}_1, \bar{\gamma}_2, \lambda)$ is conditioned on its previous SINR, and is given as:

$$\begin{aligned}
P_{\mathrm{IMOC},i}(\bar{\gamma}_1, \bar{\gamma}_2, \lambda) &= \mathbb{P}\left(\frac{P \hat{g}_o r_1^{-\alpha}}{\sigma^2 + I} > \bar{\gamma}_1 \mid \frac{P g_o r_1^{-\alpha}}{\sigma^2 + I} > \bar{\gamma}_2 \right) \\
&\overset{a}{=} \frac{\mathbb{P}\left(\frac{P \hat{g}_o r_1^{-\alpha}}{\sigma^2 + I} > \bar{\gamma}_1, \frac{P g_o r_1^{-\alpha}}{\sigma^2 + I} > \bar{\gamma}_2 \right)}{\mathbb{P}\left(\frac{P g_o r_1^{-\alpha}}{\sigma^2 + I} > \bar{\gamma}_2 \right)} \\
&\overset{b}{=} \frac{\mathbb{P}\left(\frac{P \hat{g}_o r_1^{-\alpha}}{\sigma^2 + I} > \max\{\bar{\gamma}_1, \bar{\gamma}_2\} \right)}{\mathbb{P}\left(\frac{P g_o r_1^{-\alpha}}{\sigma^2 + I} > \bar{\gamma}_2 \right)} \\
&\overset{c}{\leq} \frac{\mathbb{E}\left\{ \sum_{n=1}^{N_1} \binom{N_1}{n} (-1)^{n+1} e^{-\frac{n \zeta_1 \max\{\bar{\gamma}_1, \bar{\gamma}_2\} r_1^{\alpha} (\sigma^2 + I)}{P}} \right\}}{\mathbb{E}\left\{ \sum_{m=1}^{N_2} \binom{N_2}{m} (-1)^{m+1} e^{-\frac{m \zeta_2 \bar{\gamma}_2 r_1^{\alpha} (\sigma^2 + I)}{P}} \right\}}
\end{aligned} \tag{B.6}$$

where in (a) stems from Bayes' rule, (b) is due to the fact that the two terms in numerator have the same interference and fading channel, and (c) stems from applying (B.5). Concentrating on numerator term, and conditioning on r_1, the numerator term in (B.6) can be evaluated as follows:

$$\begin{aligned}&\mathbb{E}\Big\{\sum_{n=1}^{N_1}\binom{N_1}{n}(-1)^{n+1}e^{-\frac{r_1^{\alpha}(\sigma^2+I)n\zeta_1\max\{\bar{\gamma}_1,\bar{\gamma}_2\}}{P}}\Big\}\\&=\sum_{n=1}^{N_1}\binom{N_1}{n}(-1)^{n+1}e^{-\frac{r_1^{\alpha}\sigma^2 n\zeta_1\max\{\bar{\gamma}_1,\bar{\gamma}_2\}}{P}}\mathbb{E}_I\Big\{e^{-\frac{r_1^{\alpha}n\zeta_1\max\{\bar{\gamma}_1,\bar{\gamma}_2\}I}{P}}\Big\}\end{aligned}\tag{B.7}$$

Again, the expectation in (B.7) is the Laplace transform, i.e. $\mathscr{L}(s_o r_1^{\alpha})$, where $s_o = n\zeta_1\max\{\bar{\gamma}_1,\bar{\gamma}_2\}$, which can be evaluated using the same approach in Appendix A.1, hence, is given as

$$\mathbb{E}_I\big\{e^{-\frac{r_1^{\alpha}s_o I}{P}}\big\}=\exp(-2\pi\lambda\psi(s_o)r_1^2)\tag{B.8}$$

where $\psi(s_o)=\frac{s_o}{\alpha-2}{}_2F_1\left(1,1-\frac{2}{\alpha};2-\frac{2}{\alpha};-s_o\right)$. Plugging (B.8) in (B.7), de-conditioning on r_1, and doing simple algebraic manipulations, the numerator in (4.5) yields. Following the same approach, the denominator in (B.6) can be obtained as in (4.5).

B.3 Proof of Corollary 4.1

In the special case of $\alpha = 4$, the integration with respect to r_1 can be obtained by changing the variable $r_1^2 = x$ and invoking the integral equality: $\int_0^{\infty} x^{\nu-1}e^{-\beta x^2-\gamma x}\mathrm{d}x = \frac{\Gamma(\nu)}{(2\beta)^{\nu/2}}\exp\big(\frac{\gamma^2}{8\beta}\big)D_{-\nu}\big(\frac{\gamma}{\sqrt{2\beta}}\big)$ [107]. By plugging for both numerator and denominator, (4.7) follows immediately.

B.4 Proof of Proposition 4.3

A user with SINR $< \bar{\gamma}_2$ is considered as an outer region user, and is therefore allocated a new subband w_e, and served by CBF. The user will experience a new channel fading $\hat{g}_o$ with a parameter $N_1 = N_t - K + 1$ and an interference $\hat{I} = \sum_{i \in \Phi / \{\mathrm{BS}_1, \ldots, \mathrm{BS}_K\}} P \hat{g}_i r_i^{-\alpha}$, the previous channel fading, i.e., g_o has a parameter $N_2 = N_t$. The upper bound of CCDF of the outer region user $P_{\mathrm{IMOC},e|\rho}(\bar{\gamma}_1, \bar{\gamma}_2, \lambda)$ is conditioned on its previous SINR. Thus, by applying Bays' rule and (B.5), the coverage probability is expressed as

$$
\begin{aligned}
&P_{\mathrm{IMOC},e|\rho}(\bar{\gamma}_1, \bar{\gamma}_2, \lambda) \\
&= \mathbb{P}\left(\frac{P \hat{g}_o r_1^{-\alpha}}{\sigma^2 + \hat{I}} > \bar{\gamma}_1 \mid \frac{P g_o r_1^{-\alpha}}{\sigma^2 + I} < \bar{\gamma}_2 \right) \\
&= \frac{\mathbb{P}\left(\frac{P \hat{g}_o r_1^{-\alpha}}{\sigma^2 + \hat{I}} > \bar{\gamma}_1, \frac{P g_o r_1^{-\alpha}}{\sigma^2 + I} < \bar{\gamma}_2 \right)}{\mathbb{P}\left(\frac{P g_o r_1^{-\alpha}}{\sigma^2 + I} < \bar{\gamma}_2 \right)} \\
&\leq \frac{\mathbb{E}\left\{ \sum_{n=1}^{N_1} \binom{N_1}{n} (-1)^{n+1} e^{-\frac{n \zeta_1 \bar{\gamma}_1 r_1^{\alpha} (\sigma^2 + \hat{I})}{P}} \left(1 - \sum_{m=1}^{N_2} \binom{N_2}{m} (-1)^{m+1} e^{-\frac{m \zeta_2 \bar{\gamma}_2 r_1^{\alpha} (\sigma^2 + I)}{P}} \right) \right\}}{\mathbb{E}\left\{ 1 - \sum_{m=1}^{N_2} \binom{N_2}{m} (-1)^{m+1} e^{-\frac{m \zeta_2 \bar{\gamma}_2 r_1^{\alpha} (\sigma^2 + I)}{P}} \right\}}
\end{aligned}
\tag{B.9}
$$

$$
\begin{aligned}
&P_{\mathrm{IMOC},e|\rho}(\bar{\gamma}_1, \bar{\gamma}_2, \lambda) \\
&\leq \frac{\overbrace{\mathbb{E}\left\{ \sum_{n=1}^{N_1} \binom{N_1}{n} (-1)^{n+1} e^{-\mathcal{A}_1 r_1^{\alpha}} e^{-\frac{n \zeta_1 \bar{\gamma}_1 r_1^{\alpha} \hat{I}}{P}} \left(1 - \sum_{m=1}^{N_2} \binom{N_2}{m} (-1)^{m+1} e^{-\mathcal{A}_2 r_1^{\alpha}} e^{-\frac{m \zeta_2 \bar{\gamma}_2 r_1^{\alpha} I}{P}} \right) \right\}}^{\mathcal{I}_1}}{\underbrace{\mathbb{E}\left\{ 1 - \sum_{m=1}^{N_2} \binom{N_2}{m} (-1)^{m+1} e^{-\mathcal{A}_2 r_1^{\alpha}} e^{-\frac{m \zeta_2 \bar{\gamma}_2 r_1^{\alpha} I}{P}} \right\}}_{\mathcal{I}_2}}
\end{aligned}
\tag{B.10}
$$

Now by distributing, factoring out the noise term due to its independence from the interference term in $\mathcal{I}_1$, and conditioning on r_1, $\mathcal{I}_1$ can be written as

$$\mathcal{I}_1 = \overbrace{\sum_{n=1}^{N_1} \binom{N_1}{n} (-1)^{n+1} e^{-\mathcal{A}_1 r_1^{\alpha}} \mathbb{E}_{\hat{I}}\Big\{ e^{-\frac{n\zeta_1 \bar{\gamma}_1 r_1^{\alpha} \hat{I}}{P}} \Big\}}^{\Upsilon_1(\rho,\bar{\gamma}_1)} - \underbrace{\mathbb{E}\Big\{ \sum_{n=1}^{N_1} \sum_{m=1}^{N_2} \binom{N_1}{n} \binom{N_2}{m} (-1)^{n+m} e^{-(\mathcal{A}_1+\mathcal{A}_2) r_1^{\alpha}} e^{-\frac{n\zeta_1 \bar{\gamma}_1 r_1^{\alpha} \hat{I}}{P}} e^{-\frac{m\zeta_2 \bar{\gamma}_2 r_1^{\alpha} I}{P}} \Big\}}_{\Upsilon_2(\rho,\bar{\gamma}_1,\bar{\gamma}_2)} \tag{B.11}$$

Concentrating on the second term of the numerator $\Upsilon_2(\rho, \bar{\gamma}_1, \bar{\gamma}_2)$, it can be noticed that the term $\exp\big(-r_1^{\alpha}(n\zeta_1\bar{\gamma}_1\hat{I}+m\zeta_2\bar{\gamma}_2 I)\big)$ is the joint Laplace transform of both $\hat{I}$ and I evaluated at $(n\zeta_1 r_1^{\alpha}\bar{\gamma}_1,\, m\zeta_2 r_1^{\alpha}\bar{\gamma}_2)$. The reason is that both $\hat{I}$ and I have now different channel fadings but with the same point process Φ, so they must be jointly evaluated. Now, define Φ_d and Φ_2 as the point process in the region from $\overline{b(0,r_1)} \bigcap b(0,r_K)$ such that $\Phi = \Phi_2 \bigcup \Phi_d$, where $b(0,x)$ denotes a circle of radius x centred at the origin, thus, Φ_d represents the point process consisting of K BSs participating in coordination. Let I_d and I_K denote the aggregate interference over subband w_c from BSs in Φ_d and Φ_2, respectively.

The joint Laplace transform $\mathscr{L}(s_1 r_1^{\alpha}, s_2 r_1^{\alpha})$ denotes as $\mathcal{Q}(r_1, \rho, s_1, s_2)$ is evaluated as follows

$$\begin{aligned}
&= \mathbb{E}\big\{\exp(-s_1 r_1^{\alpha}\hat{I} - s_2 r_1^{\alpha} I)\big\} \\
&= \mathbb{E}\big\{\exp(-s_1 r_1^{\alpha} \sum_{i\in\Phi_2} \hat{g}_i r_i^{-\alpha} - s_2 r_1^{\alpha} \sum_{i\in\Phi_1} g_i r_i^{-\alpha})\big\} \\
&\overset{a}{=} \mathbb{E}\Big\{\exp(-s_1 r_1^{\alpha} \sum_{i\in\Phi_2} \hat{g}_i r_i^{-\alpha} - s_2 r_1^{\alpha} \sum_{i\in\Phi_d} g_i r_i^{-\alpha} - s_2 r_1^{\alpha} \sum_{i\in\Phi_2} g_i r_i^{-\alpha})\Big\} \\
&\overset{b}{=} \mathbb{E}\Big\{ \prod_{i\in\Phi_d} \mathbb{E}_{g_i}\Big\{\exp(-s_2 r_1^{\alpha} g_i r_i^{-\alpha})\Big\}\Big\} \mathbb{E}\Big\{ \prod_{i\in\Phi_2} \mathbb{E}_{\hat{g}_i, g_i}\Big\{\exp(-s_1 r_1^{\alpha}\hat{g}_i r_1^{-\alpha} - s_2 r_1^{\alpha} g_i r_i^{-\alpha})\Big\}\Big\}
\end{aligned}$$

$$\stackrel{c}{=} \mathbb{E}\Big\{ \prod_{i\in\Phi_d} \frac{1}{1+s_2 r_1^{\alpha} r_i^{-\alpha}} \Big\} \mathbb{E}\Big\{ \prod_{i\in\Phi_2} \frac{1}{1+s_2 r_1^{\alpha} r_i^{-\alpha}} \times \frac{1}{1+s_1 r_1^{\alpha} r_i^{-\alpha}} \Big\}$$
$$\stackrel{d}{=} \exp\Big(-2\pi\lambda \int_{r_1}^{r_K} \big(1 - \frac{1}{1+s_2 r_1^{\alpha}\nu^{-\alpha}}\big)\nu \mathrm{d}\nu \Big)$$
$$\times \exp\Big(-2\pi\lambda \int_{r_K}^{\infty} \big(1 - \frac{1}{1+s_2 r_1^{\alpha}\nu^{-\alpha}} \times \frac{1}{1+s_1 r_1^{\alpha}\nu^{-\alpha}}\big)\nu \mathrm{d}\nu \Big) \tag{B.12}$$

In (a), the interference terms I_d and I_K are separated in order to jointly evaluate the Laplace terms of $\hat{I}$ and I_K as they belong to the same point process Φ_2. In (b), the Laplace of product is equal to the product of Laplace transforms of each part due to independence between disjoint regions. (c) stems from evaluating the expectation of channel fading. (d) stems from applying PGFL property. Then by substituting $r_K = r_1/\rho$, de-conditioning on r_1, and conditioning on ρ, $\Upsilon_2(\rho, \bar{\gamma}_1, \bar{\gamma}_2)$ is obtained as in (4.11).

The first term in numerator $\Upsilon_1(\rho, \bar{\gamma}_1)$ can be evaluated similar to (B.7) where the Laplace term is given by:

$$\mathbb{E}_{\hat{I}}\big\{ e^{-\frac{n\zeta_1\bar{\gamma}_1 r_1^{\alpha}\hat{I}}{P}} \big\} = \exp(-2\pi\lambda\psi(s_3) r_K^2) \tag{B.13}$$

where $\psi(.)$ is given by (4.6), and $s_3 = n\rho^{\alpha}\zeta_1\bar{\gamma}_1$. By substituting $r_K = r_1/\rho$, conditioning on ρ, and de-conditioning on r_1, $\Upsilon_1(\rho, \bar{\gamma}_1)$ is deduced as in (4.10).
Similarly, $\mathcal{I}_2$ can also be evaluated in a way similar to that of Appendix B.2.

B.5 Proof of Corollary 4.2

First, the PDF of ρ is needed, which can be derived using the following lemma.
Lemma 2 : The PDF of the ratio of the distance between a typical user at the origin and the serving BS over the distance to the Kth BS, i.e. $\rho = \frac{r_1}{r_K}$, is given by:

$$f_{\rho}(x) = 2(K-1)x(1-x^2)^{K-2} \tag{B.14}$$

The proof is as follows: starting from the distribution of $Y = \frac{r_K}{r_1}$ given by eq. (15) in [124] as

$$\mathbb{P}\big(Y \leq y\big) = (1 - 1/y^2)^{K-1} \tag{B.15}$$

Let $g(y) = 1/y$, then we have $g^{-1}(x) = 1/x$, and $\rho = X = 1/Y$. By applying the chain rule of PDF transformation given as: $f_\rho(x) = f_Y(g^{-1}(x))|\frac{d}{dx}g^{-1}(x))|$, where $f_Y(g^{-1}(x)) = 2(K-1)(1-x^2)^{K-2}x^3$ and $|\frac{d}{dx}g^{-1}(x))| = 1/x^2$, the (B.14) follows immediately.

The expectation with respect to ρ can be approximated by Gaussian-Hermite quadrature given by [105]:

$$\int_0^1 x^k f(x) \approx \sum_{n=1}^{N} w_n f(x_n) \tag{B.16}$$

Plugging the results in the main expression yields (4.13).

B.6 Proof of Proposition 4.4

A user with SINR $> \bar{\gamma}_2$ on the subband w_c is considered as an inner region user and served via CBF, i.e., its serving BS coordinates towards Δ outer region users served by other BSs, however, the other BSs do not coordinate toward it. Thus, the user experiences a new small-scale channel fading, i.e., $\tilde{g}_o$ with a parameter $N_1 = N_t - \Delta$, while the interference given by $I = \sum_{i \in \Phi/\{\mathrm{BS}_1\}} P g_i r_i^{-\alpha}$ remains unchanged. The CCDF of the inner region user $P_{\mathrm{ICOM},i}(\bar{\gamma}_1, \bar{\gamma}_2, \lambda)$ is conditioned on its previous SINR as follows:

$$P_{\mathrm{ICOM},i}(\bar{\gamma}_1,\bar{\gamma}_2,\lambda)=\mathbb{P}\left(\frac{P\tilde{g}_o r_1^{-\alpha}}{\sigma^2+I}>\bar{\gamma}_1 \mid \frac{Pg_o r_1^{-\alpha}}{\sigma^2+I}>\bar{\gamma}_2\right) \tag{B.17}$$

$$=\frac{\mathbb{P}\left(\frac{P\tilde{g}_o r_1^{-\alpha}}{\sigma^2+I}>\bar{\gamma}_1, \frac{Pg_o r_1^{-\alpha}}{\sigma^2+I}>\bar{\gamma}_2\right)}{\mathbb{P}\left(\frac{Pg_o r_1^{-\alpha}}{\sigma^2+I}>\bar{\gamma}_2\right)} \tag{B.18}$$

Note that I is the interference field calculated from r_1. Hence, the BS will coordinate its transmission toward Δ users belonging to other cells, while its user is exposed to the whole interference field, i.e. no coordination toward it is implemented. Following the same steps of the Proof of Proposition 4.2, the expression of $P_{\mathrm{ICOM},i}(\bar{\gamma}_1,\bar{\gamma}_2,\lambda)$ can be derived as follows:

$$\leq \frac{\mathbb{E}\left\{\sum_{n=1}^{N_1}\binom{N_1}{n}(-1)^{n+1}e^{-\frac{n\zeta_1\bar{\gamma}_1 r_1^{\alpha}(\sigma^2+I)}{P}}\sum_{m=1}^{N_2}\binom{N_2}{m}(-1)^{m+1}e^{-\frac{m\zeta_2\bar{\gamma}_2 r_1^{\alpha}(\sigma^2+I)}{P}}\right\}}{\mathbb{E}\left\{\sum_{m=1}^{N_2}\binom{N_2}{m}(-1)^{m+1}e^{-\frac{m\zeta_2\bar{\gamma}_2 r_1^{\alpha}(\sigma^2+I)}{P}}\right\}} \tag{B.19}$$

The numerator term in (B.19) can be evaluated as follows:

$$\mathbb{E}\left\{\sum_{n=1}^{N_1}\sum_{m=1}^{N_2}\binom{N_1}{n}\binom{N_2}{m}(-1)^{n+m}e^{-\frac{r_1^{\alpha}(\sigma^2+I)(n\zeta_1\bar{\gamma}_1+m\zeta_2\bar{\gamma}_2)}{P}}\right\}$$

$$=\sum_{n=1}^{N_1}\sum_{m=1}^{N_2}\binom{N_1}{n}\binom{N_2}{m}(-1)^{n+m}e^{-\frac{r_1^{\alpha}\sigma^2(n\zeta_1\bar{\gamma}_1+m\zeta_2\bar{\gamma}_2)}{P}}\mathbb{E}_I\left\{e^{-\frac{r_1^{\alpha}(n\zeta_1\tau_1+m\zeta_2\bar{\gamma}_2)I}{P}}\right\} \tag{B.20}$$

Following the same steps of evaluating the Laplace transform for both numerator and denominator and de-conditioning on r_1 as in Appendix B.2, (4.14) yields.

B.7 Proof of Proposition 4.5

A user with SINR $<\bar{\gamma}_2$ on the subband w_c is considered as an outer region user and allocated subband w_e. Its serving BS will coordinate toward $\Delta-1$ users (when

$\Delta = 1$, it transmits using MRT with full diversity), while the other BSs coordinate toward it. Thus, the user experiences a new channel fading, i.e. $\tilde{g}_o$ with a parameter $N_1 = N_t - \Delta + 1$, and new interference given by $\hat{I} = \sum_{i \in \Phi / \{\mathrm{BS}_1, \ldots, \mathrm{BS}_K\}} P g_i r_i^{-\alpha}$. The CCDF of the inner region user, $P_{\mathrm{ICOM},e}(\bar{\gamma}_1, \bar{\gamma}_2, \lambda)$, is conditioned on its previous SINR and can be written as:

$$P_{\mathrm{ICOM},e}(\bar{\gamma}_1, \bar{\gamma}_2, \lambda) = \mathbb{P}\left(\frac{P \tilde{g}_o r_1^{-\alpha}}{\sigma^2 + \hat{I}} > \bar{\gamma}_1 \mid \frac{P g_o r_1^{-\alpha}}{\sigma^2 + I} < \bar{\gamma}_2 \right) \tag{B.21}$$

$$= \frac{\mathbb{P}\left(\frac{P \tilde{g}_o r_1^{-\alpha}}{\sigma^2 + \hat{I}} > \bar{\gamma}_1, \frac{P g_o r_1^{-\alpha}}{\sigma^2 + I} < \bar{\gamma}_2 \right)}{\mathbb{P}\left(\frac{P g_o r_1^{-\alpha}}{\sigma^2 + I} < \bar{\gamma}_2 \right)} \tag{B.22}$$

Following the same steps of deriving coverage probability in Proposition 4.3 and Corollary 4.2, $P_{\mathrm{ICOM},e}(\bar{\gamma}_1, \bar{\gamma}_2, \lambda)$ can be obtained.

B.8 Proof of Proposition 4.6

Staring from the fact that $\mathbb{E}\{X\} = \int_0^\infty \mathbb{P}(X > t) \mathrm{d}t$, for positive X, the average rate of IMOC scheme can be expressed as

$$\widetilde{R}_{\mathrm{IMOC},e} = \mathbb{E}\left\{ \ln\left(1 + \frac{\mathrm{P} g_o r_1^{-\alpha}}{\sigma^2 + I} \right) \right\} \tag{B.23}$$

$$= \int_{r_1 > 0} e^{-\pi \lambda r_1^2} \mathbb{E}\left\{ \ln\left(1 + \frac{\mathrm{P} g_o r_1^{-\alpha}}{\sigma^2 + I} \right) \right\} 2\pi \lambda r_1 \mathrm{d}r_1 \tag{B.24}$$

By considering the upper bound of coverage probability as in the Proposition 4.2 and conditioning the outer region user's SINR on the previous one, we have:

$$\widetilde{R}_{\mathrm{IMOC},e} \leq 2\pi\lambda \int_{r_1 > 0} e^{-\pi \lambda r_1^2} \int_{t > 0} \mathbb{P}(*) \mathrm{d}t r_1 \mathrm{d}r_1 \tag{B.25}$$

where

$$\begin{aligned}
\mathbb{P}(*) &= \mathbb{P}\left(\ln\left(1+\frac{\mathrm{P}\hat{g}_o r_1^{-\alpha}}{\sigma^2+\hat{I}}\right) > t \mid \frac{\mathrm{P}g_o r_1^{-\alpha}}{\sigma^2+I} < \bar{\gamma}_2\right) \\
&= \frac{\mathbb{P}\left(\ln\left(1+\frac{\mathrm{P}\hat{g}_o r_1^{-\alpha}}{\sigma^2+\hat{I}}\right) > t, \frac{\mathrm{P}g_o r_1^{-\alpha}}{\sigma^2+I} < \bar{\gamma}_2\right)}{\mathbb{P}\left(\frac{\mathrm{P}g_o r_1^{-\alpha}}{\sigma^2+I} < \bar{\gamma}_2\right)} \\
&= \frac{\mathbb{P}\left(\frac{\mathrm{P}\hat{g}_o r_1^{-\alpha}}{\sigma^2+\hat{I}} > (e^t-1), \frac{\mathrm{P}g_o r_1^{-\alpha}}{\sigma^2+I} < \bar{\gamma}_2\right)}{\mathbb{P}\left(\frac{\mathrm{P}g_o r_1^{-\alpha}}{\sigma^2+I} < \bar{\gamma}_2\right)} \\
&\leq \int_{t>0}^{\infty} P_{\mathrm{IMOC},e}(e^t-1, \bar{\gamma}_2, \lambda)\mathrm{d}t
\end{aligned} \tag{B.26}$$

Bibliography

[1] Cisco, "Cisco visual networking index: global mobile data traffic forecast update, 2013–2018," White Paper, Feb. 2014. [Online]. Available: http://www.cisco.com.

[2] WWRF, L. Sorensen and K. E. Skouby, "User scenarios 2020,"Report, July 2009, [online]. Available: http://www.wireless-world-research.org.

[3] M. Agiwal, A. Roy, and N. Saxena, "Next generation 5G wireless networks: a comprehensive survey," *IEEE Commun. Surveys Tuts.*, early access, Feb. 2016.

[4] T. O Olwal, K. Djouani, and A. M Kurien, "A survey of resource management towards 5G radio access networks," *IEEE Commun. Surveys Tuts.*, early access, Apr. 2016.

[5] J. Lee, Y. Kim, H. Lee, B. Ng,D. Mazzarese, J. Liu, W. Xiao, and Y. Zhou, "Coordinated multipoint transmission and reception in LTE-Advanced systems," *IEEE Trans. Wireless Commun.*, vol. 50, no. 11, pp. 44-50, Nov. 2012.

[6] S. Sun, Q. Gao, Y. Peng, Y. Wang, and L. Song, "Interference management through CoMP in 3GPP LTE-Advanced networks," *IEEE Trans. Wireless Commun.*, vol. 20, no. 1, pp. 59-66, Feb. 2013.

[7] V. Ntranos, M. A. Maddah-Ali, and G. Caire, "Cellular interference alignment, " *Trans. Inf. Theory*, vol. 61, no. 3, pp. 1194–1217, Mar. 2015.

[8] 3GPP, TS 36.201 V8.3.0, "Evolved universal terrestrial radio access (E-UTRA); LTE physical layer - general description," Rel. 8, Mar. 2009.

[9] A. Hashimoto, H. Yorshino, and H. Atarashi, "Roadmap of IMT-Advanced development," *IEEE Microw. Mag.*, vol. 9, no. 4, pp. 80–88, Aug. 2008.

[10] 3GPP, TS 36.104 V10.0.0, "Evolved universal terrestrial radio access (EUTRA); base station (BS) radio transmission and reception," Rel. 10, Oct. 2010.

[11] A. Goldsmith, "*Wireless communications*", Cambridge University Press, 2005.

[12] D. Tse and P. Viswanath, "*Fundamentals of Wireless Communications*", Cambridge University Press, 2005.

[13] C. E. Shannon, "A mathematical theory of communication," *Bell system technical journal*, vol. 27, 1948.

[14] Y. Cui, V. K. N. Lau, R. Wang, H. Huang, S. Zhang, "A survey on delay-aware resource control for wireless systems-large deviation theory, stochastic Lyapunov drift, and distributed stochastic learning," *IEEE Trans. Inf. Theory*, vol. 58, no. 3, pp. 1677-1701, Mar. 2012.

[15] C.-S. Chang, "Effective bandwidth in high-speed digital networks," *IEEE J. Sel. Areas Commun.*, vol. 13, no. 6, pp. 1091-1100, Aug. 1995.

[16] D. Wu and R. Negi, "Effective capacity: A wireless link model for support of quality of service," *IEEE Trans. Wireless Commun.*, vol. 2, no. 4, pp. 630-643, July 2003.

[17] Gartner, "Gartner estimates ICT industry accounts for 2 percent of global CO2 emissions,"Press Release, Apr. 2007. [Online]. Available: http://www.gartner.com.

[18] Y. Chen, S. Zhang, S. Xu, and G. Y. Li, "Fundamental tradeoffs on green wireless networks," *IEEE Wireless Commun. Mag.*, vol. 49, no. 6, pp.30-37, Jun. 2011.

[19] D. Feng, C. Jiang, G. Lim, L. J. Cimini, G. Feng, and G. Y. Li, "A survey of energy-efficient wireless communication," *IEEE Commun. Surveys Tuts.*, vol. 15, no. 1, pp. 167-178, Feb. 2012.

[20] T. Chen, H. Kim and Y. Yang, "Energy efficiency metrics for green wireless communications," in *Proc. IEEE WCSP'10*, Oct. 2010.

[21] H. M. Kwon and T. G. Birdsall, "Channel capacity in bits per joule," *IEEE J. Ocean. Eng.*, vol. 11, no. 1, pp. 97–99, Jan. 1986.

[22] V. Rodoplu and T. H. Meng, "Bits-per-joule capacity of energy-limited wireless networks," *IEEE Trans. Wireless Commun.*, vol. 6, no. 3, pp. 857–865, Mar. 2007.

[23] F. Khan, "*LTE for 4G Mobile Broadband: Air Interface Technologies and performance*", Cambridge University Press, 2009.

[24] M.-S. Alouini and A. Goldsmith, "Area spectral efficiency of cellular mobile radio systems," *IEEE Trans. Veh. Technol.*, , vol. 48, pp. 1047-1066, July 1999.

[25] H. ElSawy, E. Hossain, and M.Haenggi, "Stochastic geometry for modeling, analysis, and design of multi-tier and cognitive cellular wireless networks: a Survey," *IEEE Commun. Surveys Tuts.*, vol. 15, no. 3, pp. 996-1019, third quarter 2013.

[26] A. Wyner, "Shannon-theoretic approach to a gaussian cellular multiple-access channe, " *Trans. Inf. Theory*, vol. 40, no. 6, pp. 1713-1727, Nov. 1994.

[27] J. Xu, J. Zhang, and J. G. Andrews, "On the accuracy of the Wyner model in cellular networks," *IEEE Trans. Wireless Commun.*, vol. 10, no. 9, pp. 3098–3109, Sep. 2011.

[28] J. G. Andrews, H. Claussen, M. Dohler, S. Rangan, and M. C. Reed, "Femtocells: Past, present, and future," *IEEE J. Sel. Areas Commun.*, vol. 30, no. 3, pp. 497–508, Apr. 2012.

[29] D. Stoyan, W. S. Kendall, and J. Mecke, *Stochastic Geometry and its Applications*, 2nd edition. Hoboken, NJ, USA: Wiley, 2008.

[30] J. Winters, "" On the capacity of radio communication systems with diversity in a rayleigh fading environment," *IEEE J. Sel. Areas Commun.*, vol. 5, no. 5, pp. 871-878, Jun. 1987.

[31] G. J. Foschini, "Layered space-time architecture for wireless communication in a fading environment when using multiple antennas," *Bell Labs Tech. J.*, vol. 1, no. 2, pp. 41-59, 1996.

[32] G. J. Foschini and M. J. Gans, "On limits of wireless communications in a fading environment when using multiple antennas," *Wireless Pers. Commun.*, vol. 6, no. 3, pp. 311-335, 1998.

[33] I. E. Telatar, "Capacity of multi-antenna gaussian channels," *European Trans. Telecommun.*, vol. 10, pp. 585-595, 1999.

[34] A. Goldsmith, S. A. Jafar, N. Jindal, and S. Vishwanath, "Capacity limits of MIMO channels," *IEEE J. Sel. Areas Commun.*, vol. 16, no. 8, pp. 684-702, Jun. 2003.

[35] E. Bilieri, R. Calderbank, A. Constantinides, A. Goldsmith, A. Paulraj, and H. V. Poor, "*MIMO Wireless communications*", Cambridge University Press, 2007.

[36] D. Gesbert, M. Kountouris, R. W. Heath Jr.,C. B. Chae, and T. Salzer, "Shifting the MIMO paradigm," *Trans. Signal Process. Mag.*, vol. 24, no. 5, pp. 36-46, Sep. 2007.

[37] M. Costa, "Writing on dirty paper," *IEEE Trans. Inf. Theory*, vol. 29, no. 3, pp. 439-441, May 1983.

[38] H. Wiengarten, Y. Steinberg, and S. Shamai, "The capacity region of the Gaussian multiple-input multiple output broadcast channel," *IEEE Trans. Inf. Theory.*, vol. 52, no.9, pp.3936-3964, Sept. 2006.

[39] H. Viswanathan, S. Venkatesan, and H. Huang, "Downlink capacity evaluation

of cellular networks with known-interference cancellation," in *IEEE J. Sel. Areas in Commun.*, vol. 21, no. 6, pp. 802-811, June. 2003.

[40] G. Caire and S. Shamai, "On the achievable throughput of a multiantenna Gaussian broadcast channel," *IEEE Trans. Inf. Theory.*, vol. 49, no.7, pp.1691-1706, July. 2003.

[41] T. Yoo and A. Goldsmith, "On the optimality of multiantenna broadcast scheduling using zero-forcing beamforming," *IEEE J. Sel. Areas in Commun.*, vol. 24, no. 3, pp. 528-541, Mar. 2006.

[42] Titus K. Y. Lo, "Maximum ratio transmission," *IEEE Trans. Commun.*, vol. 47, pp. 1458-1461, Oct. 1999.

[43] P. A. Dighe, R. K. Mallik, and S. S. Jamuar, "Analysis of transmit-receive diversity in Rayleigh fading," *IEEE Trans. Commun.*, vol. 51, pp. 694-703, Apr. 2003.

[44] M. Sadek, A. Tarighat, and A. Sayed, "A leakage-based precoding scheme for downlink multi-user MIMO channels," *IEEE Trans. Wireless Commun.*, vol. 6, no. 5, pp. 1711-1721, May 2007.

[45] Q. H. Spencer, A. L. Swindlehurst, and M. Haardt, "Zero-forcing methods for downlink spatial multiplexing in multiuser MIMO channels," *IEEE Trans. Signal Process.*, vol. 52, no.2, pp. 461-471, Feb. 2004.

[46] S. Shim, J. Kwak, R. W. Heath Jr., and J. Andrews, "Block diagonalization for multi-user MIMO with other-cell interference," *IEEE Trans. Wireless Commun.*, vol. 7, no. 7, pp. 2671-2681, Jul. 2008.

[47] G. Caire, N. Jindal, M. Kobayashi, and N. Ravindran, "Multiuser MIMO achievable rates with downlink training and channel state feedback," *IEEE Trans. Inf. Theory.*, vol. 56, no.6, pp. 2845-2866, Jun. 2010.

[48] P. Viswanath, D. Tse, and R. Laroia, "Opportunistic beamforming using dumb antennas, " *Trans. Inf. Theory*, vol. 48, no. 6, pp. 1277–1294, Jun. 2002.

[49] M. Sharif and B. Hassibi, "On the capacity of MIMO broadcast channel with partial side information, " *Trans. Inf. Theory*, vol. 51, no. 2, pp. 506–522, Feb. 2005.

[50] E. A. Jorswieck, P. Svedman, and B. Ottersten, "Performance of TDMA and SDMA based opportunistic beamforming," *IEEE Trans. Wireless Commun.*, vol. 7, no. 11, pp. 4058-4063, Nov. 2008.

[51] S. H. Moon, S. R. Lee, and I. Lee,, "Sum-rate capacity of random beamforming for multi-antenna broadcast channels with other cell interference," *IEEE Trans. Wireless Commun.*, vol. 10, no. 8, pp. 2440–2444, Aug. 2011.

[52] D. J. Love, R. W. Heath, V. K. N. Lau, D. Gesbert, B. D. Rao, M. Andrews, "An overview of limited feedback in wireless communication systems," *IEEE J. Sel. Areas Commun.*, vol. 26, no. 8, pp. 1341-1365, Oct. 2008.

[53] N. Jindal, "MIMO broadcast channels with finite-rate feedback, " *Trans. Inf. Theory*, vol. 52, no. 11, pp. 5045-5060, Nov. 2006.

[54] N. Ravindran and N. Jindal, "Multi-user diversity vs. accurate channel state information in MIMO downlink channels," *IEEE Trans. Wireless Commun.*, vol. 59, no. 3, pp. 803-814, Dec. 2008.

[55] N. Ravindran and N. Jindal, "Limited feedback-based block diagonalization for the MIMO broadcast channel," *IEEE J. Sel. Areas Commun.*, vol. 26, no. 8, pp. 1473–1482, Oct. 2008.

[56] D. Gesbert, S. Hanly, H. Huang, S. Shamai Shitz, O. Simeone, and W. Yu, "Multi-cell MIMO cooperative networks: A new look at interference," *IEEE J. Sel. Areas Commun.*, vol. 28, no. 9, pp. 1380-1408, Dec. 2010.

[57] H. Holma and A. Toskala, Eds., "*WCDMA for UMTS: Radio Access for Third*

Generation Mobile Communications", John Wiley & Sons, Inc., New York, NY, USA, 1st edition, 2001.

[58] M. Sawahashi, Y. Kishiyama, A. Morimoto, and M. Nishikawa, and D. Tanno, "Coordinated multipoint transmission/reception techniques for LTE-Advanced," *IEEE Trans. Wireless Commun.*, vol. 17, no. 3, pp. 26–34, June 2010.

[59] R. Zhang, "Cooperative multi-cell block diagonalization with per-base station power constraints," *IEEE J. Sel. Areas in Commun.*, vol. 28, no. 9, pp. 1435-1445, Dec. 2010.

[60] A. Lozano and J.G. Andrews, "Fundamental limits of cooperation ," *IEEE Trans. Inf. Theory.*, vol. 59, no.9, pp. 5213-5226, Sept. 2013.

[61] C. T. K. Ng and H. Huang, "Linear precoding in cooperative MIMO cellular networks with limited coordination clusters," *IEEE J. Sel. Areas in Commun.*, vol. 28, no. 9, pp. 1446–1454, 2010.

[62] J. Zhang, R. Chen,J. Andrews, A. Ghosh, and R. Heath, "Network MIMO with clustered linear precoding," *IEEE Trans. Wireless Commun.*, vol. 8, no. 4, pp.1910-1921, Apr. 2009.

[63] B. Ng, J. Evans, S. Hanly, and D. Aktas, "Distributed downlink beamforming with cooperative base stations," *IEEE Trans. Inf. Theory.*, vol. 54, no.12, pp. 5491-5499, Dec. 2008.

[64] H. J. Choi, S. H. Park, S. R. Lee, and I. Lee, "Distributed beamforming techniques for weighted sum-rate maximization in MISO interfering broadcast channels," *IEEE Trans. Wireless Commun.*, vol. 11, no. 4, pp. 1314-1320, Apr. 2012.

[65] R. Zakhour and S. Hanly, "Base station cooperation on the downlink: large system analysis," *IEEE Trans. Inf. Theory.*, vol. 58, no. 4, pp. 2064–2078, Apr. 2012.

[66] K. Karakayali, G.J. Foschini, and R.A. Valenzuela, "Network coordination for spectrally efficient communications in cellular systems," *IEEE Trans. Wireless Commun.*, vol. 13, no. 4, pp. 56-61, Aug. 2006.

[67] H. Dahrouj and W. Yu, "Coordinated beamforming for the multicell multi-antenna wireless system," *IEEE Trans. Wireless Commun.*, vol. 9, no. 5, pp. 1748-1759, May. 2010.

[68] S. Lakshminarayana, M. Assaad, and M. Debbah,, "Coordinated multicell beamforming for massive MIMO: a random matrix approach," *IEEE Trans. Inf. Theory.*, vol. 61, no. 6, pp. 3387-3412, Apr. 2015.

[69] H. Huh, A. M. Tulino, and G. Caire,, "Network MIMO with linear zero-forcing beamforming: large system analysis, impact of channel estimation and reduced-complexity scheduling," *IEEE Trans. Inf. Theory.*, vol. 58, no. 5, pp. 2911-2934, Dec. 2011.

[70] R. Bhagavatula and R. W. Heath Jr., "Adaptive bit partitioning for multicell intercell interference nulling with delayed limited feedback," *Trans. Signal Process.*, vol. 59, no. 8, pp. 3824-3836, Aug. 2011.

[71] H. Zhang, N. B. Mehta, A. F. Molisch, J. Zhang, and H. Dai, "Asynchronous interference mitigation in cooperative base station systems," *IEEE Trans. Wireless Commun.*, vol. 7, no. 1, pp. 155-165, Jan. 2008.

[72] A. Tolli, H. Pennanen, P. Komulainen, "Distributed coordinated multi-cell transmission based on dual decomposition," in *Proc. IEEE GLOBECOM'09*, Dec. 2009, pp. 1-6.

[73] J. Zhang, J. Andrews, "Adaptive spatial intercell interference cancellation in multicell wirless networks," *IEEE J. Sel. Areas in Commun.*, vol. 28, no. 8, pp. 1455-1468, Dec. 2010.

[74] S. Moon, C. Lee, S. Lee, and I. Lee, "Joint user scheduling and adaptive intercell

interference cancellation for MISO downlink cellular systems," *IEEE Trans. Veh. Technol.*,vol. 62, no. 1, pp. 172-181, Jan. 2013.

[75] M. Sternad, T. Svensson, and T. Ottosson, A. Ahlen, A. Svensson, and A. Brunstrom, "Towards systems beyond 3G on adaptive OFDMA transmission," in *Proc. IEEE*, vol. 95, pp. 2432–2455, December 2007.

[76] S. Sadr, A. Anpalagan, and K. Raahemifar, "Radio resource allocation algorithms for the downlink of multiuser OFDM communication systems," *IEEE Commun. Surveys Tuts.*, vol. 11, no. 3, pp. 92-106, third quarter 2009.

[77] G. Song and Y. G. Li, "Cross-layer optimization for OFDM wireless networks-Part I: theoretical framework," *IEEE Trans. Wireless Commun.*, vol. 4, pp. 614–624, Mar. 2005.

[78] G. Song and Y. G. Li, "Cross-layer optimization for OFDM wireless networks-Part II: Algorithm development," *IEEE Trans. Wireless Commun.*, vol. 4, pp. 625–634, Mar. 2005.

[79] G. Song, Y. Li, and L. J. Cimini, Jr,"Joint channel- and queue-aware scheduling for multiuser diversity in wireless OFDMA networks," *IEEE Trans. Commun.*, vol. 57, no. 7, pp. 2109–2121, Jul. 2009.

[80] A. Asadi and V. Mancuso, "A survey on opportunistic scheduling in wireless communications," *IEEE Commun. Surveys Tuts.*, vol. 15, no. 4, pp. 1671-1688, Jan. 2013.

[81] G. Boudreau, J. Panicker, N. Guo, R. Chang, N. Wang, and S. Vrzic, "Interference coordination for 4G networks," *IEEE Commun. Mag.*, vol. 47, no. 4, pp. 74-81, Apr. 2009.

[82] N. Saquib, E. Hossain, L. B. Le, and D. I. Kim, "Interference management in OFDMA femtocell networks: Issues and approaches," *IEEE Trans. Wireless Commun.*, vol. 19, no. 3, pp. 86–95, Jun. 2012.

[83] E. Pateromichelakis, M. Shariat, A. ul Quddus, and R. Tafazolli "On the evolution of the multi-cell scheduling in 3GPP LTE/LTE-A," *IEEE Commun. Surveys Tuts.*, vol. 15, no. 2, pp. 701-717, second quarter 2013.

[84] 3GPP LTE Release 10 & Beyond (LTE-Advanced), 3rd Generation Partnership Project (3GPP), 2009. [Online]. Available:http://www.3gpp.org/

[85] R. Baldemair, E. Dahlman, G. Fodor, G. Mildh, S. Parkvall, Y. Selén, H. Tullberg, and K. Balachandran, "Evolving wireless communications: addressing the challenges and expectations of the future," *IEEE Trans. Veh. Mag.*, vol. 8, no. 1, pp. 24-30, Mar. 2013.

[86] J. G. Andrews, S. Buzzi, W. Choi, S. V. Hanly, A. Lozano, A. C. K. Soong, and J. Charlie, "What will 5G be?," *IEEE J. Sel. Areas Commun.*, vol. 32, no. 6, pp. 1065–1082, Jun. 2014.

[87] A. Gupta and R. Kumar Jha, " A survey of 5G networks: architecture and emerging technologies," *IEEE Access.*, vol. 2, pp. 1187–1195, Jul. 2014.

[88] T. M. Cover and J. A. Thomas, *Elements of Information Theory*, New York: Wiley, 1991.

[89] X. Zhang and J. Tang, "Power-delay tradeoff over wireless networks," *IEEE Trans.Commun.*, vol. 61, no. 9, pp. 3673-3684, Sept. 2013.

[90] X. Lin, N. B. Shroff, and R. Srikant, "A tutorial on cross-layer optimization in wireless networks," *IEEE J. Sel. Areas Commun.*, vol. 24, no. 8, pp. 1452-1463, Aug. 2006.

[91] C.-S. Chang, "Stability, queue length, and delay of deterministic and stochastic queueing networks," *IEEE Trans. Automat. Control.*, vol. 39, no. 5, pp. 913-931, May 1994.

[92] L. Musavian and S. Aissa, "Effective capacity of delay-constrained cognitive radio

in Nakagami fading channels," *IEEE Trans. Wireless Commun.*, vol. 9, no. 3, pp. 1054-1062, Mar. 2010.

[93] L. Musavian and S. Aissa, and S. Lambotharan, "Effective capacity for interference and delay constrained cognitive radio relay channels," *IEEE Trans. Wireless Commun.*, vol. 9, no. 5, pp. 1698-1707, May. 2010.

[94] J. Tang and X. Zhang, "Quality-of-Service driven power and rate adaptation for multichannel communications over wireless links," *IEEE Trans. Wireless Commun.*, vol. 6, no. 12, pp. 4349-4360, Dec. 2007.

[95] J. Tang and X. Zhang, "Cross-layer resource allocation over wireless relay networks for quality of service provisioning," *IEEE J. Sel. Areas Commun.*, vol. 25, no. 4, pp. 2318-2328, May 2007.

[96] J. Tang and X. Zhang, "Cross-layer-model based adaptive resource allocation for statistical qos guarantees in mobile wireless networks," *IEEE Trans. Wireless Commun.*, vol. 7, no. 6, pp. 2318-2328, Jun. 2008.

[97] M. Haenggi, J. Andrews, F. Baccelli, O. Dousse, and M. Franceschetti, "Stochastic geometry and random graphs for the analysis and design of wireless networks," *IEEE J. Sel. Areas in Commun.*, vol. 27, no. 7, pp. 1029–1046, Sept. 2009.

[98] J. Andrews, F. Baccelli, and R. Ganti, "A tractable approach to coverage and rate in cellular networks," *IEEE Trans. Commun.*, vol. 59, no. 11, pp. 3122-3134, Nov. 2011.

[99] N. Jindal, S. Weber, and J. Andrews, "Fractional power control for decentralized wireless networks," *IEEE Trans. Wireless Commun.*, vol. 7, no. 12, pp. 5482-5492, Dec. 2008.

[100] H. Haas, S. McLaughli, *Next Generation Mobile Access Technologies: Implementing TDD*, Cambridge University Press, 2007.

[101] B. Rong, C.-H. Liu and S. Cui, "Discrete location-dependent power control in wireless clustered ad hoc networks," in *Proc. IEEE GLOBECOM '13*, Dec. 2013.

[102] T. Novlan, H. Dhillon, and J. Andrews, "Analytical modelling of uplink cellular networks," *IEEE Trans. Wireless Commun.*, vol. 12, no. 6, pp. 2669-2679, June 2013.

[103] M. Haenggi, "On distances in uniformly random networks," *IEEE Trans. Inf. Theory.*, vol. 51, no. 10, pp. 3584-3586, Oct. 2005.

[104] H. Dhillon, M. Kountouris and J. Andrews, "Downlink MIMO HetNets: modeling, ordering results and performance analysis ," *IEEE Trans. Wireless Commun.*, vol. 12, no. 10, pp. 5208-5222, Oct. 2013.

[105] M. Abramowitz and I. A. Stegun, *Handbook of Mathematical Functions with Formulas, Graphs, and Mathematical Tables*, 9th edition. Dover, 1965.

[106] K. Huang, R. W. Heath, and J.G. Andrews, "Space division multiple access With a sum feedback rate constraint,"*IEEE Trans. Signal Process.*, vol. 55, no.7, pp.3879-3891, July 2007.

[107] I. S. Gradshteyn and I. M. Ryzhik, *Table of Integrals, Series, and Products*, 7th edition. Academic Press, 2007.

[108] W. Choi and J. G. Andrews, "The capacity gain from intercell scheduling in multi-antenna systems ," *IEEE Trans. Wireless Commun.*, vol. 7, no. 2, pp. 714-725, Feb. 2008.

[109] C. Kosta, B. Hunt, A. U. Quddus, R. Tafazolli, "On interference avoidance through inter-cell interference coordination (ICIC) based on OFDMA mobile systems," *IEEE Commun. Surveys Tuts.*,vol. 15, no. 3, pp. 973–995, Mar. 2013.

[110] T. D. Novlan, R. K. Ganti, A. Ghosh, and J. G. Andrews, "Analytical evaluation of fractional frequency reuse of OFDMA cellular networks," *IEEE Trans. Wireless Commun.*, vol. 10, no. 12, pp. 4294-4305, Dec. 2011.

[111] A. H. Sakr and E. Hossain, "Location-aware cross-tier coordinated multipoint transmission in two-tier cellular networks ," *IEEE Trans. Wireless Commun.*, vol. 13, no. 11, pp. 6311-6325, Sept. 2014.

[112] M. Haenggi, *Stochastic Geometry for Wireless Networks* , Cambridge, UK, Cambridge University Press, 2012.

[113] R. Tanbourgi, S.Singh, J. G. Andrews, and F. K. Jondral, "A tractable model for noncoherent joint-transmission base station cooperation ," *IEEE Trans. Wireless Commun.*, vol. 13, no. 9, pp. 1536-1276, Nov. 2014.

[114] G. Nigam, P. Minero, and M. Haenggi, "Coordinated multipoint joint transmission in heterogeneous networks," *IEEE Trans. Commun.*, vol. 62, no. 11, pp. 4134-4146, Nov. 2014.

[115] F. Baccelli and A. Giovanidis, "A stochastic geometry framework for analyzing pairwise-cooperative cellular networks ," *IEEE Trans. Wireless Commun.*, vol. 14, no. 2, pp. 1536-1276, Feb. 2015.

[116] K. Huang and J.G. Andrews, "An analytical framework for multi-cell cooperation via stochastic geometry and large deviations," *IEEE Trans. Inf. Theory.*, vol. 59, no. 4, pp. 2501-2516, Apr. 2013.

[117] X. Zhang and M. Haenggi, "A stochastic geometry analysis of inter-cell interference coordination and intra-cell diversity," *IEEE Trans. Wireless Commun.*, vol. 13, no. 12, pp. 6655-6669, Dec. 2014.

[118] M. Wildemeersch, T. Quek, M. Kountouris, A. Rabbachhin, and C. Slump, "Successive interference cancellation in heterogeneous networks," *IEEE Trans. Commun.*, vol. 62, no. 12, pp. 4440-4453, Dec. 2014.

[119] S. Akoum and R. W. Heath, "Interference coordination: Random clustering and adaptive limited feedback," *IEEE Trans. Signal Process.*, vol. 61, no. 7, pp. 1822-1834, Apr. 2013.

[120] N. Lee, D. M. Jimenez, A. Lozano, R. Heath, "Spectral efficiency of dynamic coordinated beamforming: a stochastic geometry approach," *IEEE Trans. Wireless Commun.*, vol. 14, no. 1, pp. 230-241, Jan 2015.

[121] B. Błaszczyszyn, M. K. Karray, and H. P. Keeler, "Using Poisson processes to model lattice cellular networks," in *Proc. IEEE INFOCOM*, Apr. 2013, pp. 773–781.

[122] A. Behnad and X. Wang,"Distance statistics of the communication best neighbour in a Poisson field of nodes," *IEEE Trans. Commun.*, vol. 63, no. 3, pp. 997-1005, Mar. 2015.

[123] S. Roman, "The formula of Faa di Bruno," *Amer. Math. Monthly* 87, 805-809, 1980.

[124] T. Brown, "Cellular performance bounds via shotgun cellular systems," *IEEE J. Sel. Areas in Commun.*, vol. 18, no. 11, pp. 2443–2455, Nov. 2000.

[125] A. S. Hamza, S. S. Khalifa, H. S. Hamza, and K. Elsayed, "A survey on inter-cell interference coordination techniques in OFDMA-based cellular networks," *IEEE Commun. Surveys Tuts.*, vol. 15, no. 4, pp. 1642–1670, Jan. 2013.

[126] J. Mietzner, R. Schober, L. Lampe, W. Gerstacker, and P. Hoeher, "Multiple-antenna techniques for wireless communications - a comprehensive literature survey," *IEEE Commun. Surveys Tuts.*, vol. 11, no. 2, pp. 87-105, Feb. 2009.

[127] G. Dimic and N. D. Sidiropoulos, "On downlink beamforming with greedy user selection: performance analysis and a simple new algorithm," *IEEE Trans. Signal Process.*, vol. 53, no. 10, pp. 3857-3868, Oct. 2005.

[128] Z. Shen, R. Chen, J. G. Andrews, R. W. Heath, and B. L. Evans, "Low complexity user selection algorithm for multiuser MIMO systems with block diagonalization," *IEEE Trans. Signal Process.*, vol. 54, no.9, pp. 3658-3663, Sep. 2006.

[129] M. Fuchs, G. D. Galdo, and M. Haardt, "Low complexity space-time-frequency scheduling for MIMO systems with SDMA," *IEEE Trans. Veh. Technol.*, vol. 56, no. 5, pp. 2775-2784, Sep. 2007.

[130] L. N. Tran, M. Bengtsson, and B. Ottersten, "Iterative precoder design and user scheduling for block-diagonalized systems," *IEEE Trans. Signal Process.*, vol. 60, no.7, pp.3726-3739, Jul. 2012.

[131] T. F. Maciel and A. Klein, "On the performance, complexity, and fairness of suboptimal resource allocation for multiuser MIMO-OFDMA systems," *IEEE Trans. Veh. Technol.*, vol. 59, no. 1, pp. 406-419, Jan. 2010.

[132] X. Yi and E. K. S. Au, "User scheduling for heterogeneous multiuser MIMO systems: a subspace viewpoint," *IEEE Trans. Veh. Technol.*, vol. 60, no. 8, pp. 4004-4013, Oct. 2011.

[133] S. Nam, J. Kim, and Y. Han,"A user selection algorithm using angle between subspaces for downlink MU-MIMO systems," *IEEE Trans. Commun.*, vol. 62, no. 2, pp. 616-624, Feb. 2014.

[134] S. Sigdel and W. A. Krzymien, "Simplified fair scheduling and antenna selection algorithms for multiuser MIMO orthogonal space-division multiplexing downlink," *IEEE Trans. Veh. Technol.*, vol. 58, no. 3, pp. 1329-1344, Mar. 2009.

[135] R. Chen, Z. Shen, J.G. Andrews, and R. W. Heath, "Multimode transmission for multiuser MIMO systems with block diagonalization," *IEEE Trans. Signal Process.*, vol. 56, no.7, pp. 3294-3302, Jul. 2008.

[136] L. Ventruino, N. Prasad, and X. D. Wang, "Coordinated linear beamforming in downlink multi-cell wireless networks," *IEEE Trans. Wireless Commun.*, vol. 9, no. 4, pp. 1451-1461, Apr. 2010.

[137] Y. F. Liu and Z. Q. Luo, " Coordinated beamforming for MISO interference channel: Complexity analysis and efficient algorithms," *IEEE Trans. Signal Process.*, vol. 59, no.3, pp. 1142-1157, Mar. 2011.

[138] D. Choi, D. Lee, and J. H. Lee, "Resource allocation for CoMP with multiuser MIMO-OFDMA," *IEEE Trans. Veh. Technol.*, vol. 60, no. 9, pp. 4626-4632, Nov. 2011.

[139] U. Jang, H. Son, J. Park, and S. Lee, "CoMP-CSB for ICI nulling with user selection," *IEEE Trans. Wireless Commun.*, vol. 10, no. 9, pp. 2982-2993, Sep. 2011.

[140] S. Sigdel, W. A. Krzymien, and M. Al-Shalash, "Greedy and progressive user scheduling for CoMP wireless networks," in *Proc. IEEE ICC'12*, Ottawa, Canada, Jun. 2012, pp. 4218-4223.

[141] S. Kaviani and W. A. Krzymien, "Multicell scheduling in network MIMO," in *Proc. IEEE Globecom'10*, Miami, Dec. 2010, pp. 1-5.

[142] G. H. Golub and C. F. V. Loan, *Matrix Computations*,3rd ed. Baltimore, MD: The John Hopkins Univ. Press, 1996.

[143] H. Gunawan, O. Neswan, and W. Setya-Budhi, "A formula for angles between two subspaces of inner product spaces," *Beitrage zur Algebra und Geometrie*, vol. 46, no. 2, pp. 311-320, 2005.

[144] A. Bjorck and G. H. Golub, "Numerical methods for computing angles between linear subspaces," *Math. Comput.*, vol. 27, no. 123, pp. 579-594, Jul. 1973.

[145] I. B. Risteski and K. G. Trencevski, "Principal values and principal subspaces of two subspaces of vector spaces with inner product," *Beitrage zur Algebra und Geometrie*, vol. 42, pp. 289-300, 2001.

[146] M. Hong and Z.-Q. Luo, "E-reference signal processing," *ch. Signal Processing and Optimal Resource Allocation for the Interference Channel*. Elsevier, 2013.

[147] L. Venturino, N. Prasad, and X. Wang, "Coordinated scheduling and power allocation in Downlink multicell OFDMA networks," *IEEE Trans. Veh. Technol.*, vol. 58,no. 6, pp. 2835-2848, Jul. 2009.

[148] D. Lopez-Perez, A. Juttner, J.Zhang, "Dynamic frequency planning versus frequency reuse schemes in OFDMA networks," in *Proc. IEEE VTC'09*, Apr. 2009, pp. 1-5.

[149] G. Miao, N. Himayat, Y. Li, and A. Swami, "Cross-layer optimization for energy efficient wireless communication: a survey," *Wireless Comm. and Mobile Computing,*, vol. 9, no. 4, pp. 529–542, Apr. 2009.

[150] F. Haider, C.-X. Wang, H. Haas, E. Hepsaydir, and X. Ge, "Energy-efficient subcarrier-and-bit allocation in multi-user OFDMA systems," in *Proc. IEEE VTC'12*, May 2012, pp. 1-5.

[151] C. Isheden and G. P. Fettweis, "Energy-efficient multi-carrier link adaptation with sum rate-dependent circuit power," in *Proc. IEEE GLOBECOM'10*, Dec. 2010, pp. 1-6.

[152] G. Miao, N. Himayat, Y. Li, A. T. Koc, and S. Talwar, "Interference-aware energy-efficient power optimization," in *Proc. IEEE ICC'09*, Dresden, Germany, Jun. 2009, pp. 14-18.

[153] J. Xu, L. Qiu, and C. Yu, "Improving network energy efficiency through cooperative idling in the multi-cell systems," in *EURASIP J. Wireless Communication and Networking*, Jan. 2011.

[154] X. Wang, P. Zhu, B. Sheng, X. You, "Energy-efficient downlink transmission in multi-cell coordinated beamforming systems," in *Proc. IEEE WCNC'09*, Apr. 2013. pp. 2554-2558.

[155] G. Miao, N. Himayat, Y. Li, "Energy-efficient link adaptation in frequency selective channels," *IEEE Trans. Commun.*, vol. 58, no. 2, pp. 545-554 , Feb. 2010.

[156] Z. Mao and X. Wang, "Efficient optimal and suboptimal radio resource allocation in OFDMA system," *IEEE Trans. Wireless Commun.*, vol. 7, no. 2, pp. 440-445, Feb. 2008.

[157] C. Y. Wong, R. S. Cheng, K. B. Letaief, and R. D. Murch, "Multiuser OFDM with adaptive subcarrier, bit and power allocation," *IEEE J. Sel. Areas Commun.*, vol. 17, no. 10, pp. 1747-1758, Oct. 1999.

[158] I. Kim, I. Park, and Y. Lee, "Use of linear programming for dynamic subcarrier and bit allocation in multiuser OFDM," *IEEE Trans. Veh. Technol.*, vol. 55, no. 4, pp. 1195-1207, July 2006.

[159] E. Bajalinov, "*Linear-fractional programming: theory, methods, applications and software*," Springer, 2003.

[160] W. Dinkelbach, "On nonlinear fractional programming", *Management Science*, vol. 13, pp. 492-498, 1967.

[161] J. Laiho, A. Wacker, T. Novosad, "*Radio Network Planning and Optimisation for UMTS*", John Wiley & Sons, Chichester, 2002.

Papers Submitted as Publications

The work presented in this thesis has led to the following publications:

Journals

1. **M. Al-Saedy**, H. S. Al-Raweshidy, and F. Haider, "Stochastic geometry modelling of adaptive coordination inter-cell interference cancellation in downlink cellular networks," *IEEE Trans. Veh. Technol.*, submitted for publication.

2. **M. Al-Saedy**, H. S. Al-Raweshidy, and F. Haider, "Coverage and effective capacity in downlink MIMO multi-cell networks with power control: stochastic geometry modelling," *IEEE Trans. Commun.*, submitted for publication.

3. **M. Al-Saedy**, H. S. Al-Raweshidy, and M. Sabah, "User scheduling and multimode selection in coordinated MIMO multicell downlink cellular networks," *IEEE Trans. Veh. Technol.*, submitted for publication.

Conferences

1. **M. Al-Saedy** and H. S. Al-Raweshidy, "Energy-spectral efficiency trade-off in coordinated multi-cell OFDMA systems," in *Proc. IEEE FGCT'15*, Luton, UK, Jul. 2015.